



Technische Universität München

Klinikum rechts der Isar

Klinik und Poliklinik für Chirurgie

Direktor: Prof. Dr. Helmut Friess

**Signalling of the neuropeptide CGRP via its receptor
component RAMP1 promotes liver fibrosis upon chronic liver
injury through controlling YAP activity**

Yang Wang

Vollständiger Abdruck der von der Fakultät für Medizin der Technischen Universität München
zur Erlangung des akademischen Grades eines

Doktors der Medizin (Dr. med.)

genehmigten Dissertation.

Vorsitzender: Prof. Dr. Florian Eyer

Prüfende der Dissertation: 1. Priv.-Doz. Dr. Melanie Laschinger

2. Priv.-Doz. Dr. Fabian Geisler

Die Dissertation wurde am 15.04.2021 bei der Technischen Universität München eingereicht
und durch die Fakultät für Medizin am 10.08.2021 angenommen.

Table of Contents

1. Introduction	4
1.1 The liver and its functions under physiological conditions	4
1.1.1 Parenchyma and non-parenchymal cells.....	4
1.1.2 Functions of hepatic stellate cells	5
1.2 Liver fibrosis upon injury	6
1.2.1 Development of liver fibrosis	6
1.2.2 Role of hepatic stellate cells in liver fibrosis	7
1.2.3 TGF β 1 signalling is activated during liver fibrosis.....	9
1.3 Hepatocyte proliferation during liver fibrosis	10
1.4 Role of YAP signalling in liver fibrosis.....	11
1.4.1 YAP signalling pathway	11
1.4.2 Effect of YAP signalling on liver fibrosis	13
1.5 Liver innervation and fibrosis	13
1.5.1 Distribution of perihepatic nerves	14
1.5.2 Distribution of intrahepatic nerves	15
1.5.3 Connection between liver innervation and fibrosis	15
1.6 Role of CGRP/RAMP1 signalling in liver fibrosis	16
1.6.1 Complex of CGRP receptors	16
1.6.2 Transduction of G protein signalling	17
1.6.3 Effect of CGRP/RAMP1 signal on YAP activity	18
2. Aims of the study	19
3. Materials and methods	20
3.1 Materials	20
3.1.1 Chemicals and reagents.....	20
3.1.2 Buffers and solutions.....	22
3.1.3 Antibodies.....	23
3.1.4 Primers	24

3.1.5 Technical devices	27
3.1.6 Cell line.....	28
3.1.7 Kits	28
3.2 Methods.....	28
3.2.1 RAMP1 ^{-/-} mouse model	28
3.2.2 Induction of liver fibrosis by injection of carbon tetrachloride.....	28
3.2.3 Generation of formalin-fixed paraffin-embedded sections	29
3.2.4 Immunohistochemistry.....	29
3.2.5 Sirius Red staining.....	30
3.2.6 Immunofluorescence staining.....	31
3.2.7 Isolation of RNA using Qiagen RNeasy kit	32
3.2.8 Complementary DNA reverse transcription	33
3.2.9 Quantitative real-time PCR (qRT-PCR)	34
3.2.10 Cell culture and passaging	35
3.2.11 Cell freezing	35
3.2.12 Cell thawing.....	35
3.2.13 Migration assay	36
3.2.14 <i>In vitro</i> stimulation of cells	36
3.2.15 Isolation of protein	37
3.2.16 Detection of protein by Western Blotting	38
3.2.17 ELISA for alanine aminotransferase (ALT)	39
3.3 Statistics	40
4. Results.....	41
4.1 Induction of CGRP and RAMP1 upon chronic liver injury	41
4.2 CGRP/RAMP1 signalling increases liver-to-body weight ratio and impairs liver function during chronic liver injury	42
4.3 CGRP/RAMP1 signalling promotes hepatocyte proliferation after CCl ₄ administration.....	45
4.4 CGRP/RAMP1 signalling promotes collagen deposition in the fibrotic liver	48

4.5 CGRP/RAMP1 signalling might not affect the immune response in the process of fibrosis.....	51
4.6 CGRP/RAMP1 signalling promotes the activation of hepatic stellate cells in the fibrotic liver.....	52
4.7 <i>In vitro</i> CGRP/RAMP1 signalling contributes to the activation of hepatic stellate cells and collagen production.....	54
4.8 CGRP/RAMP1 signalling positively regulates YAP activity during liver fibrosis.....	57
4.9 CGRP/RAMP1 signalling increases YAP activity via G α ₁₁ signalling during liver fibrosis.....	60
4.10 <i>In vitro</i> CGRP/RAMP1 signalling increases YAP activity in hepatic stellate cells.....	61
4.11 CGRP/RAMP1 signalling does not promote the migration of LX-2 cells.....	63
4.12 CGRP/RAMP1 promotes TGF β 1 signalling by activating Smad2.....	65
4.13 CGRP/RAMP1 signalling enhances YAP activity in the human primary hepatic stellate cells.....	66
5. Discussion.....	68
6. Summary.....	79
7. Abbreviations.....	80
8. List of Figures.....	82
9. References.....	84
10. Curriculum Vitae.....	98
11. Acknowledgements.....	100

1. Introduction

1.1 The liver and its functions under physiological conditions

1.1.1 Parenchyma and non-parenchymal cells

The liver is the largest solid gland of the human body and an organ with complex metabolic functions. It has a dual blood supply of the hepatic artery and hepatic vein, and both the hepatic vein and biliary systems of the liver parenchyma (Si-Tayeb et al., 2010). The liver has rich blood sinuses and a structure of repeating anatomical units termed liver lobules, hence it can undertake diverse metabolic works (Ben-Moshe et al., 2019).

The liver parenchyma is the functional tissue of the organ, accounting for 78% of the liver volume; these cells are known as hepatocytes (Frevert et al., 2005) (Figure 1). Hepatocytes depend on the developed smooth endoplasmic reticulum to achieve metabolic and detoxification effects, such as drug metabolism (Franco-Belussi et al., 2012). Hepatocytes can synthesise cholesterol and triglycerides, and bile is also secreted by hepatocytes. In addition, hepatocytes synthesise a tremendous amount of different proteins, including serum albumin. In the case of hepatocyte loss due to liver damage, hepatocytes can quickly enter the cell cycle and undergo rapid division.

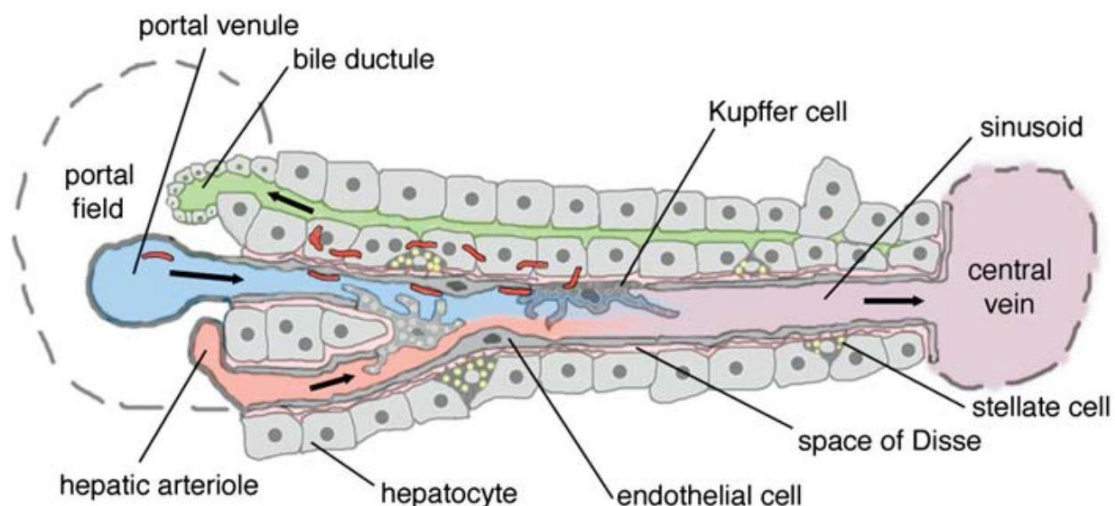


Figure 1. The location of liver cells and the dual blood supply (Frevert et al., 2005). The liver parenchyma is mainly composed of hepatocytes. Non-parenchymal cells include cholangiocytes of the bile duct, (sinusoidal) endothelial cells, (hepatic) stellate cells and Kupffer cells. As the blood supply of the liver, the portal vein and hepatic artery join upon entering the liver lobule at the portal area.

Another major type of liver cell is non-parenchymal cells, making up 40% of the total number of liver cells, but only 6.5% of the volume (Kmieć, 2001). These non-parenchymal cells include cholangiocytes, sinusoidal endothelial cells (LSECs), stellate cells (HSCs), Kupffer cells and intrahepatic lymphocytes. Cholangiocytes are arranged into the intrahepatic bile duct tree, modifying the ingredients of bile produced by hepatocytes (Banales et al., 2019). Also, cholangiocytes play an important role in maintaining and adjusting the structure of the bile duct by controlling the absorption of hormones. Moreover, they are responsible for innate and adaptive immune responses (Banales et al., 2019). Liver sinusoidal endothelial cells (LSECs) are located between hepatocytes and hepatic sinuses, and ingest macromolecular substances in the blood to remove harmful enzymes and pathogens (Figure 1) (Sørensen et al., 2015). Kupffer cells (KCs) are liver-resident macrophages, and their main function is to remove endotoxins, bacteria, viruses and tumour cells (Dixon et al., 2013). Intrahepatic lymphocytes are mostly composed of natural killer cells, which have cytotoxic effects on tumour cells, and remove the liver cells infected by viruses (Liu et al., 2018).

1.1.2 Functions of hepatic stellate cells

As the HSC plays a detrimental role during the development of fibrosis and cirrhosis, this chapter concentrates on the molecular impact of HSC on this process.

Hepatic stellate cells are some of the interstitial cells in the liver and are located in the Disse space of the liver sinus, accounting for about 15% of the total number of liver cells (Figure 1) (Friedman, 2008). HSCs normally stay quiet, as their main function is to participate in the metabolism of vitamin A and store fat. Upon liver injury, HSCs are activated, lose vitamin A and secrete large amounts of the extracellular matrix (ECM) including collagen (Iredale et al., 2013). The activation of HSCs consists of two major phases: the initiation phase and the perpetuation phase (El Taghdouini et al., 2016). The detailed physiological changes in HSCs during activation are illustrated in the following chapter 1.2.2.

1.2 Liver fibrosis upon injury

1.2.1 Development of liver fibrosis

Liver fibrosis is a pathological process caused by various acute and chronic liver injury factors, including operations, hepatitis viruses, alcohol damage, drug abuse and autoimmune disorders (Elsharkawy et al., 2005). It is characterised by an inflammatory response and the excessive accumulation of ECM in the liver (Ellis et al., 2012). If liver fibrosis is not reversed, it quickly develops into liver cirrhosis, which results in 1.03 million deaths every year worldwide (Higashi et al., 2017). Eventually, liver cirrhosis could deteriorate to liver cancer. Moreover, as the liver fibrosis progresses, symptoms such as ascites, hepatic encephalopathy, and liver-kidney syndrome are likely to occur, damaging the health of patients. Hence, it is important to understand the molecular mechanism controlling the process.

In the normal liver, the extracellular matrix maintains cell adhesion, proliferation and differentiation by producing large amounts of molecules (Baiocchi et al., 2016). However, upon injury, excessive deposition of the ECM, mainly collagen type I, distorts the lobular structure and increases the tissue stiffness of the liver parenchyma, which affects the cells' function. This process involves resident liver parenchymal and non-parenchymal cells as well as infiltrating immune cells (Koyama et al., 2017). The initial event of liver fibrosis is hepatocyte damage, which consequently promotes the recruitment of immune cells (Tu et al., 2015). Hepatocytes can undergo pyroptotic death and release extracellular inflammasome complexes, which can be internalized by HSCs, leading to HSC activation (Gaul et al., 2021). Activated HSCs produce proteins including α -smooth muscle actin (α -SMA), collagen type I and III, and fibronectin (Tsuchida et al., 2017).

The function of immune cells is also affected during liver fibrosis. Dendritic cells (DCs) promote matrix degradation through matrix metalloproteinase (MMP)-9 expression, while natural killer cells (NK cells) induce the apoptosis of activated HSCs (myfibroblasts) through the natural killer group 2 member D (NKG2D) and targeting TNF-related apoptosis-inducing ligand (TRAIL) receptors (Fasbender et al., 2016). Myofibroblast apoptosis induces inflammation in non-parenchymal cells and immune cells, as well as the activation of pro-fibrotic pathways, thus triggering the development of liver fibrosis.

During liver fibrosis, the excessive production of immune cells eliminates damaged cells and pathogens, causing increased inflammation responses (Grunebaum et al., 2019). Pro-inflammatory cytokines including TGF β , TNF- α and interleukins (IL) are elevated in fibrotic areas, which can promote the activation of HSCs (Tu et al., 2014; Weiskirchen et al., 2017; Yang et al., 2015). These cytokines play important roles in liver fibrogenesis.

1.2.2 Role of hepatic stellate cells in liver fibrosis

HSCs are the key cells involved in the process of liver fibrosis. Upon liver injury, HSCs are activated, lose vitamin A droplets and secrete large amounts of ECM, MMP, and metalloproteinase tissue inhibitor (TIMP) (Iredale et al., 2013) (Figure 2).

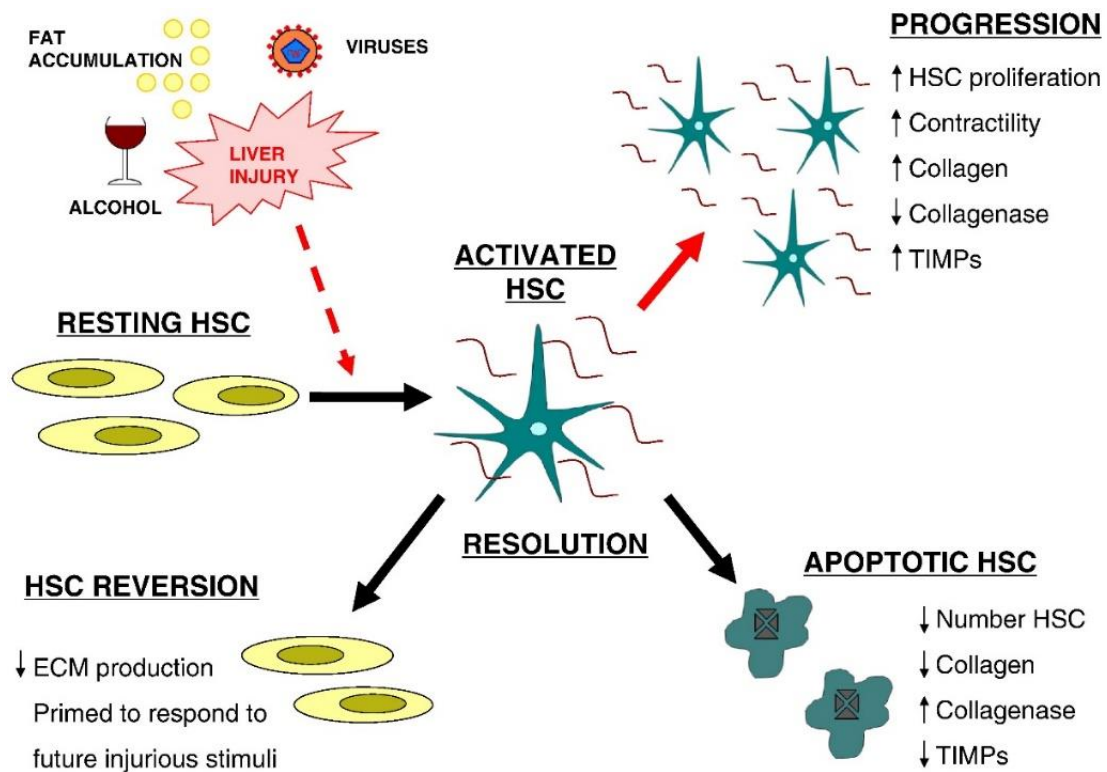


Figure 2. Liver injury leads to the conversion of quiescent HSC to activated HSC (myofibroblasts) (Iredale et al., 2013). Upon activation, HSCs secrete large amounts of extracellular matrix proteins, including collagens, with the reduced production of collagenase. When liver fibrosis is alleviated, HSCs undergo apoptosis or are transformed into a quiescent state, producing less collagen.

In the early stage of liver injury, HSCs enter the initiation phase of activation. Phenotype changes occur to HSCs, which are manifested as transcription activation, signal molecule activation, and the induction of early structural gene expression (El Taghdouini et al., 2016). Receptors of cytokines and growth factors are expressed on the cell membrane, including platelet derived growth factor (PDGF) receptors, transforming growth factor- β (TGF β) receptors, and vascular endothelial growth factor (VEGF) receptors (Dewidar et al., 2019). HSCs generate the ability to respond to these mediator molecules, turning them into myofibroblast cells.

During the perpetuation activation phase, HSCs further undergo a series of phenotypic changes, including: (1) cell proliferation: especially in the newly formed fibrous compartment of the area of inflammatory necrosis (Huang et al., 2017); (2) phenotypic transformation: HSCs lose droplets and their retinoid content, and instead synthesise the ECM; (3) contractility: the expression of α -SMA induces microcirculation changes and platelet aggregation (Friedman, 2008); (4) chemotaxis: HSCs migrate to the damaged area, resulting in increased fibroblasts in the damaged area; (5) the enhanced expression of cytokines and their receptors: increased sensitivity to stimulation by chemical factors; and (6) the release of collagenase and its inhibitor: the subendothelial matrix is destroyed (Robert et al., 2016). In addition, the increased secretion of MMP inhibitors reduces the degradation of newly generated collagen, eventually leading to excessive ECM deposition. The HSC continuously stimulates its own cell division and proliferation through the autocrine system, and secretes various kinds of ECM to promote the development of liver fibrosis (Schon et al., 2016).

During liver fibrosis, HSCs interact with hepatocytes, LSECs, KCs, etc., accelerating the fibrosis process (Hinz et al., 2007). When massive ECM is accumulated in the Disse space, it becomes a repository of cytokines, chemokines and growth factors, including TGF- β , PDGF, hepatocyte growth factor (HGF), fibroblast growth factor (FGF), epidermal growth factor (EGF), VEGF and connective tissue growth factor (CTGF) (Bonnans et al., 2014). These factors together form the micro-environment of the fibrotic tissue. Furthermore, the mechanical stimuli form a positive feedback loop through the intrinsic protein pathway to continuously promote HSCs activation. HSCs express two types of collagen receptors, integrin and discoid cell domain receptors (DDR), which regulate cell differentiation, proliferation, and migration (Henderson et al., 2013).

1.2.3 TGF β 1 signalling is activated during liver fibrosis

TGF β is a profibrogenic cytokine and known to participate in all stages of liver fibrosis and cirrhosis. The TGF β superfamily includes three TGF β isoforms (TGF β 1, β 2, and β 3), three activin isotypes and over 10 isoforms of bone morphogenetic proteins (BMPs) (Shi et al., 2003). TGF β exerts its intracellular functions through binding to the TGF- β receptor II (T β RII), which allows T β RII to phosphorylate TGF β receptor I (T β RI), activating its catalytic ability. Subsequently, activated T β RI phosphorylates the receptor-activated (R-) Smads, particularly Smad2 and Smad3 (Yu et al., 2008). Then, the phosphorylated Smad2 and Smad3 oligomerise with Smad4 forming heterotrimeric complexes. These complexes translocate into the nucleus, regulating the transcription of target genes.

TGF β is known to be a key mediator involved in multiple injury responses of the liver, including regeneration, fibrogenesis and tumorigenesis. TGF β can be produced by HSCs, KCs, LSECs and hepatocytes (Hellerbrand et al., 1999). In normal mice livers, KCs and LSECs express high levels of TGF- β , while HSCs and hepatocytes possess very little TGF β (Bissell et al., 1995). After the induction of liver fibrosis by bile duct ligation (BDL), the expression of all three forms of TGF β dramatically increases. Among the three isoforms, TGF β 1 has been proven to be the strongest fibrogenic factor, triggering the contraction of cultured fibroblasts (Frolik et al., 1983).

In fact, TGF β 1 participates closely in HSC activation, which leads to the production of extracellular matrix. Under normal circumstances, HSCs are in a quiescent state. When liver damage happens upon external stimuli, TGF β 1 induces the conversion of HSCs to myofibroblasts (Tu et al., 2014). The initial activation phase relies strongly on TGF β 1 signalling, whereas the perpetuation phase seems to be independent of TGF β 1 (Dooley et al., 2001). Specifically, TGF β 1 promotes the activation of TGF β -responsive element (T β RE), phosphorylation of Smad2/3, and subsequently the nuclear translocation of the heterotrimeric complexes. The process is followed by the production and remodelling of ECM dominated by activated HSC, and the secretion of MMPs which are responsible for the collagen degradation (Kulkarni et al., 2016). Furthermore, TGF β 1 induces the synthesis of ECM crosslinking proteins, such as the lysyl oxidase (LOX) family of extracellular copper-dependent enzymes, to increase the intensity of the collagen networks (Busnadiago et al., 2013).

1.3 Hepatocyte proliferation during liver fibrosis

During liver injury, hepatocytes are damaged and undergo necrosis, which accounts for the loss of liver mass. In order to regain liver size and liver function, hepatocytes start to proliferate, entering the cell cycle to restore the liver function (Curado et al., 2010). The remnant hepatocytes in the liver account for most of the regeneration process (Curado et al., 2010). Interestingly, HSCs have also been shown to assist liver regeneration by secreting growth factors for epithelial cells, including hepatocytes (Fausto, 2004). When inhibiting the activation of HSCs by gliotoxin, the regenerative reaction of hepatocytes was dramatically decreased during acetaminophen-induced liver injury (Shen et al., 2011). Moreover, activated HSCs secrete various kinds of cytokines and chemokines, which promote hepatocyte proliferation (Friedman, 2008).

There have been numerous studies investigating hepatocyte proliferation. For this, two models have been commonly used: (a) partial hepatectomy (PHx); and (b) models of liver fibrosis. The mouse model of 2/3 partial hepatectomy has been widely used to imitate liver regeneration and cell cycle dynamics *in vivo* (Boyce et al., 2008). Upon 2/3 PHx, hepatocytes start to proliferate and undergo cell division. In wild type mice, the DNA replication of hepatocytes peaks between 36 and 48 hours after 2/3 PHx (Mitchell et al., 2008). However, the proliferation process can vary between different mouse strains. Although the model of PHx closely imitates the surgery situation in clinic, chemically-induced liver injury could better mimic the inflammatory and fibrotic reactions happening with regeneration. One well-known model is the carbon tetrachloride (CCl₄) treatment model (Dong et al., 2016). CCl₄ administration causes hepatocyte damage, necrosis, inflammation and fibrosis. When injected intraperitoneally, it infiltrates into the vascular structures and drains the liver sinusoid (Alatsakis et al., 2009). The continuous administration of CCl₄ can induce liver fibrosis between 36 hours and 18 weeks (Cheung et al., 2006; Peng et al., 2005).

Upon chronic liver injury induced by CCl₄, hepatocytes undergo a limited number of cell cycles to restore the liver mass (Corlu et al., 2015). The cell cycle is composed of interphase (G₁, S, and G₂ phases), the mitotic phase (mitosis and cytokinesis), and G₀ phase, which are controlled by different cyclins and cyclin-dependent kinase (CDK). Cyclin A regulates the S phase, and Cyclin D/Cyclin E regulates the G₁ to S phase, while Cyclin B/CDK1 regulates the G₂ to M phase (Lim et al., 2013). Our study used the mouse

model of liver fibrosis induced by the injection of CCl₄, and detected large amounts of proliferating hepatocytes by the marker Ki67 which reflects the entire active phases, as well as the induced cell cycle components (Laschinger et al., 2020). Also, cytokines and fibrotic markers were also involved in the fibrosis process, reflecting the actual situation during chronic injury. Notably, TGFβ has been shown to act as a key regulator during liver fibrosis, which triggers the activation of HSCs (Tu et al., 2014). An elegant study demonstrates that TGF-β and yes-associated protein (YAP) signalling cooperate to promote hepatocyte proliferation, regenerating the injured liver (Oh et al., 2018). However, the effect of the neuropeptide on hepatocyte proliferation during liver fibrosis still remains to be determined.

1.4 Role of YAP signalling in liver fibrosis

YAP signalling is known to promote liver fibrosis via activation of hepatic stellate cells upon chronic liver injury (Mannaerts et al., 2015).

1.4.1 YAP signalling pathway

YAP and the transcriptional co-activator with PDZ-binding motif (TAZ) are the downstream effectors of the Hippo pathway, a key controller of organ size which was originally identified in the genetic screening of *Drosophila* (Patel et al., 2017) (Figure 3).

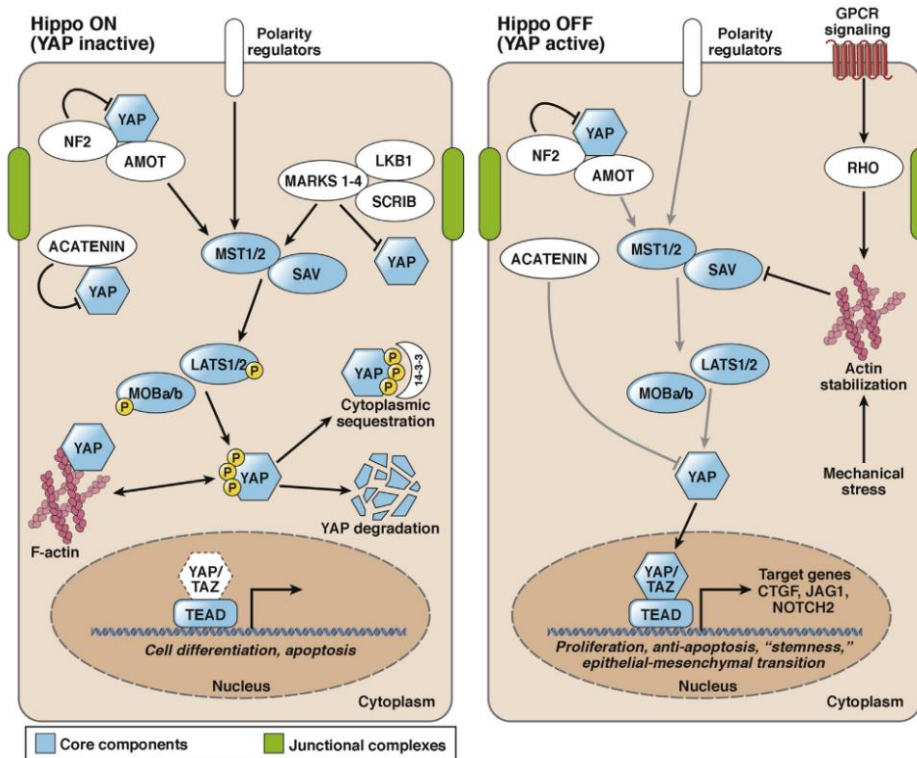


Figure 3. Regulation of the YAP signaling pathway (Patel et al., 2017). When Hippo signaling is on, YAP is phosphorylated and subjected to cytoplasmic sequestration or proteasomal degradation. When Hippo signaling is off, YAP translocates into the nucleus and binds to the TEAD family of transcription factors, leading to the transcription of genes regulating cell growth and proliferation.

The Hippo pathway generates extracellular signals and activates the Mammalian Sterile 20-like kinases 1 and 2 (Mst1/2) (Dan et al., 2001). The activated Mst1/2 phosphorylates the adaptor protein salvador (SAV) and binds with it to form a complex, together phosphorylating and activating the tumour suppressor kinases 1 and 2 (LATS1/2). Phosphorylation-activated LATS1/2 is a nuclear DBF-2-related kinase that can regulate the cell cycle, growth and development (Ma et al., 2010). Activation of LATS in turn phosphorylates YAP/TAZ, inducing cytoplasmic retention or leading to proteasomal degradation. YAP activity can be negatively regulated by the phosphorylation of either Ser397 or Ser127. Specifically, the phosphorylation of Ser397 indicates the degradation of YAP, while phosphorylation on Ser127 indicates the cytoplasmic retention of YAP (Hergovich, 2017). When the Hippo pathway is inactivated, YAP and TAZ translocate to the nucleus and bind to the TEA domain family member (TEAD) family factors, driving the transcription of the target genes related to cell proliferation and growth (Yagi et al., 1999).

Overall, the Hippo pathway controls organ size and tissue homeostasis, while in the absence of Hippo pathway activity, the excessive activation of YAP/TAZ leads to tissue overgrowth and tumorigenesis (Johnson et al., 2014).

1.4.2 Effect of YAP signalling on liver fibrosis

In the mammalian liver, Hippo/YAP signalling is involved in the regenerative response (Lu et al., 2018). Furthermore, YAP is an important regulator of hepatic stellate cell activation upon chronic liver injury (Mannaerts et al., 2015). Once activated, YAP in the cytoplasm of HSCs enters the nucleus, and binds to the transcription factor TEAD to promote the transcription of genes such as *Ctgf* and *Ankrd1*, which are related to HSC activation and matrix remodelling (Zhubanchaliyev et al., 2016). Mannaerts et al. demonstrated that the translocation of YAP into the nucleus induces HSC activation in the livers of CCl₄ injected mice, as well as in the primary HSCs *in vitro* (Mannaerts et al., 2015). Activated YAP leads to increased extracellular matrix deposition and tissue stiffness, which enhance the fibrogenic process (Herrera et al., 2018). Inhibition of YAP by verteporfin (VP) prevents the activation of hepatic stellate cells *in vitro*, and reduces the expression of α -SMA and type I collagen. Additionally, during the repair of liver ischemia-reperfusion injury, YAP in HSCs are selectively activated, with the expression of the target genes *Ctgf* and *Survivin* being up-regulated, leading to HSC activation and proliferation (Konishi et al., 2018).

Furthermore, YAP controls liver fibrosis through TGF β /Smad signalling. YAP/TAZ is essential for the nuclear accumulation of Smad2/3, and it mainly regulates the subcellular localisation of phosphorylated Smad2/3 (Varelas et al., 2010). Activated YAP translocates into the nucleus and promotes the transcription of *Ctgf*, secreted phosphoprotein 1 (*Spp1*), *Tgf β* and other genes, indicating that YAP participates in the process of liver fibrosis through the TGF β /Smad pathway (Perumal et al., 2017).

1.5 Liver innervation and fibrosis

The liver's glucose and lipid metabolism, biliary system and blood circulation are highly regulated by the innervated nerves (Kandilis et al., 2015). The anatomy of the hepatic innervating nerves and its influence on hepatic haemodynamics have been studied for over 30 years. Stimulation of the sympathetic and parasympathetic nerves causes the release of classical neurotransmitters, as well as the vasoactive neuropeptide (Streba et

al., 2014). Hence, the regulation of liver function by neurological factors becomes complicated.

1.5.1 Distribution of perihepatic nerves

The liver is innervated by sympathetic and parasympathetic nerves (vagus nerve) off the celiac nerve plexus (T7-T10) (Berthoud et al., 1996). The celiac nerve plexus is divided into the anterior plexus and the posterior plexus. The anterior plexus is composed of left and right celiac ganglia and the left vagus nerve branches, including the branches of cystic duct, gallbladder, and pancreas-common bile duct, which form a sheath around the hepatic artery and enter the liver (Natsis et al., 2004). The posterior plexus consists of the right celiac ganglion and the branches of the right vagus nerve. It is mainly distributed along the extrahepatic bile duct and portal vein, and has branches communicating with the branches of the anterior plexus nerve (Figure 4) (Berthoud, 2004).

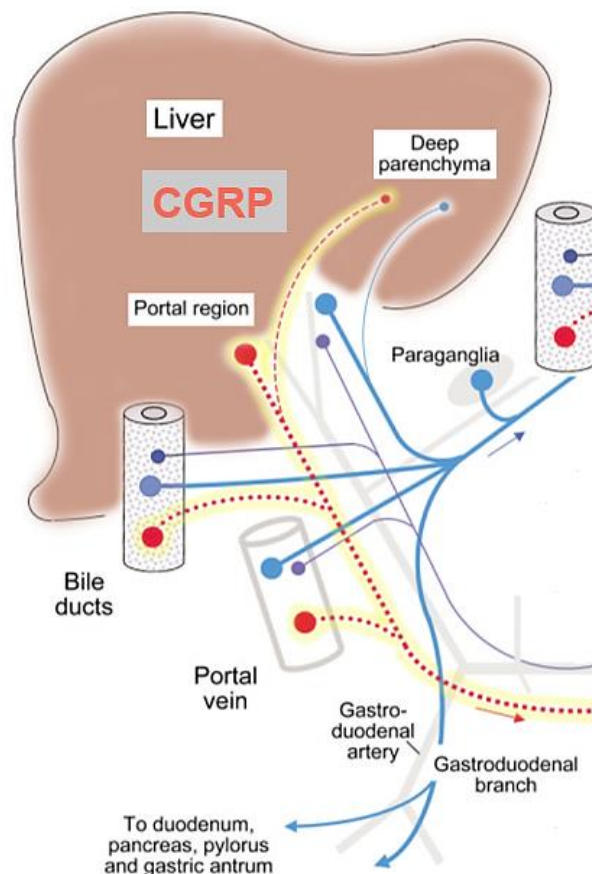


Figure 4. Anatomy of vagal and spinal afferent innervation of the liver (Berthoud, 2004). Vagal innervation is shown in blue solid lines, with spinal afferent innervation in red broken lines. The hepatic branch innervates not only the liver parenchyma, bile ducts, and portal vein, but also the duodenum, pancreas, pylorus, and distal gastric antrum.

The afferent nerves innervating the liver are sensory nerves, which transmit nerve impulses from receptors related to liver metabolism to the central nervous system (Berthoud, 2004). The efferent nerve (motor nerve) regulates blood flow, bile flow, carbohydrate and lipid metabolism, and regeneration of the liver parenchymal cells.

1.5.2 Distribution of intrahepatic nerves

The sympathetic nerves are the main nerves in the liver, distributed around blood vessels in the portal area (Reilly et al., 1978). There are also branches of sympathetic nerve endings distributed in the liver lobules. Adrenergic nerve fibres are distributed in large numbers around the portal vein and hepatic artery, but are rarely seen around the bile duct (Gardemann et al., 1992). Most cholinergic nerves are parasympathetic. In the livers of humans and rats, they are mainly located around the hepatic artery and the bile duct (Akiyoshi et al., 1998). The cholinergic fibres also exist in the hilar nerve bundle, distributed along the hepatic sinusoidal wall.

The autonomic nerves contain abundant regulatory peptides, including neuropeptide tyrosine (NPY), vasoactive intestinal polypeptide (VIP), substance P and calcitonin gene-related peptide (CGRP). NPY is mainly found in sympathetic adrenergic fibres, while VIP, substance P and CGRP are found in parasympathetic cholinergic fibres (Franco-Cereceda et al., 1987; Lundberg et al., 1982).

1.5.3 Connection between liver innervation and fibrosis

The sympathetic nervous system (SNS) plays a regulatory role in the development of liver fibrosis. Upon liver injury induced by CCl₄ injection, the fibrosis in the spontaneously hypertensive rat, which has an active SNS, appears to be more severe than in normal Wistar-Kyoto rats (Hsu, 1992). Besides, in CCl₄-induced injury, mice subjected to the chemical sympathectomy have significantly alleviated lipid peroxidation and oxidative DNA damage (Lin et al., 2016). Furthermore, selective adrenoceptor antagonists attenuate the extent of fibrogenesis and HSC activation (Oben et al., 2004). Therefore, the activation of sympathetic nerves positively regulates the progress of liver fibrosis.

Structurally, the sympathetic nerve endings are located in the Disse space, where the HSCs are distributed. HSCs express adrenoceptors and dopamine receptors, which are regulated by the autonomous nervous system (Oben et al., 2004). The deficiency of norepinephrine impairs HSC activation as well as collagen deposition. Moreover, HSCs isolated from dopamine β -hydroxylase-deficient mice proliferate poorly in medium, which can be rescued by norepinephrine treatment (Oben et al., 2004). Taken together, SNS promotes the progress of liver fibrosis by activating HSCs.

Although CGRP mainly exists in parasympathetic cholinergic fibres, it was reported to selectively stimulate the noradrenergic outflow from the sympathetic nerves, causing tachycardia and blood pressure elevation in rats (Fisher et al., 1983). Moreover, studies have shown that CGRP exerts its central pressor and tachycardiac effects by increasing the catecholamine release, possibly via specific receptors (Kuo et al., 1994). Hence CGRP could have a positive effect on the sympathetic nervous system which regulates HSC activation and fibrogenesis in the liver. Clinical studies showed that the plasma CGRP level was significantly increased in liver cirrhotic patients compared with normal patients (Bendtsen et al., 1991). Therefore, it leads us to the question whether CGRP has an effect on the progress of liver fibrosis.

1.6 Role of CGRP/RAMP1 signalling in liver fibrosis

1.6.1 Complex of CGRP receptors

The neurons of spinal afferent innervation in the liver form a network in the biliary system, the portal region as well as in the deep parenchyma, secreting diverse peptides including CGRP (Figure 4) (Berthoud, 2004). There are two isoforms of CGRP, named α CGRP and β CGRP. α CGRP is distributed in the central and peripheral systems, while β CGRP is in the enteric nervous system (Russell et al., 2014). CGRP is a strong vasodilator and has a proven cardioprotective function (Kee et al., 2018). Also, antagonists targeting CGRP receptors have a clear efficacy in the treatment of neurological diseases, especially migraine (Negro et al., 2012).

CGRP is released by peripheral nerve terminals and binds to its receptor complex on the cell surface consisting of the seven-transmembrane calcitonin receptor-like receptor

(CRLR), the receptor activity modifying protein (RAMP)1 and the receptor component protein (RCP) (Russo, 2015) (Figure 5). The heterodimer of CRLR and RAMP1 exhibits a high affinity for CGRP. Although RCP is dispensable for the binding, it assists with its coupling with the downstream signals (Dickerson, 2013).

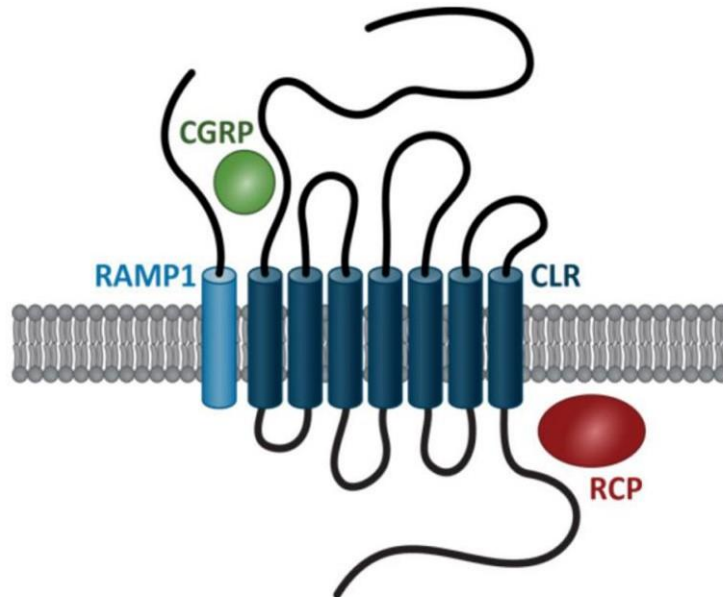


Figure 5. Composition of the CGRP receptor complex (Russo, 2015). The CGRP receptor complex contains RAMP1, CRLR and RCP. CGRP is released by peripheral nerve terminals and binds to the seven-transmembrane CRLR and RAMP1. The signaling is transmitted into the cell with the assistance of RCP.

1.6.2 Transduction of G protein signalling

In order to be transmitted into the cell, CGRP/RAMP1 signalling requires the binding of different G proteins. The $G\alpha$ subunit is the major family of proteins responsible for this transmission, including $G\alpha_s$ and $G\alpha_{q/11}$ (Downes et al., 1999). When coupling with the $G\alpha_s$ protein, the CGRP/RAMP1 signal increases the level of cyclic adenosine monophosphate (cAMP), activates protein kinase A (PKA) and phosphorylates the intranuclear transcription factor cAMP response element-binding protein (CREB) (Holzmann, 2013). The combination of CGRP/RAMP1 with $G\alpha_{q/11}$ protein promotes the expression of phospholipase C- β (PLC β), activating protein kinase C (PKC) (Drissi et al., 1998).

1.6.3 Effect of CGRP/RAMP1 signal on YAP activity

Although extensive studies have identified the upstream signals of the YAP pathway, knowledge about extracellular molecules and receptors on the cell surface regulating YAP activity still remains elusive. G Protein-Coupled Receptors (GPCRs) are the largest families of cell surface receptors. CRLR was identified as one of the GPCRs (Cottrell, 2019). GPCRs have been reported to regulate diverse physiological process, including cell proliferation and differentiation (Wang et al., 2018). Additionally, GPCRs participate in the development of liver fibrosis and tumorigenesis (Huang et al., 2018; Tan et al., 2019).

As one of the extracellular ligands, the neuropeptide CGRP binds to the complex receptor of CRLR and RAMP1, triggering the activation of different G proteins. Signalling via the $G\alpha_s$ protein has been demonstrated to have a negative effect on YAP activity, leading to growth inhibition in MDA-MB-231 cells as well as in primary Schwann cells (Deng et al., 2017; Yu et al., 2012), while signalling via the $G\alpha_{q/11}$ protein increases YAP activity and shows a stimulatory effect on the proliferation of the human embryonic kidney cell line HEK293A (Feng et al., 2014; Yu et al., 2012).

Our previous study has demonstrated that CGRP/RAMP1 signalling promotes hepatocyte proliferation through YAP activity (Laschinger et al., 2020). Given that CGRP/RAMP1 signalling regulates YAP activity via specific G proteins, and YAP controls HSC activation, it is crucial to investigate whether CGRP/RAMP1 signalling has an effect on the development of liver fibrosis through YAP activity.

2. Aims of the study

Liver fibrosis is characterised as the activation and conversion of HSCs. YAP signalling has been reported to promote the transcription of genes related to HSC activation and matrix remodelling, contributing to fibrosis development (Mannaerts et al., 2015). The neuropeptide CGRP, secreted by the hepatic sensory nerves, binds to its receptor complex, which consists of CRLR and RAMP1, together signalling via different G α proteins (Dickerson, 2013). G α protein families were found to have different effects on YAP activity (Yu et al., 2012). However, how CGRP/RAMP1 signalling regulates YAP and promotes liver fibrosis remains unclear.

Our previous *in vivo* study has demonstrated that CGRP/RAMP1 signalling promotes hepatocyte proliferation via YAP activity (Laschinger et al., 2020). Additionally, the *in vitro* data illustrated the positive effect of CGRP stimulation on YAP activation in primary human hepatocytes. Therefore, we aimed to investigate the role of CGRP/RAMP1 signalling in the development of liver fibrosis controlled by YAP.

The aims of the study are summarised as follows:

- Explore the effect of CGRP/RAMP1 signalling on the activation of HSCs and the development of liver fibrosis.
- Examine the impact of CGRP/RAMP1 signalling on hepatocyte proliferation upon CCl₄-induced liver injury.
- Investigate whether CGRP/RAMP1 is able to control YAP activity in hepatic stellate cells during liver fibrosis.

3. Materials and methods

3.1 Materials

3.1.1 Chemicals and reagents

Chemicals and reagents	Company
2-Mercaptoethanol C ₂ H ₆ OS	Sigma-Aldrich, Germany
4',6-Diamidino-2-phenylindole (DAPI)	Sigma-Aldrich, Germany
Acrylamide Solution	Carl ROTH, Germany
Agarose	Carl ROTH, Germany
Albumin from bovine serum(BSA)	Sigma-Aldrich, Germany
Ammonium Persulphate (APS)	Sigma-Aldrich, Germany
CGRP	Sigma-Aldrich, Germany
DAB System	Dako, USA
DAPI	Thermo Fisher, USA
D(+)-Glucose C ₆ H ₁₂ O ₆	Sigma-Aldrich, Germany
Dimethyl sulphoxide (DMSO) C ₂ H ₆ OS	Sigma-Aldrich, Germany
DirectPCR Lysis Reagent Tail	PEQLAB, Germany
dNTP Set (10mM)	Thermo Scientific, USA
ECL detection reagent	Amersham, USA
Ethanol 70%, 96%, 100%	Carl ROTH, Germany
Ethylenediaminetetraacetic acid (EDTA)	Sigma-Aldrich, Germany
FBS Superior (FCS)	Biochrom, Germany
Fibronectin	Carl ROTH, Germany
Glycine C ₃ H ₈ O ₃	Carl ROTH, Germany
Haematoxylin	Merck, Germany
HEPES (4-(2-hydroxyethyl)-1-piperazineethanesulphonic acid)	Sigma-Aldrich, Germany
Hydrochloric acid HCl	Carl ROTH, Germany
Hydrogen Peroxide (30%)	Carl ROTH, Germany
Magnesium chloride MgCl ₂	Sigma-Aldrich, Germany
Magnesium sulphate MgSO ₄	Sigma-Aldrich, Germany

Medium DMEM (1X)	Gibco, USA
Methanol	Merck, Germany
Milk Powder (Blotting-Grade)	Carl ROTH, Germany
Mounting Medium	Dako, Agilent Technologies, USA
N,N,N',N'-tetramethylethylenediamine (TEMED)	Bio-RAD, USA
Oligo(dT)18 Primer	Thermo Scientific, USA
Page Ruler Pre-stained Protein Ladder	Thermo Scientific, USA
Paraformaldehyde (PFA)	Sigma-Aldrich, Germany
Penicillin/Streptomycin (Pen/Strep)	Biochrom, Germany
Phenol:Chloroform:Isoamyl Alcohol 25:24:1	Sigma-Aldrich, Germany
Phosphate Buffered Saline (PBS)	Biochrom, Germany
Potassium chloride KCl	Merck, Germany
Proteinase K	Carl ROTH, Germany
Random Hexamer Primer	Thermo Fisher Scientific, USA
Recombinant Human HGF	R&D Systems, USA
RevertAid H Minus Reverse Transcriptase	Thermo Fisher Scientific, USA
RiboLock RNase Inhibitor	Thermo Fisher Scientific, USA
RNA free water	Thermo Fisher Scientific, USA
Roticlear	Carl ROTH, Germany
RT-Buffer (M-MuIV RT, 5x)	Thermo Fisher Scientific, USA
Sirius Red Solution	Sigma-Aldrich, Germany
Sodium chloride NaCl	Carl ROTH, Germany
Sodium dodecyl sulphate (SDS) Pellets	Carl ROTH, Germany
Sodium hydroxide NaOH	Merck, Germany
Sodium phosphate dibasic Na ₂ HPO ₄	Sigma-Aldrich, Germany
β-Mercaptoethanol	Merck, Germany
TEMED	Carl ROTH, Germany
TRI Reagent	Sigma-Aldrich, Germany
Tris Base	Merck, Germany
Tris(triphenylphosphine)rhodium(I) chloride (Tris-CI)	Sigma-Aldrich, Germany

Triton X-100	Carl ROTH. Germany
Trypsin-EDTA (1X)	PAA Laboratories, Austria
Tween 20	Carl ROTH. Germany

3.1.2 Buffers and solutions

1x SDS lysis Buffer

Glycerol	7.5ml
10% SDS	15ml
0.5 M Tris-HCl pH 6.8	6.25ml
0.5% Bromophenol Blue	1ml
14.3 M β -mercaptoethanol	2.5ml
Fill up with ddH ₂ O to	50ml

5x Loading Buffer

Trisma base	150g
Glycine	720g
SDS	25g
Fill up with ddH ₂ O to	5L

10x Transblot Buffer

Trisma base	58.15g
Glycine	29.28g
Fill up with ddH ₂ O to	1000ml

10x Phosphate Buffered Saline (PBS)

Phosphate Buffered Saline	95.5g
Fill up with ddH ₂ O to	1000ml

10x Tris Buffered Saline (TBS)

Trisma base	12.1g
NaCl	85g
ddH ₂ O	800ml
Adjust pH to 7.4 with	5M HCl
Fill up with ddH ₂ O to	1000ml

20x Citrate Buffer

Citric acid (Monohydrate)	21g
ddH ₂ O	300ml
Adjust pH to 6.0 with	5M NaOH
Fill up with ddH ₂ O to	500ml

TBSA

10xTBS	100ml
BSA	1g
Fill up with ddH ₂ O to	1000ml

TBST

10xTBS	100ml
Tween 20	1ml
Fill up with ddH ₂ O to	1000ml

3.1.3 Antibodies

Primary antibodies	Concentration	Reference	Company
β-Actin	1:2000	8457	Sigma-Aldrich, Germany
β-Tubulin	1:2000	ab6046	Abcam, Germany

CDK1	1:1000	ab32384, Clone #E161	Abcam, Germany
Collagen, Type I	1:1000	84336	Cell Signalling, Germany
p-CREB	1:1000	9198	Cell Signalling, Germany
Cyclin A2	1:1000	ab181591, Clone #EPR17351	Abcam, Germany
Cyclin B1	1:1000	4138	Cell Signalling, Germany
GAPDH	1:5000	5174	Cell Signalling, Germany
Ki67	1:600	550609, Clone #B56	BD, Germany
p-LATS	1:1000	8654	Cell Signalling, Germany
p-MOB1	1:1000	8699	Cell Signalling, Germany
p-YAP (Ser127)	1:1000	13008	Cell Signalling, Germany
p-YAP (Ser397)	1:1000	13619	Cell Signalling, Germany
SMA (alpha-smooth Muscle actin)	1:1000	ab5694	Abcam, Germany
uPA	1:500	NBP2-66766, Clone #JM106-09	Novus, Germany
YAP	1:1000	14074	Cell Signalling, Germany

Secondary antibodies	Concentration	Reference	Company
Peroxidase-AffiniPure Goat Anti-Mouse IgG (H+L)	1:2000	A32723	Thermo Scientific, Germany
Peroxidase-AffiniPure Goat Anti-Rabbit IgG (H+L)	1:4000	111-035-144	Jackson
Goat anti-Rabbit IgG (H+L) Alexa Fluor 488	1:200	A11008	Thermo Scientific, Germany
Cy3 AffiniPure Goat Anti-Mouse IgG (H+L)	1:200	115-165-003	Jackson

3.1.4 Primers

The following primers were retrieved from Metabion International AG, Germany.

Primer	Sequence
Acta2 fwd	ctctctccagccatcttcat

Acta2 rev	tataggtggttcgtggatgc
Ankrd1 fwd	gctggagcccagattgaa
Ankrd1 rev	ctccacgacatgcccagt
Birc5 fwd	tgatttgcccagtgTTTT
Birc5 rev	caggggagtgcttctatgc
Calca fwd	tgaggactatatgcagatgaaa
Calca rev	ggatctctctgagcagtgaca
Calcb fwd	cctgcaggcctgagtcac
Calcb rev	ggcatggtgagtcaactttatg
Ccnb1 fwd	gcttagcgctgaaaattcttg
Ccnb1 rev	tcttagccaggtgctgcata
Ccne1 fwd	tttctgcagcgtcatcctc
Ccne1 rev	tggagcttatagacttcgcaca
CDK1 fwd	ggacctcaagaagtacctggac
CDK1 rev	ccctggaggatttggtgaag
Col1a1 fwd	agacatgttcagcttggagac
Col1a1 rev	gcagctgactcagggatg
Col1a2 fwd	caagcatgtctggtaggagag
Col1a2 rev	aggacacccctctacgttg
Crlr fwd	gccaataaccaggccttagtg
Crlr rev	gcccacaggtagagatgga
CTGF fwd	tgacctggaggaaaacattaaga
CTGF rev	agccctgtatgtcttcacactg
Cyclin D1 fwd	tcttccagagtcacaaagtgtg
Cyclin D1 rev	gactccagaagggcttcaatc
Foxm1 fwd	agctaagggtgtgctgttc
Foxm1 rev	ctgtgtccagcgtgcag
hGNA11 fwd	catggagacgctcaagatcc
hGNA11 rev	cgactgatgctcgaaggtg
hGNA12 fwd	ctcgtcacttcaaaccagaag

hGNA12 rev	gagttaaacggacccccacaa
hGNA13 fwd	tcaaattgaggctgttaggg
hGNA13 rev	catttctggtattaaggcgatctt
hGNAQ fwd	ttcagccatagcttgattgc
hGNAQ rev	aaaggactcctgtgtctttga
hGNAS fwd	ccgtccagattctcctgtt
hGNAS rev	tctgcttcacaatggtgctt
hRAMP1 fwd	gtgtgactggggcaggac
hRAMP1 rev	ctgaagtagcggccatgc
mCalcr fwd	tctcaacaccaagtcagga
mCalcr rev	gcaccttccaaccaagagt
mGNA11 fwd	cactggcatcatcgagtacc
mGNA11 rev	gatccacttctcgctct
mGNA12 fwd	gataactggaccggattgg
mGNA12 rev	cttggtggccttctagcc
mGNA13 fwd	ggtaccccagagtggcttg
mGNA13 rev	tctctgcagttgggaagttg
mGNAQ fwd	gactactcccagaatatgatggac
mGNAQ rev	tcaggatgaattctcgagctg
mGNAS fwd	tggaggaggagaagatggacta
mGNAS rev	gctcggcaccacttttctc
Plau fwd	gccttggtggtgaaaaactc
Plau rev	cacgcatacacctccgttc
TGF-beta1 fwd	ccttctgctcctcatgg
TGF-beta1 rev	cgcacacagcagttcttctc
TGF-beta2 fwd	aggaggttataaaatcgacatgc
TGF-beta2 rev	tagaaagtgggcgggatg
IL-33 fwd	cacattgagcatccaaggaa
IL-33 rev	aacagattggtcattgtatgtactcag

3.1.5 Technical devices

Technical device	Company
7300 Real-Time PCR System	Applied Biosystems, Germany
Autoclave Systec	Systec, Germany
Automated Microtome	Leica, Germany
Automated Vacuum Tissue Processor	Leica, Germany
Axio Observer Z1 Microscope	Zeiss, Germany
Axiovert 100	Zeiss, Germany
Biometra Fastblot	Analytik-tik-jena, Germany
Bioruptor Ultrasonic device	Diagenode, Belgium
Centrifuge	Eppendorf, Germany
Corning Stripettor Plus Pipetting Controller for 2-25ml pipettes	Corning, USA
Glass ware (Beaker glass, Erlenmeyer flask, graduated cylinder)	Schott Duran, Germany
Heating Block	Kleinfeld Labortechnik, Germany
Ice Maker	Ziega, Germany
LightCycler 480 II	Roche, Germany
Microplate Reader	Berthold Technologies, Germany
Microplate Washer	Tecan, Switzerland
Microwave Oven	Siemens, Germany
Mixing Rotor Variospeed Variotim	Renner, Germany
Multifuge 3S-R (for Falcons and Plates)	Heraeus Kendro, Germany
NanoDrop 1000 Spectrophotometer	Thermo Scientific, USA
Optimax X-Ray Film Processor (Developing machine for Western Blot films)	Protec, Germany
PH Level I (pH-meter)	WTW inoLab, Germany
Purelab (for ddH ₂ O)	Elga, UK
Sterilgard Hood	Thermo Scientific, USA
Tissue Embedder	Leica, Germany
Trans-Blot SD Semi Dry Transfer Cell	Bio-Rad, USA
Vortex-Genie 2	Scientific Industries, USA

3.1.6 Cell line

Cell line	Reference	Company
LX-2	SCC064	EMD Millipore Corporation, USA

3.1.7 Kits

Kit	Company
ALT Elisa Kit	Cloud-Clone Corp, USA
BCA Protein Assay Kit	Thermo Scientific, USA
LightCycler 480 Probes Master	Roche, Germany
QuantiTect Reverse Transcription Kit	Qiagen, Germany
RNeasy Mini Kit	Qiagen, Germany
Universal Probe Library Set	Sigma-Aldrich, Germany

3.2 Methods

3.2.1 RAMP1^{-/-} mouse model

The generation of RAMP1^{-/-} mice has been described in previous studies (Tsujikawa et al., 2007). RAMP1-deficient mice backcrossed to the C57BL/6N background for at least ten generations were bred and housed in a specified pathogen-free facility (Charles River, Calco, Italy). C57BL/6N wild type control mice were obtained from the same laboratory. All animal experiments were approved by the government of Upper Bavaria (licenses 55.2-2532.Vet_02-15-125), and were performed in accordance with Federal Animal Regulations and under institutional guidelines.

3.2.2 Induction of liver fibrosis by injection of carbon tetrachloride

In order to induce chronic liver injury, the toxin carbon tetrachloride (CCl₄) was used, which causes hepatocyte damage, necrosis, inflammation and fibrosis. When injected intraperitoneally, it infiltrates into the vascular structures and drain the liver sinusoid

(Alatsakis et al., 2009). Continuous administration of CCl₄ can induce liver fibrosis between 36 hours to 18 weeks (Cheung et al., 2006; Peng et al., 2005).

In the present study, male mice aged 10-12 weeks were subjected to the biweekly injections of CCl₄ (0.5 µl/g body weight, intraperitoneally; diluted in corn oil 1:7; Merck, Darmstadt, Germany) for 4 weeks. Animals were sacrificed 72 h after the last injection. Blood was obtained by cardiac puncture, and then centrifuged at 8000rpm (3200g) for 8 min to get the supernatant of serum before being stored at -80°C for further analysis. Liver and spleen tissues were weighed, and then fixed in 4% paraformaldehyde as well as frozen in liquid nitrogen, stored at -80°C for further analysis.

3.2.3 Generation of formalin-fixed paraffin-embedded sections

Liver tissues were fixed in 4% paraformaldehyde at room temperature for one week, followed by dehydration in the automated vacuum tissue processor (Leica, Germany) of a graded ethanol series, and embedded in paraffin with the tissue embedder (Leica, Germany). The paraffin embedded tissues were cut with the automated microtome (Leica, Germany) to generate 2.5 µm tissue sections.

3.2.4 Immunohistochemistry

In order to detect specific cells or proteins within the liver parenchyma, indirect immunohistochemistry was used.

1. Paraffin embedded tissue sections were deparaffinised in 3 cycles of Roticlear for 10 min each, then sections were rehydrated using a descending ethanol series (100%, 100%, 100%, 96%, 70%, 50%, 3 min each), and were put in dH₂O for 3 min.
2. Antigen retrieval was performed to unmask the antigenic epitope. The slides were arranged in a staining container with 1x citrate buffer (pH 6.0), and incubated in a 600W microwave oven for 15 min. Then, the slides were cooled for 20-30 min at room temperature.
3. The slides were rinsed once in TBSA for 5 min and incubated in 3% peroxidase diluted with absolute methanol for 10 min in the dark to inactivate horseradish peroxidase. The slides were then rinsed three times in TBSA, 5 min each.
4. The unspecific binding of secondary antibodies was blocked by incubation tissue

sections with 10% goat serum for 1 h at room temperature.

5. The primary antibodies (listed in the table 3.1.3) were diluted to the final concentrations in PBS, added to the slides, and incubated overnight at 4°C in a humid chamber.
6. The slides were rinsed three times in TBSA, and incubated with HRP-conjugated secondary antibody for 1 h at room temperature in a humid chamber.
7. The slides were rinsed three times in TBSA. Then, a DAB substrate solution (0.5 mg DAB/ 1ml PBS; Dako, USA) was applied to the slides to reveal the colour of the antibody staining. The reaction was terminated by water when the desired colour intensity was reached.
8. The slides were counterstained with haematoxylin for 10-30 sec and rinsed under running tap water for more than 15 min.
9. The slides was dehydrated through an ascending ethanol series (50%, 70%, 96%, 100%, 100%, 100%, 3 min each) and cleared in 3 changes of Roticlear for 10 min each.
10. The slides were mounted using mounting solution (VectaMount Mounting Medium, Vectorlabs, USA).
11. Images were acquired using an Axiolab attached to an AxioCamMRc5 camera, an Achromplan 20x/0.45 NA objective and the AxioVision software (all Zeiss Microscopy). For quantification, five random high-power fields for each tissue were counted using the Zen 3.0 software (Zeiss, Germany).

3.2.5 Sirius Red staining

To detect the collagen deposition in the liver tissue, Sirius Red staining was used.

1. The paraffin sections were deparaffinised in 3 times of Roticlear for 10 min each, then arranged in a descending ethanol series (100%, 100%, 100%, 96%, 70%, 50%, 3 min each), and were put in dH₂O for 3 min.
2. The slides were applied with the Sirius Red solution (Sigma-Aldrich) for 1 h.
3. The slides were rinsed with 5% acetic acid for 3 times (4 min, 14 min and 17 min respectively).
4. The slides were dehydrated through the 100% ethanol series for 3 times, and cleared once in Roticlear for 10 min.
5. The slides were mounted using mounting solution (VectaMount Mounting Medium,

Vectorlabs, USA).

6. Images were acquired using an Axiolab attached to an AxioCamMRc5 camera, an EC Plan-NEOFLUAR 10x/0.3 NA objective and the AxioVision software (all Zeiss Microscopy).
7. The collagen deposition areas were quantified by ImageJ v1.51 (National Institutes of Health, USA).

3.2.6 Immunofluorescence staining

To reveal the location of specific proteins within the liver parenchyma, indirect immunofluorescence was used.

1. Paraffin embedded tissue sections were deparaffinised in 3 changes of Roticlear for 10 min each, then put through a descending ethanol series (100%, 100%, 100%, 96%, 70%, 50%, 3 min each), and placed in dH₂O for 3 min.
2. Antigen retrieval was performed to unmask the antigenic epitope. The slides were arranged in a staining container with 1x citrate buffer (pH 6.0), and incubated in a 600W microwave oven for 15 min. Then, the slides were cooled for 20-30 min at room temperature.
3. Unspecific binding of secondary antibodies was blocked by incubation tissue sections with 10% goat serum for 1 h at room temperature.
4. The primary antibodies were diluted to the recommended concentrations in PBS, added to the slides, and incubated overnight at 4°C in a humid chamber.
5. The slides were rinsed three times with TBSA, and incubated with the secondary antibody for 1 h at room temperature in a humid chamber.
6. The slides were rinsed three times with TBSA, incubated with DAPI for 2 min, and then rinsed with TBSA once. DAPI has a high binding affinity for DNA and therefore was used to stain nuclei.
7. The slides were mounted using mounting solution (Prolong Gold anti-fade reagent, Invitrogen, USA), and were placed flat in the dark until further analysis.
8. Images were acquired using a Zeiss Axio Observer Z1 microscope attached to an AxioCamMRm camera, an EC Plan-NEOFLUAR 40x/0.75 NA objective and the Zen 3.0 software (all Zeiss Microscopy).

3.2.7 Isolation of RNA using Qiagen RNeasy kit

To test the expression of specific genes in tissues or cells on mRNA level, RNA was extracted.

From liver tissues:

1. 750µl of TRI Reagent was added to approximately 30mg tissue in a 2ml safelock Eppendorf tube on ice to disrupt and break down cells and cell components.
2. Tissue was lysed using Tissue Lyser II with metal beads, 30 1/min, -20°C, 3 min.
3. 200µl Phenol:Chloroform:Isoamyl Alcohol (25:24:1) was added to each sample, mixed by vortex to promote phase separation so that RNA was isolated from DNA and protein.
4. Centrifuged for 10 min, 14000rpm (9800g), 4°C. After centrifuging, 3 layers were separated.
5. The top clear supernatant phase (containing the RNA) was transferred into a new collection tube.
6. To precipitate nucleic acids, 350µl 70% ethanol was added to the tube, mixed by pipetting up and down.
7. All of the mixture was transferred into the Qiagen RNA tubes (pink), and centrifuged 1000rpm (5000g) for 30 sec, before the flow-through was discarded.
8. 350µl Buffer RW1 was added to remove biomolecules that were non-specifically bound to the silica membrane of column, centrifuged for 30 sec, 10000rpm (5000g), before the flow-through was discarded.
9. 10µl DNase (prepared in 70µl Buffer RDD) was added, and incubated for 15 min at room temperature to digest endogenous DNA that might affect the qRT-PCR analysis.
10. 350µl Buffer RW1 was added, centrifuged for 30 sec, 10000rpm (5000g), and then the flow-through was discarded.
11. 500µl Buffer RPE was added to remove traces of salts which were still on the column due to the buffers used earlier, centrifuged for 30 sec, 10000rpm (5000g), and then the flow-through was discarded.
12. The sample was centrifuged for 1 min at full speed (14000rpm, 9800g) to dry the spin column.
13. The spin column was placed in a new 1.5ml collection tube and 30-50µl RNase free water was added, centrifuged for 1 min at 10000rpm (5000g) to elute the RNA.
14. The RNA concentration was measured by NanoDrop and the RNA was stored at -80°C.

From cultured cells:

1. A maximum of 1×10^7 cells were harvested, and resuspended in 350 μ l-600 μ l of Buffer RLT.
2. 350 μ l 70% ethanol was added to the tube to precipitate out nucleic acids, and then mixed by pipetting up and down.
3. All of the mixture was transferred into the Qiagen RNA tubes (pink), centrifuged 1000rpm (5000g) for 30 sec, then the flow-through was discarded.
4. 350 μ l Buffer RW1 was added to remove biomolecules that were non-specifically bound to the silica membrane of column, centrifuged for 30 sec, 10000rpm (5000g), and then the flow-through was discarded.
5. 10 μ l DNase (prepared in 70 μ l Buffer RDD) was added, placed on the bench for 15 min at room temperature to digest endogenous DNA that might affect the qRT-PCR analysis.
6. 350 μ l Buffer RW1 was added, centrifuged for 30 sec, 10000rpm (5000g), and then the flow-through was discarded.
7. 500 μ l Buffer RPE was added to remove traces of salts which were still on the column due to the buffers used earlier, centrifuged for 30 sec, 10000rpm (5000g), after which the flow-through was discarded.
8. The sample was centrifuged for 1 min at full speed (14000rpm, 9800g) to dry the spin column.
9. The spin column was placed in a new 1.5ml collection tube and 30-50 μ l RNase free water was added, and then centrifuged for 1 min at 10000rpm (5000g) to elute the RNA.
10. The RNA concentration was measured by NanoDrop and the RNA was stored at -80°C.

3.2.8 Complementary DNA reverse transcription

To indirectly test the mRNA expression of genes, complementary DNA reverse transcription was used.

1. 1 μ g of RNA was added with RNase free water to a total volume of 10 μ l.
2. 0.5 μ l of Random primer (1:150), 0.5 μ l of Oligo dt primer (1:20) and 2.5 μ l of RNase free water were added to prime single-stranded RNA for extension by reverse

transcriptase.

3. The sample was incubated for 10 min at 70°C, placed on ice and centrifuged briefly.
4. 4µl of 5x RT Buffer, 1µl of dNTPs, 0.5µl of RNasin and 1µl of RevertAid reverse transcriptase were added to provide nucleotides to the unzipped strand using the template of the single side.
5. The sample was incubated for 10 min at room temperature.
6. The sample was incubated for 60 min at 42°C.
7. The sample was incubated for 5 min at 95°C. The cDNA was stored at -20°C.

3.2.9 Quantitative real-time PCR (qRT-PCR)

To detect the cDNA expression, and thus reveal the mRNA level, quantitative real-time PCR was used.

The cDNA was diluted 1:5 with the RNase free water for use. The expression of genes was determined by qPCR using the LightCycler 480 II system (Roche) and corresponding universal probe library (UPL) probes. The expression of β actin was used for normalisation.

The qPCR setup was made as follows in 96-well plates:

Component	Volume per well
Mastermix	10µl
Forward primer (20µM)	0.2µl
Reverse primer (20µM)	0.2µl
UPL probe	0.2µl
Diluted cDNA	5µl
ddH ₂ O	4.4µl
Total	20µl

The qPCR program “monocolour hydrolysis probe UPL” was used according to the manufacture’s protocol. The data was analysed using the LightCycler 480 v1.5 software.

3.2.10 Cell culture and passaging

The LX-2 cell line is a human hepatic stellate cell line, generated by spontaneous immortalisation in low serum conditions (Xu et al., 2005). According to the protocol, LX-2 cells were maintained at 37°C, 7% CO₂, 95% humidity in Dulbecco's Modified Eagle Medium (DMEM) containing 100U/ml Penicillin, 2mM 2-Mercaptoethanol, 2mM L-glutamine and 7% foetal calf serum (FCS) in flasks (T75). In order to propagate LX-2, cells were grown to confluence, washed once with PBS and incubated in Trypsin for 3-5 min at 37°C. Medium containing 7% FCS was added to stop the digestion process, and cells were collected in 15ml Falcon tubes. The cells were centrifuged for 4 min at 1400rpm (500g). The supernatant was discarded, and the resuspended LX-2 cells were placed on new plates with culture medium. To quantify and seed a certain number of cells, the resuspended cells were counted using a 0.0025 mm² glass counting chamber (Marienfeld, Germany) with the Zeiss Invertoskop ID 03 Inverted & phase contrast microscope with a 10x/0.22 NA objective.

3.2.11 Cell freezing

For the long-term storage of LX-2 cells, they were trypsinised as described above. The received cell pellet was resuspended in DMEM (50% FCS, 10% DMSO) and immediately placed into a cryovial. In order to allow for the controlled freezing of cells with a temperature decrease of 1°C /min, the cryovial was placed in a cryo freezing container (Nunc Nalgene, USA) for 48 hours at -80°C. The cryovial was then transferred into the liquid nitrogen.

3.2.12 Cell thawing

To avoid damage to cells caused by DMSO, cells were quickly defrosted in a 37°C water bath. Then the cells in the cryovial were transferred to a 15ml Falcon tube prepared with 10ml medium containing 7% FCS, and centrifuged for 4 min at 1400rpm (500g). The cell pellet was resuspended in DMEM containing 100U/ml Penicillin, 2mM 2-Mercaptoethanol, 2 mM L-glutamine and 7% FCS, and cultured as described before (3.2.10).

3.2.13 Migration assay

To explore whether the migration of LX-2 cells could be affected by specific stimulation, the migration assay was used.

A total of 1.5×10^5 cells in 90 μ l DMEM with 1% FCS were seeded into both separated chambers of the Culture-Insert 2 Well in a 35 mm μ -Dish (IBIDI, Germany), which was pre-coated with 5 μ g/ml fibronectin for 1 hour at 37°C. After the cells were attached in the medium containing 1% FCS overnight, the silicon insert was removed to generate a gap of exactly 500 μ m. Cells were cultivated for up to 24h in the medium without FCS. During the time period, most cells migrated towards the generated gap. Choosing this time period prevented closure of the generated gap solely by the proliferation of LX-2 cells. In addition, cells could survive while not proliferating with 1% FCS. The images were taken by the Axio Observer Z1 microscope with an A-Plan 10x/0.25 NA objective at the time-points of 0 h, 14 h, 18 h and 22 h. Migration was measured in relation to the cell-free area at 0 hour time-points using ImageJ v1.51 (National Institute of Health, USA). The migration area was calculated as the percentage relative to the 0 h time-point.

3.2.14 *In vitro* stimulation of cells

To investigate the influence of the neuropeptide calcitonin gene-related peptide (CGRP) on cell activation and the expression of yes-associated protein (YAP) in hepatic stellate cells (HSCs), HSCs were stimulated with CGRP *in vitro*.

For LX-2 cells:

1. Analysis of α -SMA and Collagen expression: LX-2 cells were grown to confluence. Cells were trypsinised and 150,000 cells per well of a 6-well plate were placed in DMEM, 7% FCS, 100U/ml Penicillin, 2mM 2-Mercaptoethanol and 2mM L-glutamine. LX-2 cells were cultivated for 24 hours, followed by stimulation with CGRP (100nM) for 1, 2, 3 and 6 hours, respectively. Proteins or RNA were isolated from stimulated LX-2 cells as described in Methods 3.2.7 and 3.2.15.
2. Analysis of YAP expression: LX-2 cells were seeded as described above. The cells were cultivated in DMEM containing 7% FCS, 100U/ml Penicillin, 2mM 2-Mercaptoethanol and 2mM L-glutamine for 24 hours, followed by serum starvation in 0% FCS DMEM for another 24 hours. Then LX-2 cells were stimulated with CGRP

(100nM) for 1, 2, 3 and 6 hours, respectively. Proteins or RNA were isolated from stimulated LX-2 cells as described in Methods 3.2.7 and 3.2.15.

For human primary hepatic stellate cells:

Human primary HSCs were obtained from our cooperation partner from the Department of Medicine II, University Hospital, Ludwig-Maximilians-University of Munich (Germany). Human liver tissue for HSC isolation was provided by the Biobank under institutional guidelines of the Human Tissue and Cell Research (HTCR, LMU). HTCR obtained signed informed consent from all donors before the use of liver tissues. The use of HSCs from human liver tissues for the present study was approved by the ethics committee of the Faculty of Medicine of the Ludwig-Maximilians-University of Munich (Project ID: 17-619). The study procedure followed the guidelines of the 1975 Declaration of Helsinki.

1. Isolation of human primary HSCs: A suspension of liver cells was prepared using the technique of tissue perfusion and collagen digestion, as described previously (Lee et al., 2017). Hepatocytes were removed by nylon mesh and multiple cycles of low speed centrifugation (50g). Following this procedure, the supernatant contained only non-parenchymal cells. Human primary HSCs were further purified from the supernatant by centrifugation using a discontinuous Percoll density gradient. Isolated HSCs were washed twice and maintained at 37°C, 7% CO₂, 95% humidity in Iscove's Modified Dulbecco's Medium (IMDM) containing 100U/ml Penicillin, 100µg/mL streptomycin, 4mM L-glutamine and 10% FCS in 6-well plates (40,000 cells per well).
2. Analysis of YAP expression: Isolated human primary HSCs were cultivated for 2 days, and starved with 0% FCS IMDM for 40 hours. Then human primary HSCs were stimulated with CGRP (100nM) for 3 hours. Proteins were isolated from stimulated HSCs, as described in Methods 3.2.7.

3.2.15 Isolation of protein

To investigate the expression of certain proteins in the liver tissues, protein was isolated.

From liver tissues:

1. 600µl of a lysis buffer containing 0.1% SDS, 1% Triton X100, 150 mM NaCl, 20 mM

TrisHCl pH 7.5, protease/phosphatase inhibitors and 1 mM β -glycerophosphate were added to approximately 30mg tissue in a 2ml safelock Eppendorf tube on ice.

2. Tissue was lysed using Tissue Lyser II with metal beads, 30 1/min, -20°C, 3 min.
3. The sample was transferred for sonification for 5min.
4. The sample was put on ice and centrifuged briefly.
5. The sample was transferred to a new safelock Eppendorf tube.
6. The sample was heated for 5 min at 95°C, and stored at -20°C.

From cultured cells:

1. After cell stimulation, the media was discarded.
2. Cells were washed with PBS, and lysed in a lysis buffer of 320 μ l containing 0.1% SDS, 1% Triton X100, 150 mM NaCl, 20 mM TrisHCl pH 7.5, protease/phosphatase inhibitors and 1 mM β -glycerophosphate in a 1.5ml safelock Eppendorf tube on ice.
3. The sample was transferred for sonification for 5 min.
4. The sample was heated for 5 min at 95°C, and stored at 20°C.

3.2.16 Detection of protein by Western Blotting

SDS-polyacrylamide gel electrophoresis

1. The protein samples were boiled for 3 min at 70°C. The resolving and stacking gels were made and filled with the running buffer.
2. 5 μ l of the Page ruler and 10-20 μ l of each sample were loaded in the columns of stacking gel. The run was started at 70V and run until the samples reached the resolving gel.
3. The voltage was increased to 120V until the marker reached the bottom.

Transfer the gel to the membrane

4. The gel was transferred into a chamber filled with transblot buffer, and then put onto the Biometra Fastblot together with three layers of thick Whatman paper, a nitrocellulose blotting membrane and another three layers of thin Whatman paper.
5. The gel was transferred for 1 h at 300-400 mA.

Incubation of antibodies

6. To avoid the non-specific binding of antibodies to the membrane, the membrane was

blocked with 5% milk for 1 h at room temperature.

7. The membrane was washed once with TBST, and was incubated with the primary antibody on the shaker at 4°C overnight.
8. The membrane was washed three times with TBST, and was incubated with the secondary antibody on the shaker for 1 h at room temperature. Then the membrane was washed three times with TBST.

Detection of proteins

9. The membrane was incubated with the mixture of Detection Reagent 1 and 2 (1:1) for 2min.
10. Proteins were visualized using the chemiluminescent detection with an imaging system (Analytik Jena).
11. The relative protein expression was analysed using ImageJ v1.51 (National Institute of Health, USA).

3.2.17 ELISA for alanine aminotransferase (ALT)

To detect the amount of the alanine aminotransferase (ALT) in the serum of mice, the technique of ELISA was used. Blood was collected from male WT and RAMP1^{-/-} mice when they were sacrificed. Serum samples were acquired as described in chapter 3.2.1 and ALT activity was detected using the ELISA Kit SEA207Mu (Cloud-Clone Corp, USA) according to the manufacturer's protocol.

1. The wells were prepared for diluted standard (7 wells, for standard curve construction), blank (1 well) and samples. 100µL of each dilution was added to the determined wells pre-coated with a biotin-conjugated antibody specific to ALT. The plate was covered with the sealer and incubated for 1 hour at 37°C.
2. The samples were removed from the wells. 100µL of Detection Reagent A solution (Avidin conjugated to Horseradish Peroxidase) was added to each well. The plate was covered and incubated for 1 h at 37°C.
3. Detection Reagent A solution was removed from the plate, and then the wells were washed with 350µL of Wash Solution by the Microplate Washer (Tecan, Switzerland) three times.
4. 100µL of Detection Reagent B solution was added to each well. The plate was covered and incubated for 30 min at 37°C.

5. The wash procedure in step 3 was repeat five times in total.
6. 90 μ L of Substrate Solution (tetramethylbenzidine substrate) was added to each well. The plate was covered and incubated for 20 min at 37°C. The plate was protected from light. Upon reaction, the blue colour of liquid was observed. Only those wells that contain ALT exhibited a change in colour.
7. 50 μ L of Stop Solution (sulphuric acid) was added to each well and the liquid was mixed by tapping the side of the plate gently. The yellow colour of the liquid was observed upon the addition.
8. The bottom of the plate was cleaned in case there was any drop of water or fingerprint which could cause issues. The plate was loaded onto the Microplate Reader (Berthold Technologies, Germany) and immediately measured at 450nm.
9. A standard curve was constructed by plotting the mean O.D. and concentration for each standard and drawing a best fit curve through the points on the graph with ALT concentration on the y-axis and absorbance on the x-axis. Then, the value of each sample was calculated according to the standard curve.

3.3 Statistics

The generation of graphs and statistical analysis was performed using GraphPad Prism 7.0 (GraphPad Software, San Diego, USA). The standard deviation was represented by error bars. Statistical differences were analysed using the two-tailed unpaired Student's t-test or the Mann-Whitney test. The difference was considered significant for a p value less than 0.05. Statistical significant differences were marked as follows: * $p \leq 0.05$, ** $p \leq 0.01$, *** $p \leq 0.001$, **** $p \leq 0.0001$.

4. Results

4.1 Induction of CGRP and RAMP1 upon chronic liver injury

In the liver, neurons containing the calcitonin gene-related peptide (CGRP) form a network in the biliary system, the portal region and the deep parenchyma. There are two isoforms of CGRP, named α CGRP and β CGRP. α CGRP is distributed in the central and peripheral system, while β CGRP is in the enteric nervous system (Russell et al., 2014). Clinical studies showed that plasma CGRP levels were significantly increased in the liver of cirrhotic patients compared with normal patients (Bendtsen et al., 1991). This leads to the question of whether CGRP has an effect on the development of liver fibrosis.

To investigate the role of CGRP in liver fibrosis, we used the mouse model of intraperitoneal carbon tetrachloride (CCl_4) injections, which induces necrosis and inflammation within the liver. The biweekly injection of CCl_4 for 4 week leads to chronic liver injury and induces liver fibrosis. In order to find out whether the components of the CGRP signalling pathway are differentially expressed during liver fibrosis, we applied qRT-PCR to quantify the RNA expression of CGRP and its co-receptor, the receptor activity modifying protein 1 (RAMP1). Four weeks after CCl_4 injection, it appeared that the expression of *Calca* (α CGRP) and *Ramp1* (RAMP1) was highly induced in the liver, whereas *Calcb* (β CGRP) and *Crlr* (CRLR) expression did not increase (Figure 6). These results demonstrate that expression of the CGRP signalling components CGRP and RAMP1 was induced during liver fibrosis in mice.

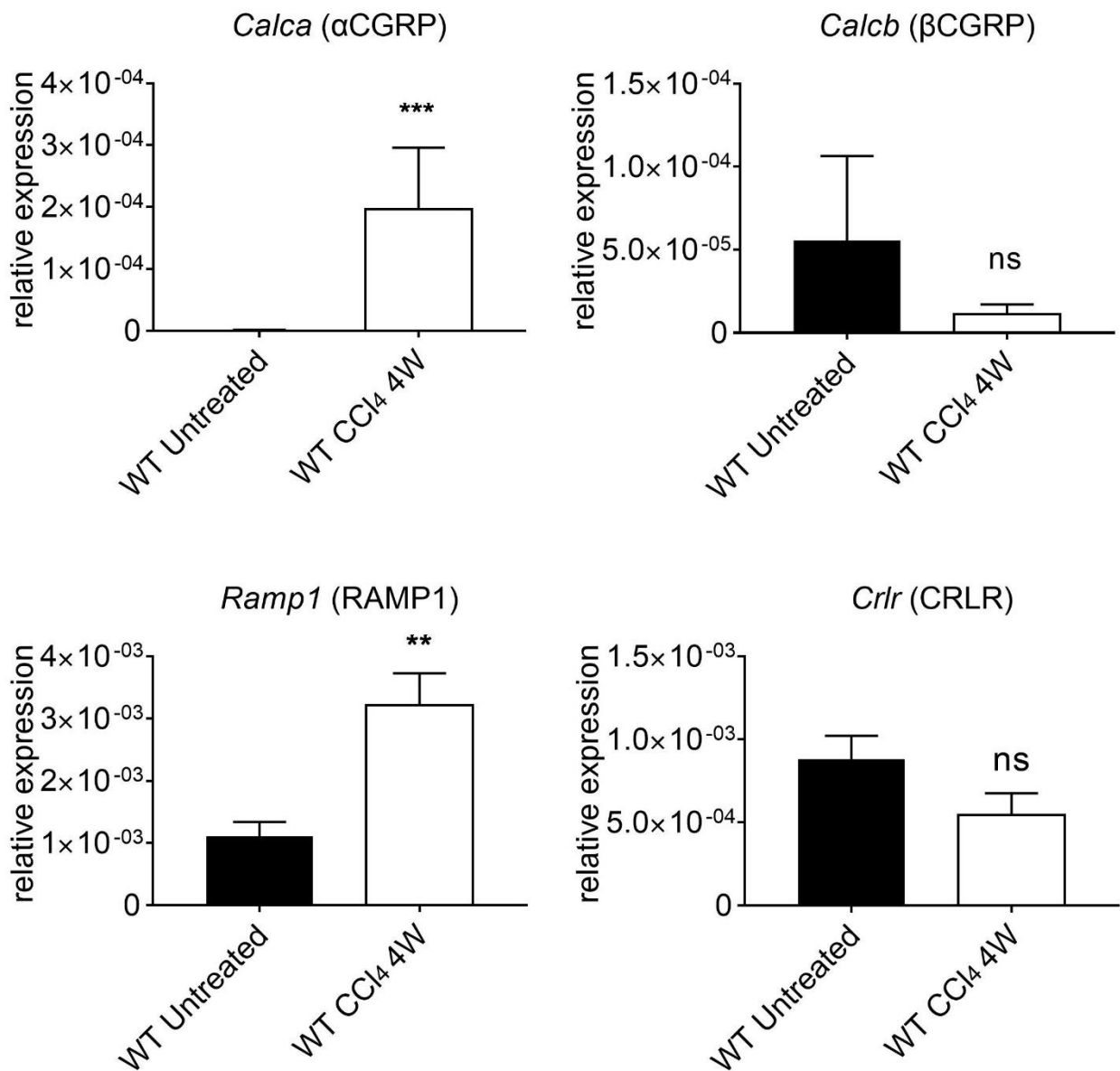


Figure 6. Induced expression of CGRP isoforms and receptor subunits during liver fibrosis in mice. mRNA levels of αCGRP, βCGRP, RAMP1 and CRLR were determined in livers of CCl₄-treated mice and were shown relative to those of β-actin (n = 8-9 mice). Results are represented as mean ± SEM. **P < 0.01, ***P < 0.001 (two-tailed unpaired Student's t-test or Mann-Whitney U test).

4.2 CGRP/RAMP1 signalling increases liver-to-body weight ratio and impairs liver function during chronic liver injury

To study the role of CGRP/RAMP1 signalling in liver fibrosis, we used a mouse strain that is deficient for RAMP1, which has been generated in previous studies (Tsuji-kawa et al.,

2007). RAMP1 deficiency in this mouse strain leads to the global deletion of RAMP1 in all cells. C57BL/6N wild type mice were used as control mice. There was no difference in the liver-to-body weight (LBW) ratio between untreated wild type and RAMP1 deficient mice. To induce fibrosis within the liver, intraperitoneal injections of CCl₄ were administered as described before (Shrestha et al., 2016). CCl₄ causes hepatocyte damage, necrosis, inflammation and fibrosis. Upon the 4 weeks of CCl₄ treatment, the liver-to-body weight ratios of both wild type and RAMP1 deficient mice increased significantly (Figure 7A). This suggests that biweekly injection of CCl₄ induced chronic damage to the liver parenchyma and led to fibrosis. The CCl₄ injected RAMP1 deficient mice had a significantly reduced liver-to-body weight ratio compared to wild type controls, demonstrating that RAMP1 deficiency resulted in decreased liver mass after CCl₄ induced liver injury (Figure 7A). As described in the literature, the spleen-to-body weight ratio (SWR) can increase due to CCl₄ injection in wild type mice (Das et al., 2014). However, in our results, the spleen-to-body weight ratio did not show a difference between wild type and RAMP1-deficient mice after CCl₄ injection (Figure 7B), indicating that there was no difference in portal hypertension. These data suggest that CGRP/RAMP1 signalling increases the liver-to-body weight ratio during the chronic liver injury.

Serum alanine aminotransferase (ALT) is commonly used in clinic to evaluate the extent of liver injury. As a chemical reagent, CCl₄ generates chloromethyl free radicals which increase the membrane permeability of liver cells that results in the release of ALT to the serum. In our study, the ALT activity was detected in the serum of mice using an ELISA Kit. ALT dramatically increased upon CCl₄ injection in wild type mice (Figure 7C), demonstrating that CCl₄ induced chronic injury in murine livers. In the absence of RAMP1, the ALT value was significantly reduced compared to wild type mice upon chronic liver injury (Figure 7C). Taken together, these results demonstrate that the CGRP/RAMP1 signalling impairs liver function during chronic liver injury.

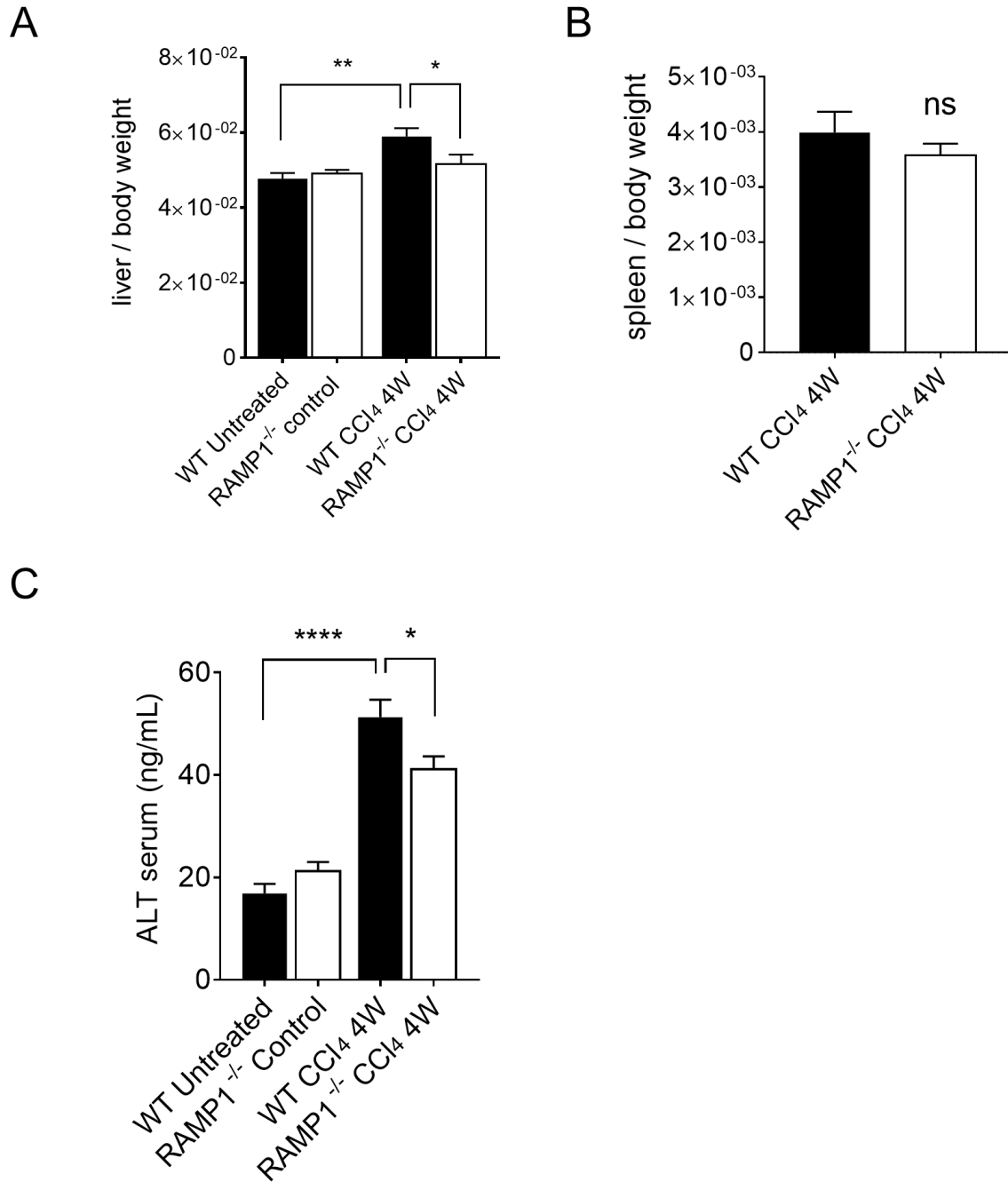


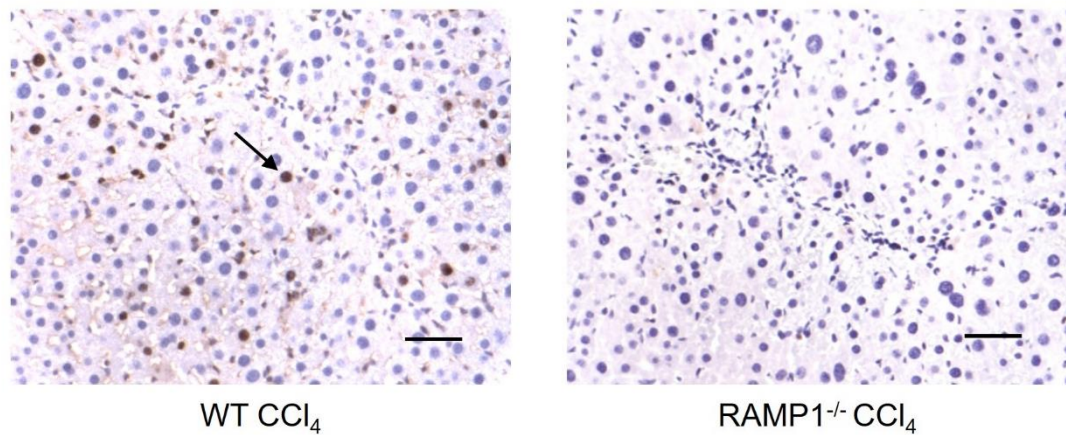
Figure 7. Liver-to-body weight ratio and serum ALT activity is affected by RAMP1 deficiency. A. Liver-to-body weight ratio of wild type and RAMP1 deficient mice. B. Spleen-to-body weight ratio of wild type and RAMP1-deficient mice. C. ALT activity in serum of wild type and RAMP1-deficient mice (n = 8-9 mice). Results are represented as mean ± SEM. *P < 0.05, **P < 0.01, ****P < 0.0001 (two-tailed unpaired Student's t-test or Mann-Whitney U test).

4.3 CGRP/RAMP1 signalling promotes hepatocyte proliferation after CCl₄ administration

In our study, we used the CCl₄ model to induce liver fibrosis in mice. The injection of CCl₄ also caused hepatocyte damage and necrosis. As demonstrated before, the absence of the CGRP co-receptor RAMP1 seems to protect liver function upon CCl₄ injection, since ALT levels in CCl₄-injected RAMP1-deficient mice were significantly lower compared to wild type mice (Figure 7C). It has been demonstrated that the liver restores its original architecture by proliferation of hepatocytes and non-parenchymal cells upon chronic injury (Tanaka et al., 2016). We therefore hypothesised that CGRP/RAMP1 signalling might have an impact on hepatocyte proliferation.

In order to address this question, we analysed proliferation markers in wild type and RAMP1^{-/-} livers subjected to CCl₄ injection. Since Ki67 is a well-known proliferation marker which is present during all active phases of the cell cycle (G₁, S, G₂ and M), we quantified its expression by immunohistochemistry. Most of the Ki67-positive cells were hepatocytes, as identified by their unique appearance of their nuclei. However, we also identified non-hepatocytes to be Ki67-positive, e.g. hepatic stellate cells (HSCs) and/or macrophages. Consistent with the result of liver-to-body weight ratio (Figure 7A), the livers of RAMP1-deficient mice showed significantly reduced amounts of Ki67-positive proliferating hepatocytes upon chronic liver injury (Figure 8A, B). This result demonstrates that CGRP/RAMP1 signalling promotes hepatocyte proliferation after CCl₄ administration.

A



B

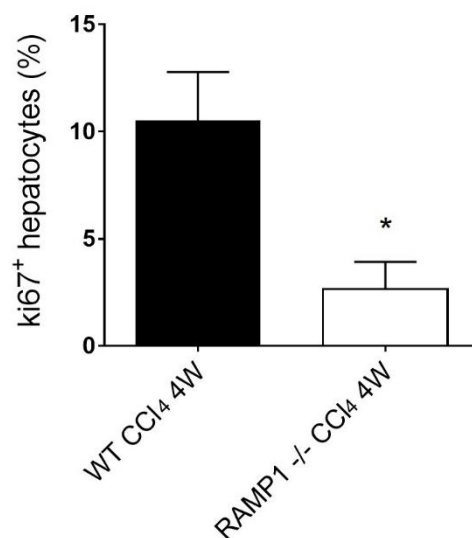
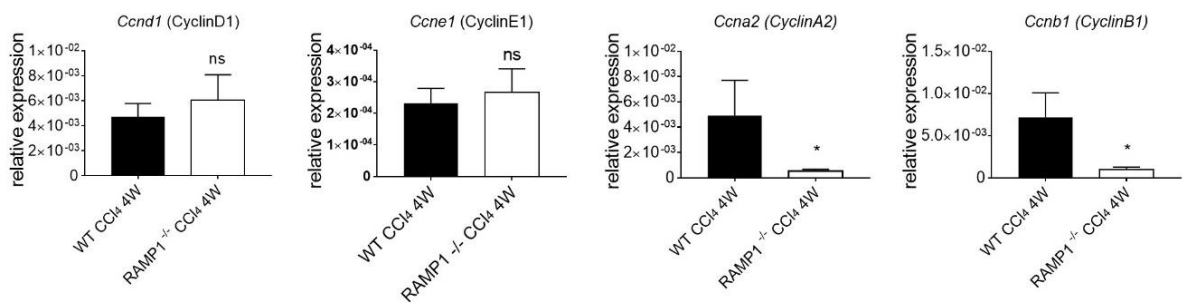


Figure 8. Reduced amounts of Ki67-positive proliferating hepatocytes in fibrotic livers of RAMP1^{-/-} mice compared to wild type mice. A. Representative images (20X) of Ki67 staining of fibrotic livers from wild type and RAMP1^{-/-} mice. Representative hepatocyte positive for Ki67 is marked by a black arrow. Scale bar: 50 μ m. B. Quantification of Ki67 positive hepatocytes in fibrotic livers of wild type and RAMP1^{-/-} mice (n = 8-9 mice). Results are represented as mean \pm SEM. *P < 0.05 (two-tailed unpaired Student's t-test or Mann-Whitney U test).

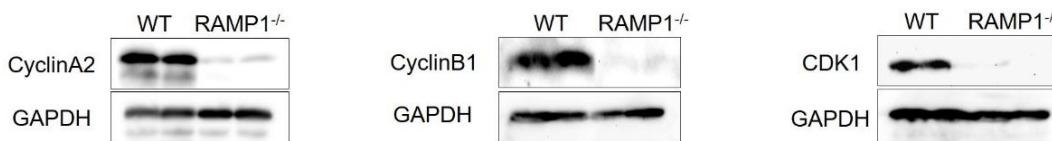
Upon chronic injury, the proliferation of hepatocytes results in liver regeneration, which undergoes a limited number of cell cycles to restore liver mass (Corlu et al., 2015). The cell cycle is composed of interphase (G₁, S, and G₂ phases), the mitotic phase (mitosis and cytokinesis), and the G₀ phase, which are controlled by different cyclins and cyclin-dependent kinases (CDKs). Cyclin A regulates the S phase, and Cyclin D/Cyclin E regulates the G₁ to S phase, while Cyclin B/CDK1 regulates the G₂ to M phase (Lim et al., 2013). To explore whether CGRP/RAMP1 signalling regulates cell cycle progression, we analysed the expression of the cell cycle regulators in wild type and RAMP1^{-/-} livers upon

chronic injury by qRT-PCR. Compared to the livers of wild type mice, the livers of RAMP1^{-/-} mice had a significantly lower RNA level of *Ccna2* (Cyclin A2) and *Ccnb1* (Cyclin B1) (Figure 9A). There was no difference between wild type and RAMP1^{-/-} mice livers in the RNA expression of *Ccnd1* (Cyclin D1) and *Ccne1* (Cyclin E1) (Figure 9A). In addition, at the protein level, there was lower expression of Cyclin A2, Cyclin B1 and the cell cycle regulator CDK1 in the livers of RAMP1-deficient mice (Figure 9B). Therefore, we conclude that CGRP/RAMP1 signalling promotes cell cycle progression during the hepatocyte proliferation process. Specific phases (S to M phases) might be differentially regulated by CGRP/RAMP1 signalling.

A



B



C

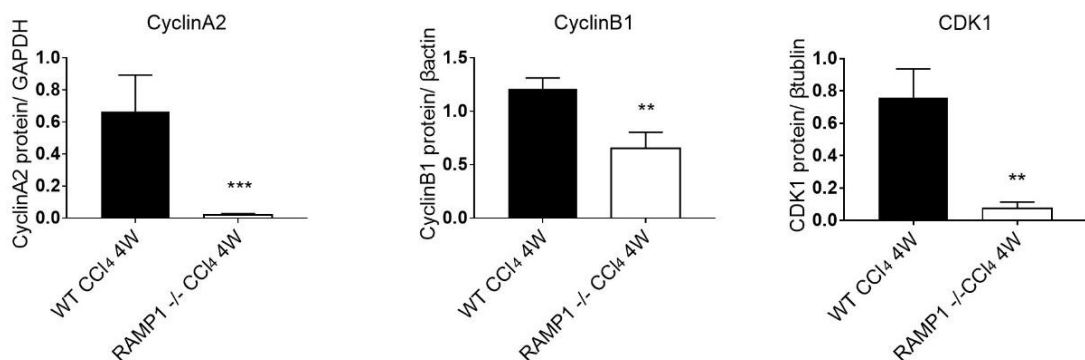


Figure 9. Decreased expression of cell cycle regulators in fibrotic livers of RAMP1^{-/-} mice compared to wild type mice. A. mRNA expression of cell cycle regulators in fibrotic livers of wild type and RAMP1^{-/-} mice (n = 8-9 mice). B. Protein expression and quantification (C) of cell cycle regulators in fibrotic livers of wild type and RAMP1^{-/-} mice (n = 8-9 mice). Results are represented as mean ± SEM. *P < 0.05, **P < 0.01, ***P < 0.001 (two-tailed unpaired Student's t-test or Mann-Whitney U test).

4.4 CGRP/RAMP1 signalling promotes collagen deposition in the fibrotic liver

A hallmark of liver fibrosis is the deposition of collagen in the injured area. Following chronic injury of the liver parenchyma, HSCs are activated and produce collagen as a consequence. To investigate the role of CGRP/RAMP1 in liver fibrosis, we visualised and quantified the collagen deposition in mice livers upon chronic injury due to CCl₄ injection by using Sirius Red staining. Previous studies have shown that Sirius Red is able to detect the fibrous septa of collagen that forms around liver lobule continuously (Huang et al., 2013). Consistent with data from the literature, we found the collagen deposition around the liver lobule to be highly induced in wild type livers upon CCl₄ treatment. In contrast, a significantly lower amount of deposition was observed in RAMP1^{-/-} fibrotic livers (Figure 10A, B).

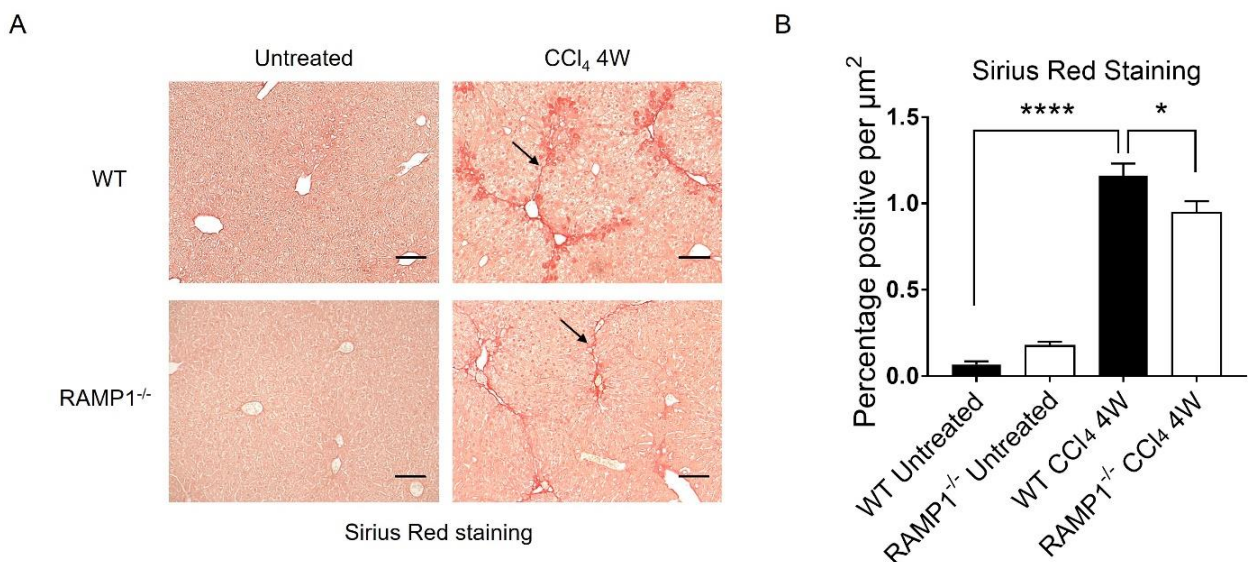
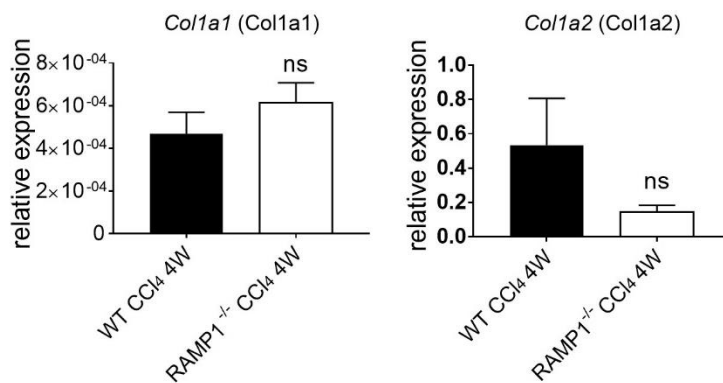


Figure 10. Reduced collagen fibers in fibrotic livers of RAMP1^{-/-} mice compared to wild type mice. A. Representative images (10X) of Sirius Red staining in fibrotic livers from wild type and RAMP1^{-/-} mice. Collagen deposition within the fibrous septa is marked by black arrows. Scale bar: 100 μm . B. Quantification of Sirius Red staining in wild type and RAMP1^{-/-} mice (n = 8-9 mice). Results are represented as mean \pm SEM. *P < 0.05, ****P < 0.0001 (two-tailed unpaired Student's t-test or Mann-Whitney U test).

To further demonstrate the impact of CGRP/RAMP1 signalling on collagen production, we quantified the collagen expression in wild type and RAMP1^{-/-} mice livers upon chronic injury by qRT-PCR. After 4 weeks of CCl₄ treatment, there was no difference in RNA level

between wild type and RAMP1^{-/-} livers in *Col1a1* (Figure 11A). The RNA expression of *Col1a2* in RAMP1^{-/-} livers tended to be lower than that in wild type livers but the difference was not significant (Figure 11A). On protein level, a strong expression of both Collagen 1a1 and 1a2 was observed in the livers from wild type mice upon chronic liver injury. On the contrary, the expression was significantly decreased in RAMP1^{-/-} mice livers (Figure 11B).

A



B

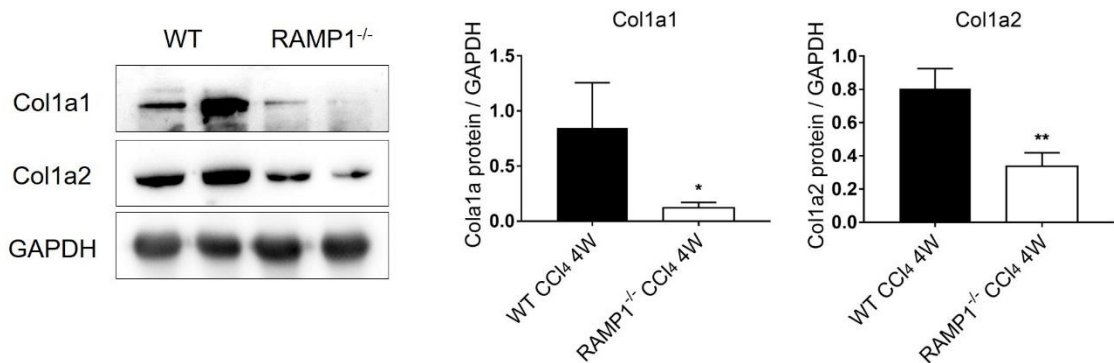


Figure 11. Reduced expression of collagen in fibrotic livers of RAMP1^{-/-} mice compared to wild type mice. A. mRNA expression of collagen in fibrotic livers of wild type and RAMP1^{-/-} mice (n = 8-9 mice). B. Representative western blots and quantification of Collagen1a1 and Collagen1a2 in fibrotic livers of wild type and RAMP1^{-/-} mice (n = 8-9 mice). Results are represented as mean ± SEM. *P < 0.05, **P < 0.01 (two-tailed unpaired Student's t-test or Mann-Whitney U test).

Since Collagen Type I is the major type of collagen involved in the process of liver fibrosis, we specifically detected its location using immunohistochemistry. Immunohistochemistry staining revealed that the livers of RAMP1^{-/-} mice expressed less Collagen Type I

compared to those of wild type mice upon chronic injury (Figure 12). Together, these findings indicate that CGRP/RAMP1 signalling promotes collagen deposition upon chronic liver injury, accelerating the process of fibrosis.

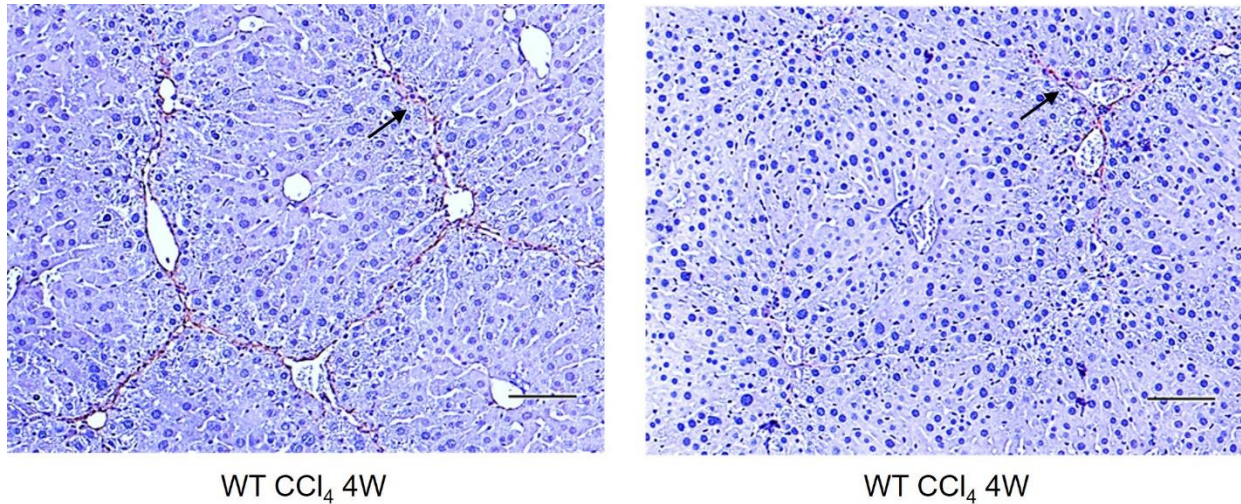


Figure 12. Less expression of collagen in fibrotic livers of RAMP1^{-/-} mice compared to wild type mice. Representative images (10X) of immunohistochemistry staining of Collagen Type I in fibrotic livers of wild type and RAMP1^{-/-} mice. Areas positive for Collagen Type I within the fibrous septa are marked by black arrows. Scale bar: 100 μ m.

The urokinase plasminogen activator (uPA) is known to be an initiator of the extracellular matrix degradation, by promoting the conversion of plasminogen to plasmin (Salas et al., 2008). Previous studies have shown that CCl₄ treatment induced uPA (*Plau*) expression, which activated matrix metalloproteinase (MMP) activity and mitigated liver injury (Li et al., 2020). In our study, we detected decreased levels of uPA mRNA expression (*Plau*) in RAMP1-deficient livers compared to wild type livers upon chronic injury (Figure 13A). At the protein level, RAMP1^{-/-} livers tended to have a lower expression of uPA compared to wild type livers, while the difference was not significant ($p = 0.07$) (Figure 13B).

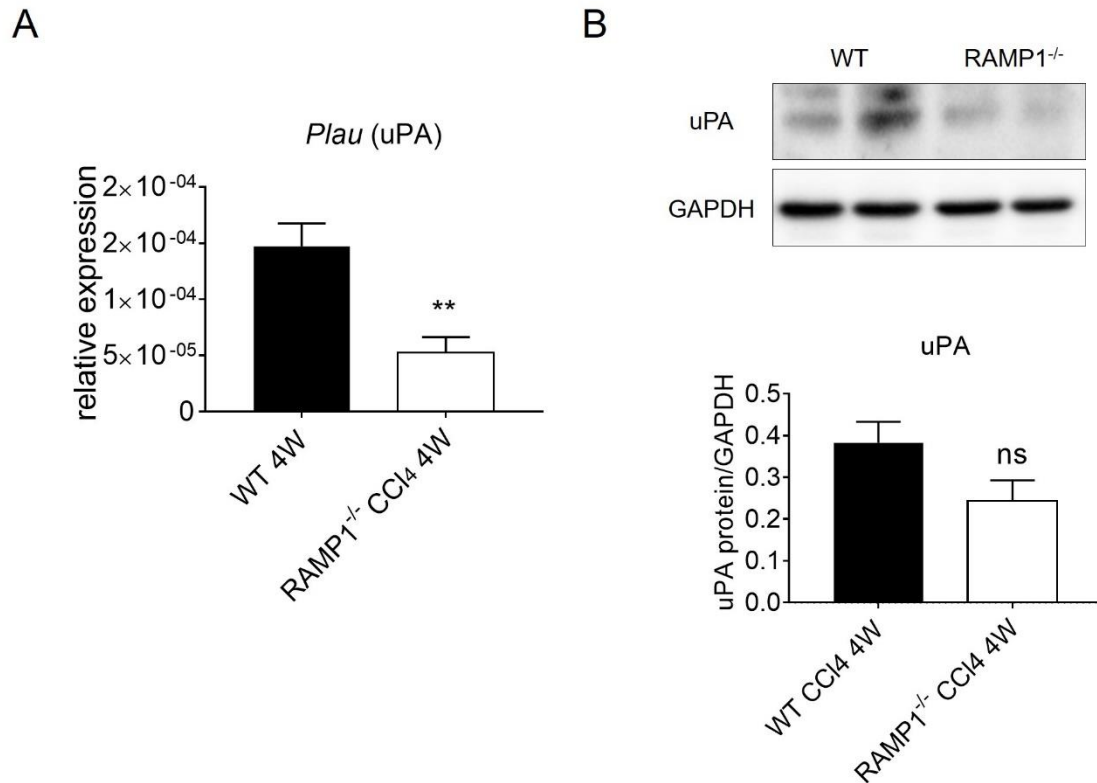


Figure 13. Decreased uPA expression on RNA and protein levels in fibrotic livers of RAMP1^{-/-} mice compared to wild type mice. A. mRNA expression of *Plau* (uPA) in fibrotic livers of wild type and RAMP1^{-/-} mice (n = 8-9 mice). B. Protein expression of uPA in fibrotic livers of wild type and RAMP1^{-/-} mice (n = 8-9 mice). Results are represented as mean \pm SEM. **P < 0.01 (two-tailed unpaired Student's t-test or Mann-Whitney U test).

4.5 CGRP/RAMP1 signalling might not affect the immune response in the process of fibrosis

Liver fibrogenesis triggers enhanced expression of inflammatory cytokines, including transforming growth factor- β (TGF β), tumour necrosis factor alpha (TNF α) and interleukins (IL) (Frolik et al., 1983; Weiskirchen et al., 2017). Specifically, TGF β 1, TGF β 2, TNF α and IL-33 were reported to promote the activation of hepatic stellate cells, which is the major event during liver fibrosis (Tu et al., 2014; Weiskirchen et al., 2017; Yang et al., 2015). In order to investigate the possibility that CGRP/RAMP1 signalling might affect these modulators during liver fibrosis, we analysed the expression of these modulators in

the fibrotic livers of wild type and RAMP1^{-/-} mice by qRT-PCR. Upon chronic injury by CCl₄, no difference was detected in the expression of *Tgfβ1*, *Tgfβ2*, *Tnfa* or *Il-33* (Figure 14). Hence, CGRP/RAMP1 signalling might not affect the immune response in the process of fibrosis.

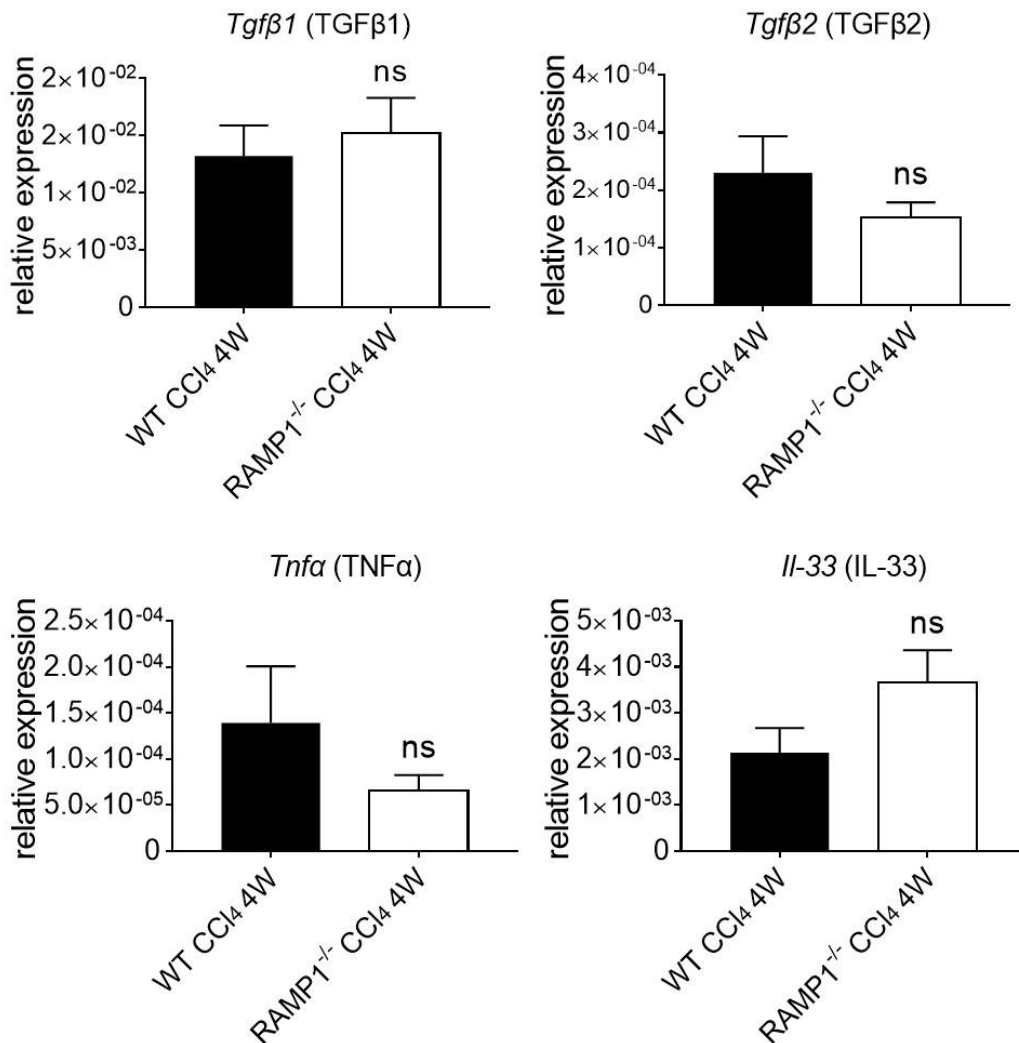


Figure 14. mRNA expression of modulators in fibrotic livers of wild type and RAMP1^{-/-} mice. mRNA expression of *Tgfβ1*, *Tgfβ2*, *Tnfa* and *Il-33* in fibrotic livers of wild type and RAMP1^{-/-} mice (n = 8-9 mice). Results are represented as mean ± SEM (two-tailed unpaired Student's t-test or Mann-Whitney U test).

4.6 CGRP/RAMP1 signalling promotes the activation of hepatic stellate cells in the fibrotic liver

The activation of HSCs is a crucial event during liver fibrogenesis, and a commonly examined fibrosis marker is α -smooth muscle actin (α -SMA). In order to find out whether CGRP/RAMP1 signalling affects the activation of HSCs during liver fibrosis, we analysed the hepatic mRNA expression of α -SMA gene *Acta2* in wild type and RAMP1^{-/-} mice after 4 weeks of CCl₄ injection. mRNA expression of *Acta2* in RAMP1^{-/-} mice livers tended to be lower than in wild type livers, but the difference was not significant (Figure 15A). At the protein level, wild type livers showed a significantly stronger expression of α -SMA compared to RAMP1^{-/-} livers upon chronic injury (Figure 15B).

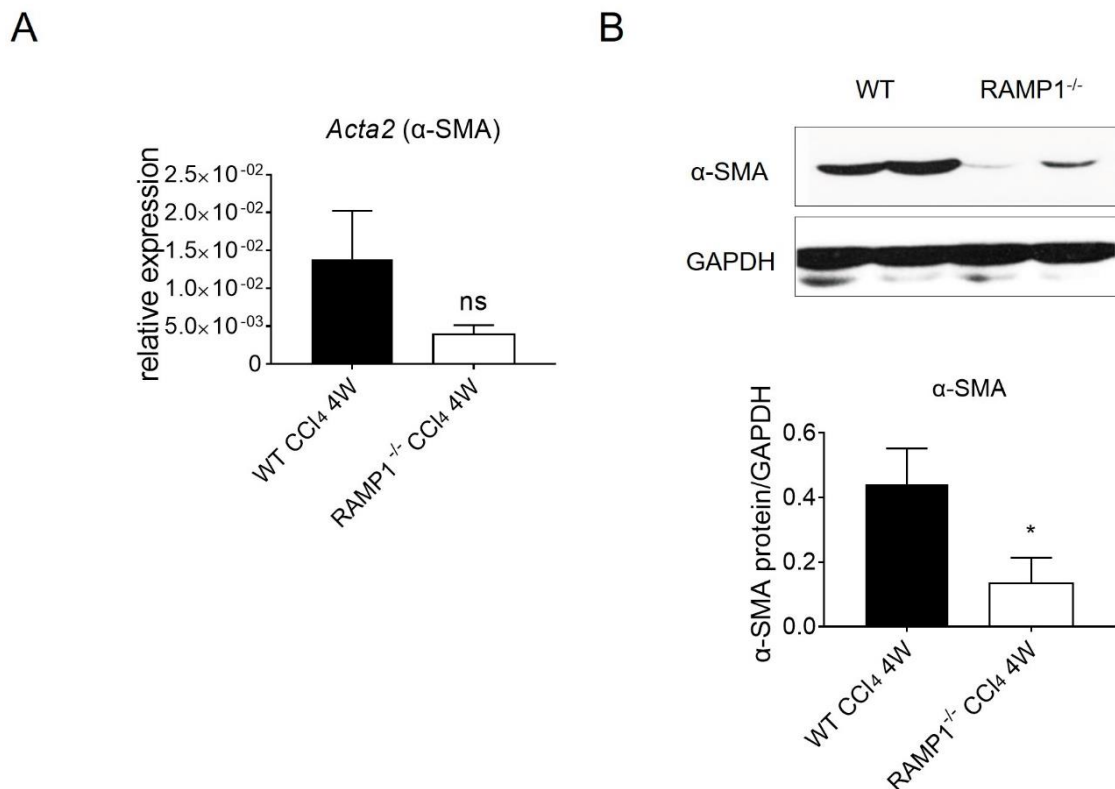


Figure 15. Reduced α -SMA expression in fibrotic livers of RAMP1^{-/-} mice compared to wild type mice. A. mRNA expression of *Acta2* in fibrotic livers of wild type and RAMP1^{-/-} mice. B. Western blot analysis and quantification of α -SMA in fibrotic livers of wild type and RAMP1^{-/-} mice (n = 8-9 mice). Results are represented as mean \pm SEM. *P < 0.05 (two-tailed unpaired Student's t-test or Mann-Whitney U test).

In contrast, western blot analysis allows only for quantification of α -SMA protein. To locate α -SMA within the liver parenchyma *ex vivo*, immunohistochemistry was used. In wild type livers, α -SMA was densely distributed around the liver lobules, forming thick stripes

(Figure 16). In contrast, in RAMP1-deficient livers, the expression was incompact with disconnected and thin stripes. Although HSCs are the main cells that are α -SMA positive in fibrotic livers, α -SMA is also expressed in lipocytes as well as vascular smooth muscle cells (Yamaoka et al., 1993). Here, α -SMA seems to be only expressed in HSCs. Taken together, these results demonstrate that *in vivo* CGRP/RAMP1 signalling promotes the activation of HSCs upon chronic injury induced by CCl₄.

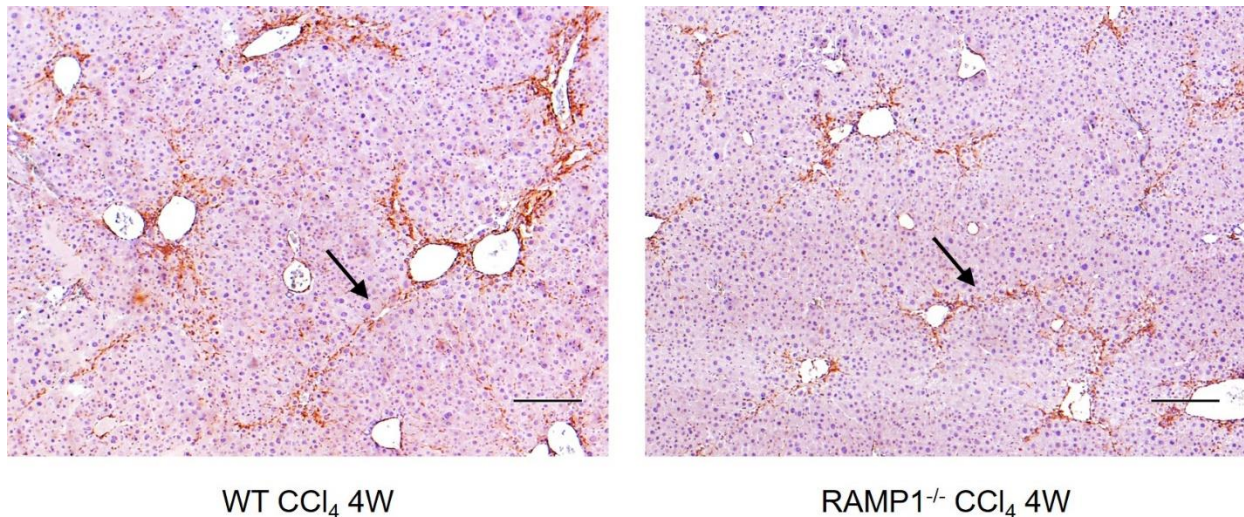


Figure 16. Reduced expression of α -SMA in fibrotic livers of RAMP1^{-/-} mice compared to wild type mice. Representative images (5X) of immunohistochemistry staining of α -SMA in fibrotic livers of wild type and RAMP1^{-/-} mice. HSCs positive for α -SMA are marked by black arrows. Scale bar: 200 μ m.

4.7 *In vitro* CGRP/RAMP1 signalling contributes to the activation of hepatic stellate cells and collagen production

In order to verify that CGRP/RAMP1 signalling promotes α -SMA expression in hepatic stellate cells, we used the human hepatic stellate cell line LX-2. LX-2 cells were seeded and cultured for 24 hours, and then stimulated with CGRP (100nM) for 1, 2, 3 and 6 hours. The HSC activation marker α -SMA was quantified by western blot analysis. Upon stimulation, we clearly detected an induction of α -SMA protein expression at 2, 3 and 6 hour time-points (Figure 17A, B). Using qRT-PCR analysis for mRNA expression, we did not observe any increase in α -SMA (Figure 17C).

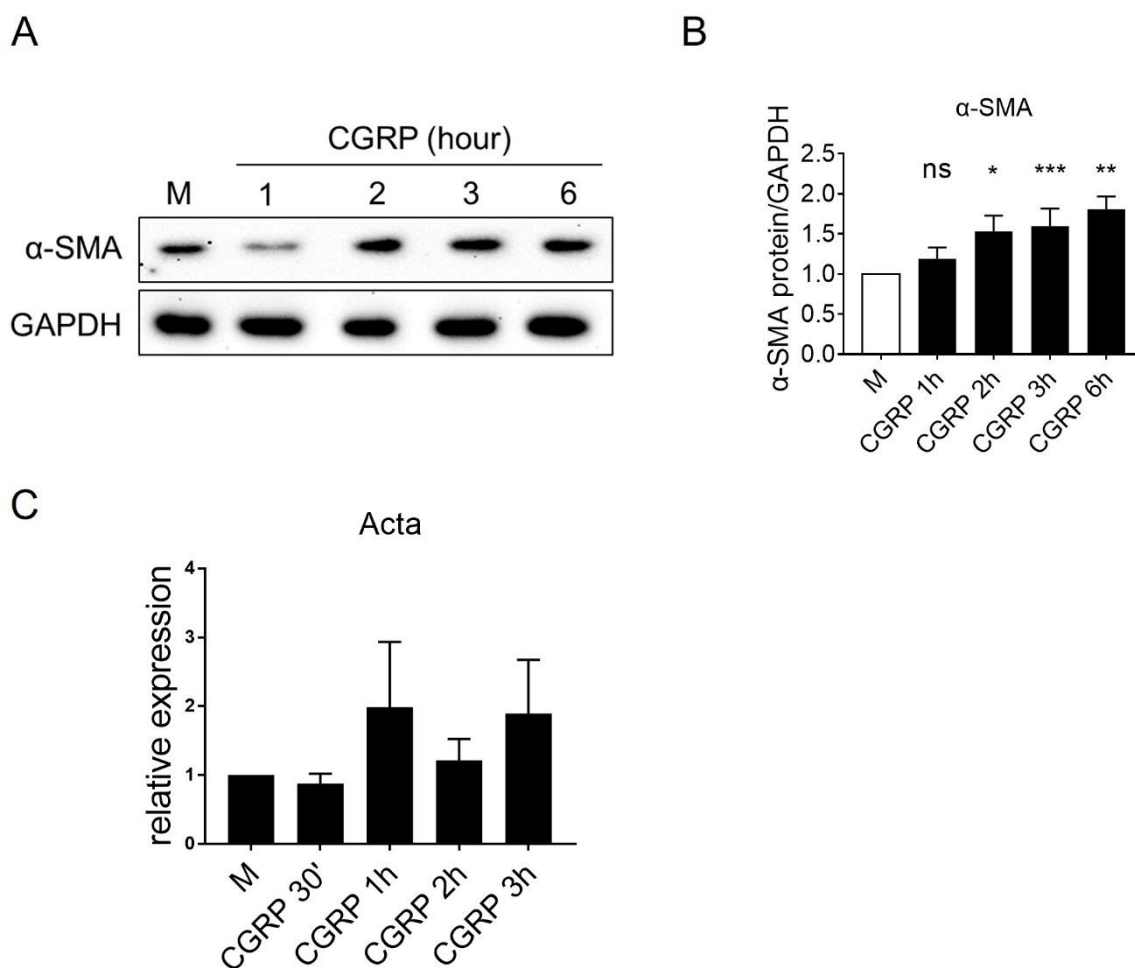


Figure 17. Induced expression of α -SMA in LX-2 cells stimulated by CGRP. A. Representative western blot analysis of α -SMA in LX-2 cells stimulated with CGRP. B. The quantification of α -SMA in LX-2 cells stimulated with CGRP (n = 4-5). C. RNA expression of α -SMA in LX-2 cells stimulated with CGRP (n = 4-5). Results are represented as mean \pm SEM. *P < 0.05, **P < 0.01, ***P < 0.001 (two-tailed unpaired Student's t-test or Mann-Whitney U test).

By using immunofluorescence staining, we detected the location of α -SMA expression either in untreated LX-2 cells or in cells stimulated with the neuropeptide CGRP. Untreated quiescent LX-2 cells displayed a relatively small and irregular cell body. However, following CGRP stimulation, activated LX-2 cells generated a large and flat morphology, with prominent perinuclear stress fibres of α -SMA (Figure 18). We observed an induction of α -SMA in LX-2 cells upon 6 hours' stimulation with CGRP. These results suggest that CGRP/RAMP1 signalling directly activates hepatic stellate cells.

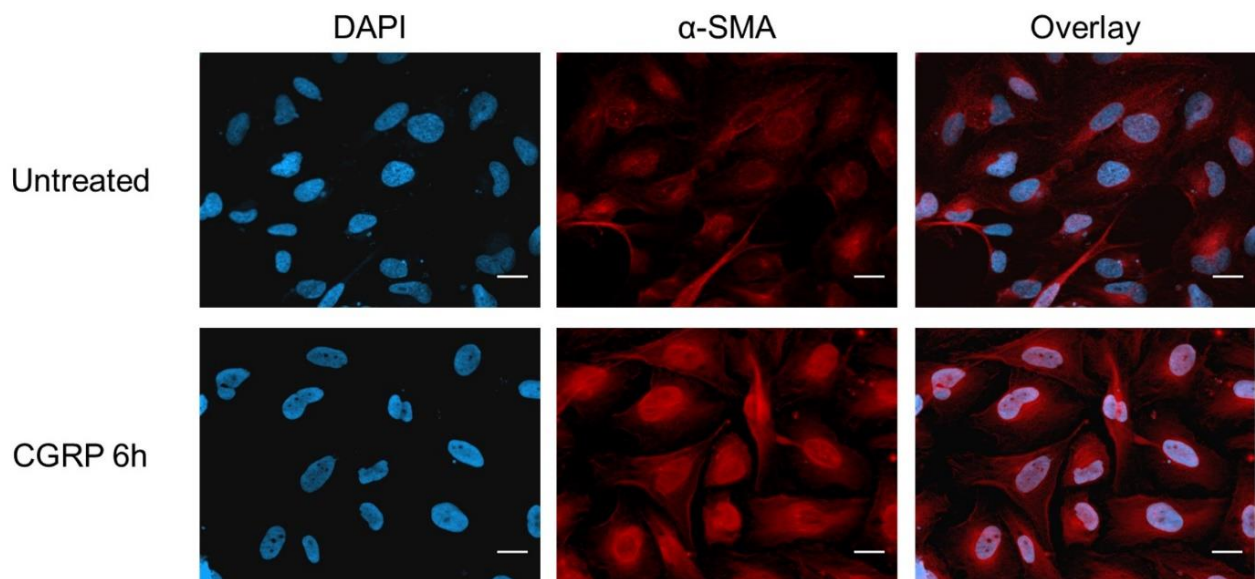


Figure 18. Induced expression of α -SMA in LX-2 cells stimulated with CGRP. Representative images (40X) of immunofluorescence staining of α -SMA in LX-2 cells stimulated with CGRP for 6 hours. Scale bar: 20 μ m.

During chronic injury, hepatic stellate cells are activated, producing large amounts of collagen, which are distributed around the liver lobules (Figure 12). In order to verify *in vitro* that CGRP/RAMP1 signalling promotes the collagen production of hepatic stellate cells, LX-2 cells were seeded and cultured for 1 day, and then stimulated with CGRP (100nM) for 1, 2, 3 and 6 hours. Collagen Type I Alpha 1 chain (Col1a1) and Collagen Type I Alpha 2 chain (Col1a2) expression was quantified by western blot analysis. At all time-points, the expression of Col1a1 was dramatically induced upon CGRP stimulation (Figure 19A). The expression of Col1a2 was elevated upon 1 hour of stimulation (Figure 19B). Together, these results suggest that CGRP/RAMP1 signalling increases the Collagen Type I production of hepatic stellate cells.

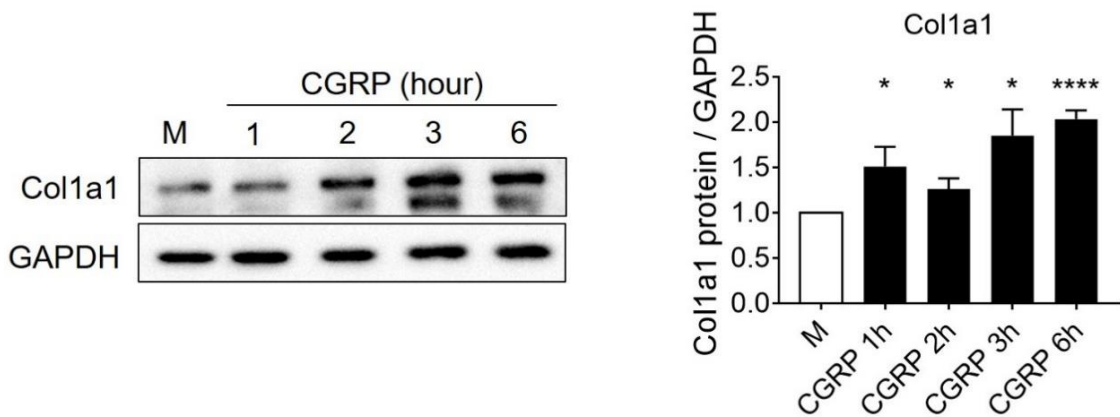
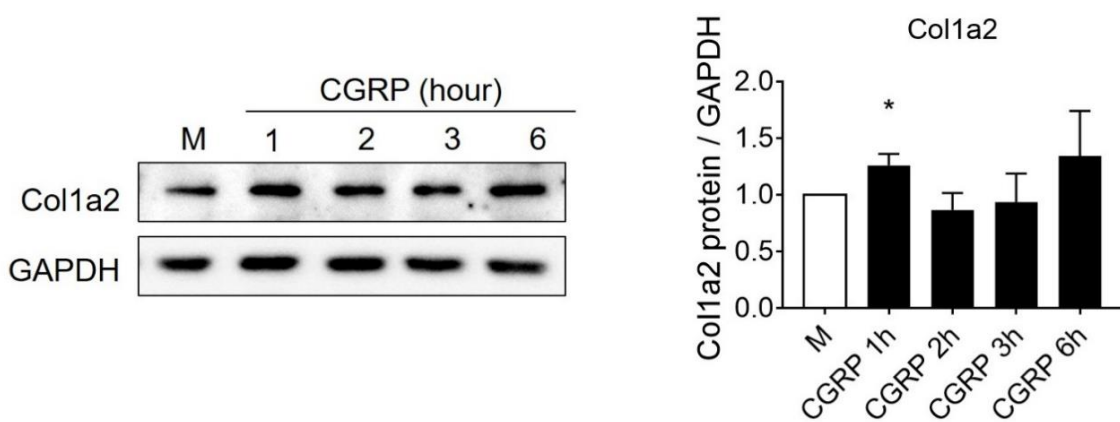
A**B**

Figure 19. Induced expression of Collagen Type I in LX-2 cells stimulated with CGRP. A. Representative western blot analysis and quantification of Col1a1 in LX-2 cells stimulated with CGRP (n = 4-5). B. Representative western blot analysis and quantification of Col1a2 in LX-2 cells stimulated with CGRP (n = 4-5). Results are represented as mean \pm SEM. *P < 0.05, ****P < 0.0001 (two-tailed unpaired Student's t-test or Mann-Whitney U test).

4.8 CGRP/RAMP1 signalling positively regulates YAP activity during liver fibrosis

The Hippo pathway effector YAP is known to control the activation of hepatic stellate cells and promote the development of liver fibrosis (Mannaerts et al., 2015). To investigate whether CGRP/RAMP1 is able to control YAP activity during liver fibrosis, the expression of YAP was analysed after 4 weeks of CCl₄ treatment. YAP activity can be negatively regulated by phosphorylation of either Ser397 or Ser127. Specifically, the phosphorylation of Ser397 leads to the degradation of YAP, while the phosphorylation of Ser127 indicates

the cytoplasmic retention of YAP (Hergovich, 2017). Phosphorylated, inactive YAP cannot translocate into the nucleus of hepatic stellate cells. Only non-phosphorylated, active YAP can be relocated into the nucleus where it serves together with the transcriptional co-activator with PDZ-binding motif (TAZ) as a transcription factor, inducing the *de novo* synthesis of YAP target genes. In our results, the deficiency of RAMP1 did not influence the total expression of YAP nor its phosphorylation on Ser397 in fibrotic murine livers (Figure 20A, B). However, the phosphorylation of YAP on Ser127 was significantly elevated in RAMP1-deficient livers compared to wild type ones (Figure 20A, B), which indicates less activated YAP in absence of the CGRP co-receptor RAMP1 in fibrotic mice livers.

The Hippo pathway is regulated by extracellular signals and activates the intracellular Mammalian Sterile 20-like kinases 1 and 2 (Mst1/2) (Dan et al., 2001). Activated Mst1/2 phosphorylates the adaptor protein salvador (SAV) and combines with it to form a complex, that jointly activates tumour suppressor kinases 1 and 2 (LATS1/2) and monopolar spindle-one-binder 1 (MOB1). LATS1/2 and MOB1 negatively regulate YAP activity (Patel et al., 2017). To explore whether CGRP/RAMP1 signalling could regulate the activation of LATS1/2 and MOB1 thus promote YAP activity, we analysed these two kinases in the CGRP co-receptor RAMP1-deficient mouse model upon liver fibrosis. At the protein level, the phosphorylation of both LATS1/2 and MOB1 protein was significantly up-regulated in RAMP1-deficient livers compared to wild type livers, suggesting that there were more activated LATS1/2 and MOB1 in the absence of RAMP1 (Figure 20C, D). These data demonstrate that CGRP/RAMP1 signalling negatively regulates LATS1/2 and MOB1, thus promoting YAP activity in fibrotic mice livers.

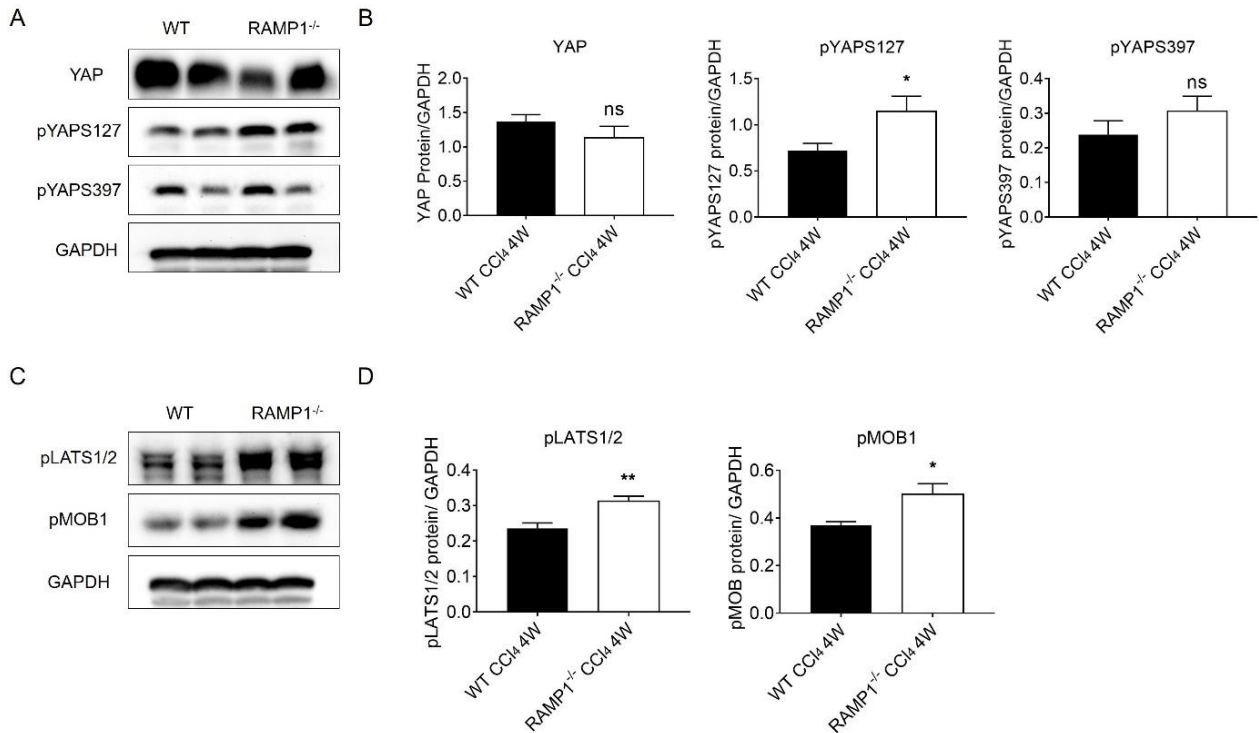


Figure 20. Decreased expression of YAP and increased expression of the upstream regulators in fibrotic livers of RAMP1^{-/-} mice compared to wild type mice. A. Representative western blot analysis and quantification (B) of total and phosphorylated YAP expression in fibrotic livers of wild type and RAMP1^{-/-} mice (n = 8-9 mice). C. Representative western blot analysis and quantification (D) of phosphorylated LATS1/2 and MOB1 expression in fibrotic livers of wild type and RAMP1^{-/-} mice (n = 8-9 mice). Results are represented as mean ± SEM. *P < 0.05, **P < 0.01 (two-tailed unpaired Student's t-test or Mann-Whitney U test).

YAP is known to control cell growth by promoting the expression of target genes, including *Ctgf*, *Thbs1*, *Ankrd1*, *Bird5* and *Foxm1* (Haskins et al., 2014). These genes are also related to HSC activation and liver fibrosis (Filliol et al., 2020; Lipson et al., 2012; Mannaerts et al., 2015; Wang et al., 2011). Therefore, to examine whether CGRP/RAMP1 signalling could regulate the expression of these YAP target genes, we analysed these target genes by qRT-PCR in fibrotic livers of wild type and RAMP1^{-/-} mice, although no difference was detectable between wild type and RAMP1^{-/-} livers regarding the expression of *Ctgf*, *Thbs1*, *Ankrd1*, *Bird5* and *Foxm1* (Figure 21). Importantly, the cell cycle regulators, *Ccna*, *Ccnb1*, and *Cdk1*, are also known as the target genes of YAP, the expression of which was reduced in RAMP1-deficient fibrotic mice livers (Figure 9). Taken together, these results demonstrate that CGRP/RAMP1 signalling promotes YAP activation and the

transcription of some of its target genes during liver fibrosis.

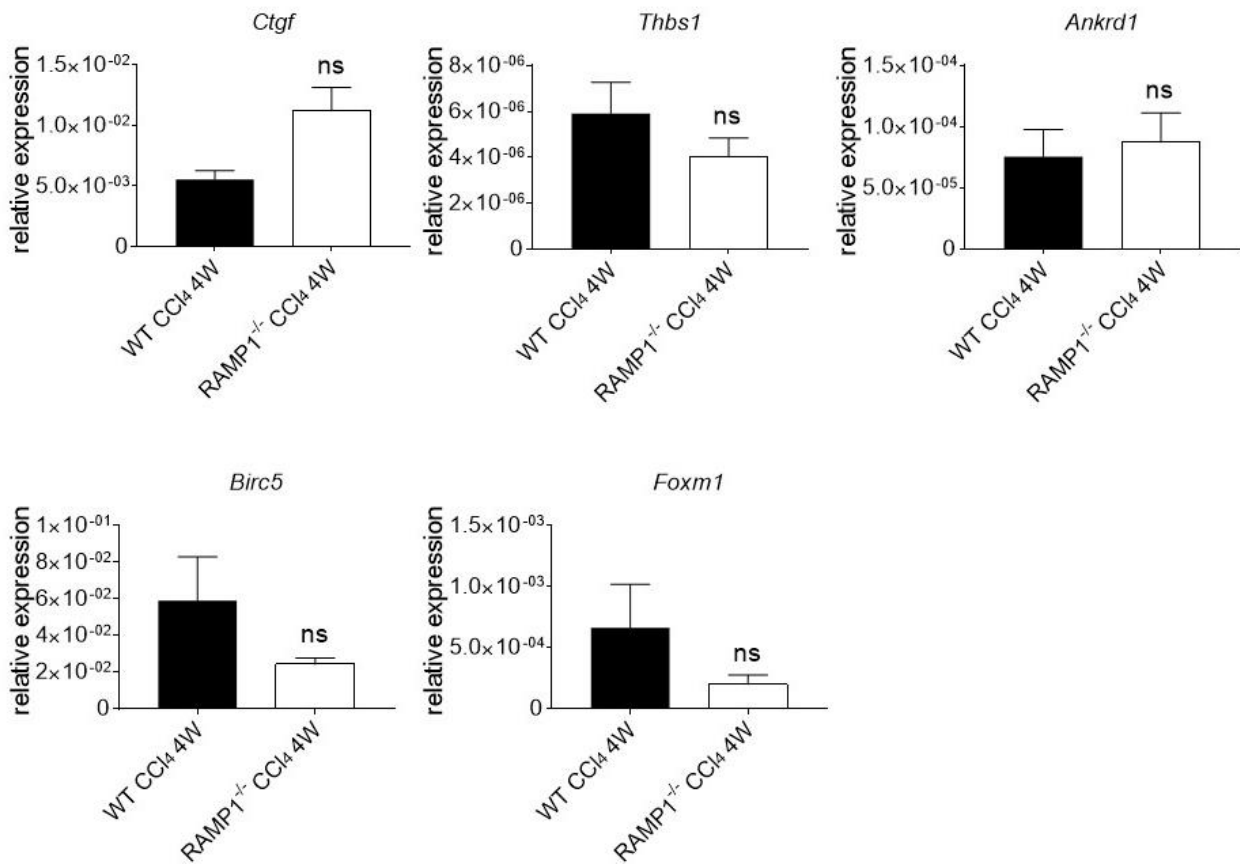


Figure 21. mRNA Expression of YAP target genes in fibrotic livers of wild type and RAMP1^{-/-} mice. mRNA expression of *Ctgf*, *Thbs1*, *Ankrd1*, *Birc5* and *Foxm1* in fibrotic livers of wild type and RAMP1^{-/-} mice (n = 8-9 mice). Results are represented as mean ± SEM (two-tailed unpaired Student's t-test or Mann-Whitney U test).

4.9 CGRP/RAMP1 signalling increases YAP activity via Gα₁₁ signalling during liver fibrosis

When CGRP binds to its receptor complex, calcitonin receptor-like receptor (CRLR) and RAMP1, the signal transmits into the cell (Russo, 2015). It has been demonstrated that CGRP/RAMP1 can signal intracellularly via Gα_{q/11} or Gα_s protein (Deng et al., 2017; Feng et al., 2014). Signalling via Gα_{q/11} protein was reported to increase YAP activity, whereas signalling via Gα_s protein negatively regulates YAP activity (Yu et al., 2012). In order to

investigate via which protein CGRP/RAMP1 signalling regulates YAP activity during liver fibrosis, we analysed these two proteins on RNA level in livers of untreated and CCl₄ injected wild type mice by qRT-PCR. Upon CCl₄ administration, the wild type livers showed the higher expression of *Gna11* (Gα₁₁) (Figure 22). The expression of *Gnaq* (Gα_q) and *Gnas* (Gα_s) tended to increase but the difference was not significant (Figure 22). These results suggest that CGRP/RAMP1 complex controls YAP activity via Gα₁₁ protein during liver fibrosis.

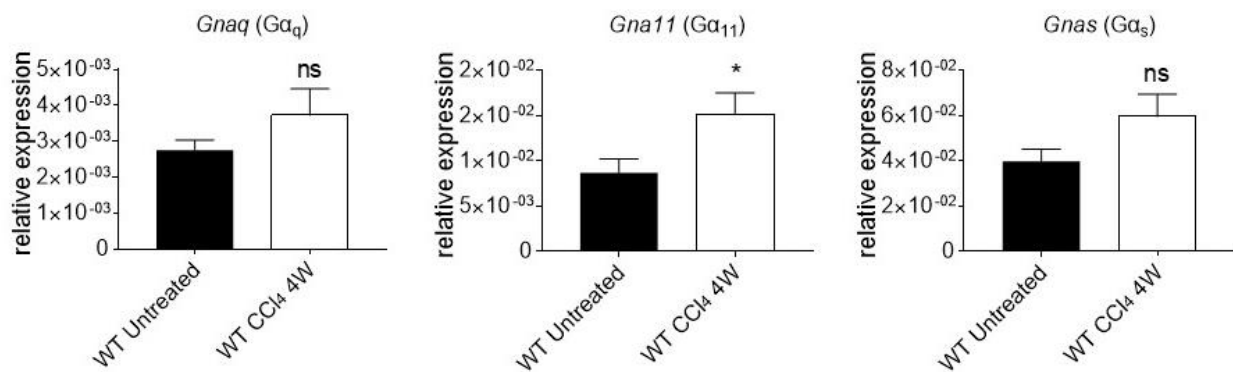


Figure 22. Induced mRNA expression of Gα₁₁ protein in wild type mice livers upon CCl₄ treatment. mRNA expression of Gα_{q/11} and Gα_s in livers of untreated and CCl₄ injected wild type mice (n = 8-9 mice). Results are represented as mean ± SEM. *P < 0.05 (two-tailed unpaired Student's t-test or Mann-Whitney U test).

4.10 *In vitro* CGRP/RAMP1 signalling increases YAP activity in hepatic stellate cells

As mentioned previously (Figure 20), CGRP/RAMP1 signalling positively regulates YAP activity by decreasing its cytoplasmic retention during liver fibrosis. To test whether CGRP/RAMP1 signalling increases YAP activity specifically in hepatic stellate cells which are highly responsible for liver fibrosis, we used the human hepatic stellate cell line LX-2. LX-2 cells were seeded and cultivated in Dulbecco's Modified Eagle Medium (DMEM) containing 100U/ml Penicillin, 2mM 2-Mercaptoethanol, 2mM L-glutamine and 7% foetal calf serum (FCS) for 24 hours, and starved with 0% FCS DMEM for another 24 hours, then stimulated with CGRP (100nM) for 1, 2, 3 and 6 hours. The total YAP expression

increased at 2 hours' time-point upon CGRP stimulation (Figure 23A, B). The treatment did not affect the phosphorylation of YAP on Ser127, but significantly decreased its phosphorylation on Ser397 at 2 and 3 hours' time-points. Thus, these data demonstrate that CGRP/RAMP1 signalling increases YAP activity specifically in hepatic stellate cells.

As mentioned before (Results 4.8), CGRP/RAMP1 signalling negatively regulates LATS1/2 and MOB1, thus promoting YAP activity in the fibrotic mice livers. To test whether CGRP/RAMP1 signalling modulates the activity of LATS1/2 and MOB1 in hepatic stellate cells, we quantified the phosphorylation of LATS1/2 and MOB1 in the LX-2 cells stimulated with CGRP (100nM). The down-regulation of phospho-LATS1/2 appeared at 3 and 6 hour time-points, and phospho-MOB1 expression was reduced at the 3 hour time-point (Figure 23C, D). Together, the results suggest that CGRP/RAMP1 signalling negatively regulates LATS1/2 and MOB1 specifically in hepatic stellate cells.

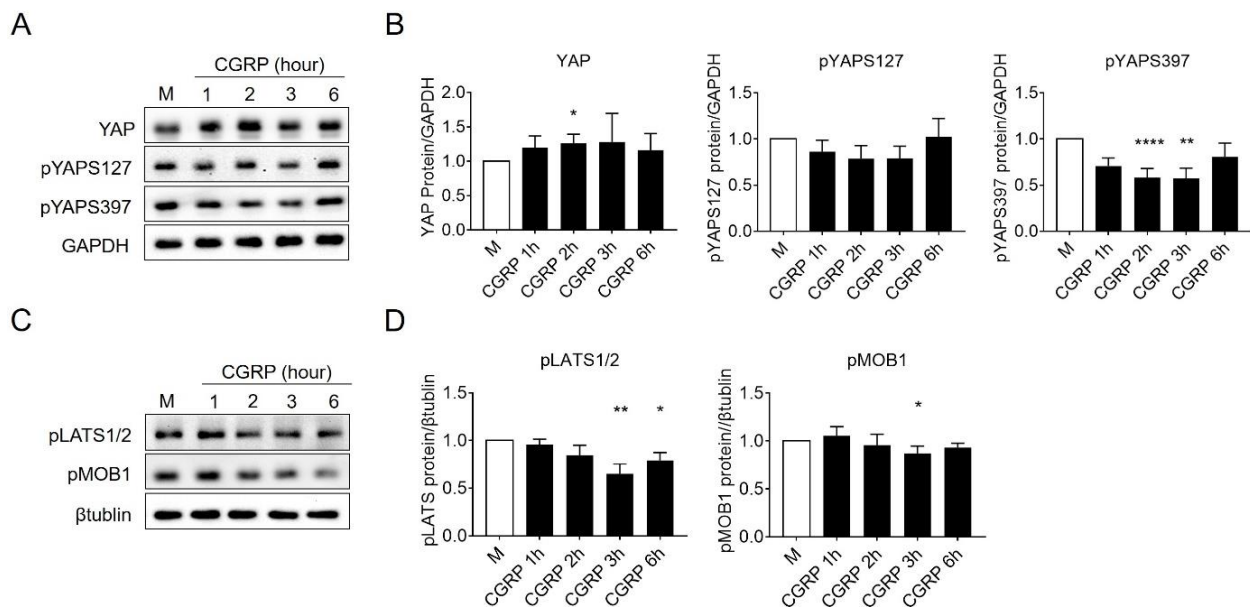


Figure 23. Increased expression of YAP and decreased expression of the upstream regulators in LX-2 cells stimulated with CGRP. A. Western blot analysis and quantification (B) of total and phosphorylated YAP expression in LX-2 cells stimulated with CGRP (n = 4-5). C. Western blot analysis and quantification (D) of phosphorylated LATS1/2 and MOB1 expression in LX-2 cells stimulated with CGRP (n = 4-5). Results are represented as mean ± SEM. *P < 0.05, **P < 0.01, ****P < 0.0001 (two-tailed unpaired Student's t-test or Mann-Whitney U test).

The immunofluorescence staining allowed us to detect the location of YAP expression in

LX-2 cells stimulated with CGRP. Untreated LX-2 cells displayed a relatively small and irregular cell body. Upon the treatment of CGRP (100nM) for 6 hours, activated LX-2 cells generated a large and flat morphology (Figure 24). Importantly, YAP translocated from the cytoplasm into the nucleus of LX-2 cells following a 6 hour stimulation of CGRP (Figure 24). All these results demonstrate that CGRP signalling triggers the activation of YAP by inducing its nucleus translocation in the hepatic stellate cells.

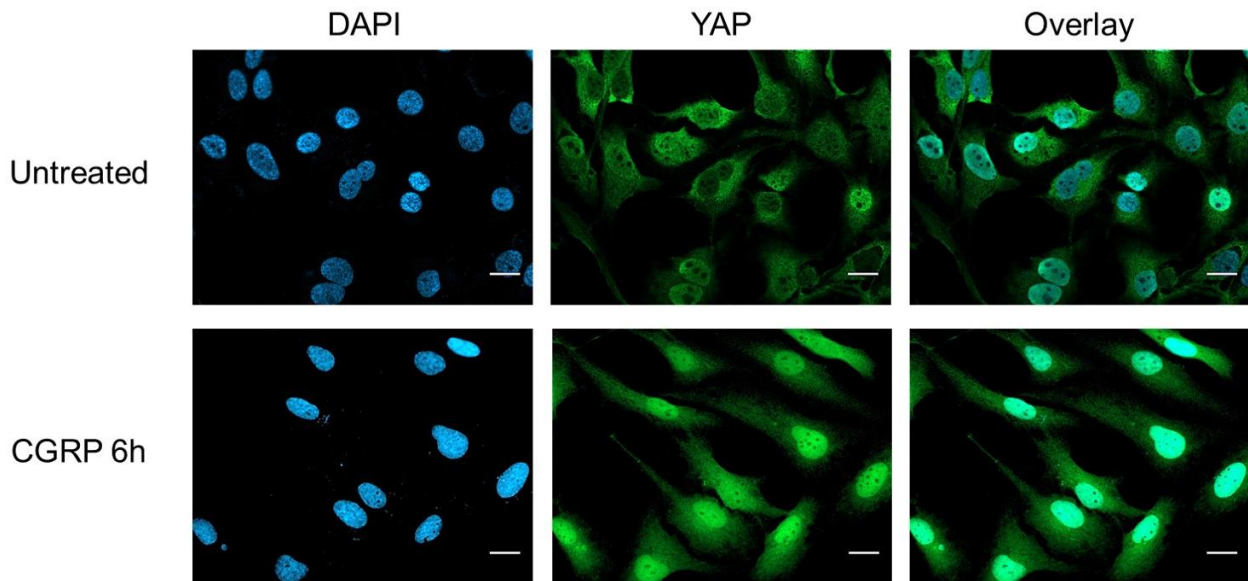


Figure 24. YAP translocated from the cytoplasm into the nucleus of LX-2 cells upon 6 hours' stimulation of CGRP. Representative images (40X) of immunofluorescence staining of YAP in LX-2 cells stimulated with CGRP for 6 hours. Scale bar: 20 μ m.

4.11 CGRP/RAMP1 signalling does not promote the migration of LX-2 cells

CGRP/RAMP1 signalling was found to promote the migration of human T lymphocytes isolated from healthy blood donors (Talme et al., 2008). Studies have demonstrated that the migration of hepatic stellate cells has an important role in liver fibrosis, promoting the production of the ECM and growth factors (Moon et al., 2019). Therefore, we tested whether CGRP could enhance the migration of hepatic stellate cells, thus accelerating the development of liver fibrosis. As mentioned in Methods 3.2.13, we applied the migration assay. LX-2 cells were seeded and cultured in a 2-well chamber, and migrated for up to

22 hours with one well stimulated with CGRP (100nM). Images were taken and the migration areas were calculated as the percentage relative to the 0 h time-point (Figure 25A). At the 14, 18 and 22 hour time-points, the closure of the generated gap increased continuously due to the migration of LX-2 cells. There was no significant difference of the closure areas between media control and CGRP stimulated cells at all of the time-points (14h, 18h, 22h) (Figure 25B). Together, the migration of LX-2 cells seemed to be not positively affected by the neuropeptide CGRP.

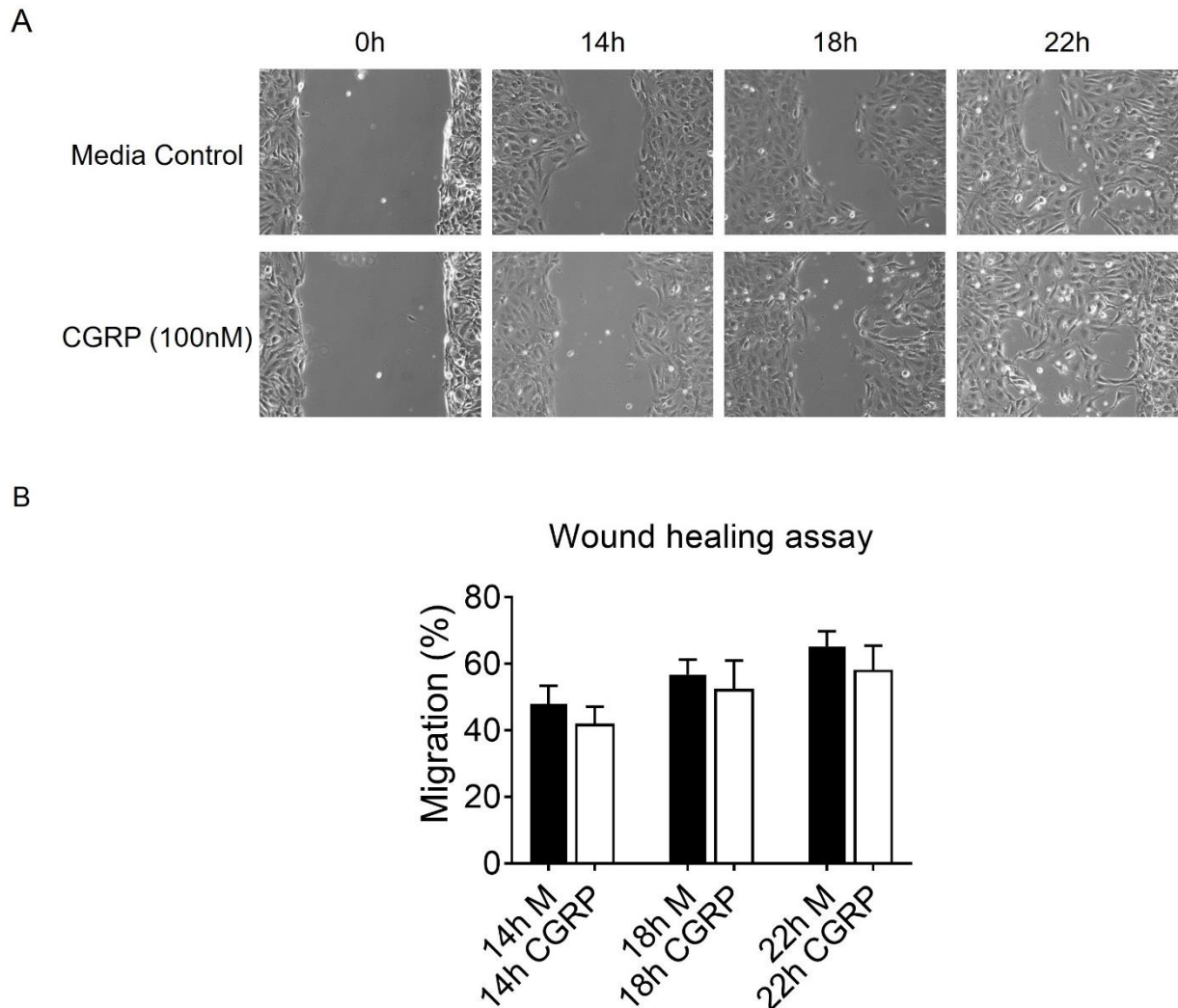


Figure 25. Migration of LX-2 cells was not affected by CGRP stimulation. A. Images (10X) of migrating LX-2 cells at 14, 18 and 22 hour time-points. B. Quantification of the migrating areas (n = 3). Results are represented as mean \pm SEM (two-tailed unpaired Student's t-test or Mann-Whitney U test).

4.12 CGRP/RAMP1 promotes TGF β 1 signalling by activating Smad2

The transforming growth factor β 1 (TGF β 1) is a profibrogenic cytokine that is known to participate in all stages of liver fibrosis and cirrhosis. TGF β 1 exerts its intracellular functions through binding to the TGF β 1 receptor II (T β RII), which allows T β RII to phosphorylate the TGF β 1 receptor I (T β RI), activating its catalytic ability (Yu et al., 2008). Subsequently, the activated T β RI phosphorylates the receptor-activated (R-) Smads, particularly Smad2 and Smad3, which form heterotrimeric complexes. The nuclear translocation of these complexes activates the hepatic stellate cells, thus producing the ECM (Kulkarni et al., 2016). The activity of Smad2 can be regulated by the phosphorylation of either Ser465/467 or Ser245/250/255. The phosphorylation of Smad2 on Ser465/467 indicates the activation of Smad2 while phosphorylation on Ser245/250/255 indicates the inactivation of Smad2. To examine whether CGRP/RAMP1 promotes TGF β 1 signalling by activating Smad2 in hepatic stellate cells, we analysed the expression of TGF β 1 as well as p-Smad2 in the LX-2 cell line stimulated with CGRP (100nM).

LX-2 cells were seeded and cultured for 24 hours, and then stimulated with CGRP (100nM) for 1, 2, 3 and 6 hours. TGF β 1 expression was quantified by qRT-PCR, and the phosphorylation of Smad2 was analysed by western blot. At the RNA level, the expression of TGF β 1 tends to increase upon CGRP stimulation. However, the difference was not significant (Figure 26A). In particular, our *in vivo* results did not show any difference in mRNA expression of TGF β 1 between wild type and RAMP1^{-/-} mice livers upon chronic injury (Results 4.5, Figure 14). At the protein level, the stimulation of CGRP did not affect the total expression of Smad2 or its phosphorylation on Ser245/250/255 (Figure 26B, C). Importantly, the phosphorylation of Smad2 on Ser465/467, was significantly elevated upon CGRP stimulation at all time-points. These results suggest that CGRP/RAMP1 promotes TGF β 1 signalling by activating Smad2 in hepatic stellate cells.

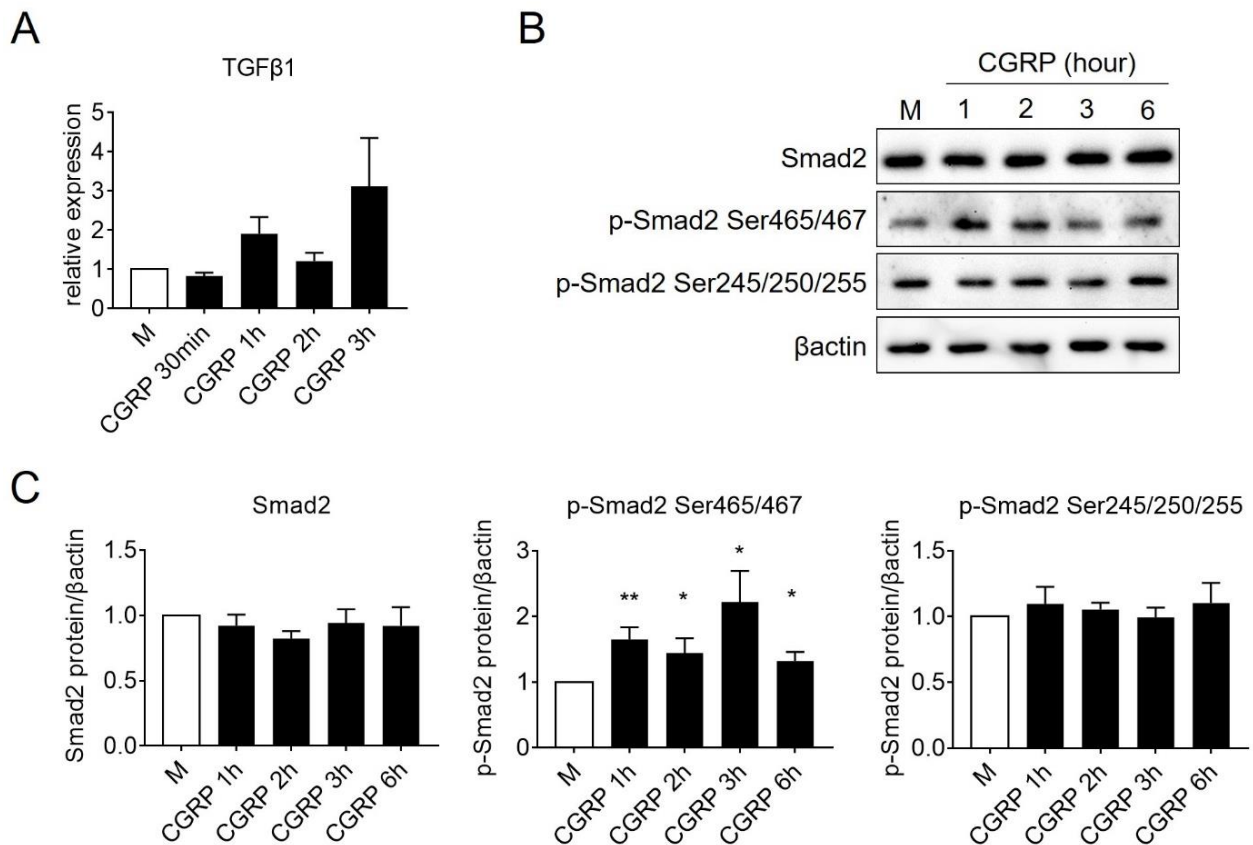


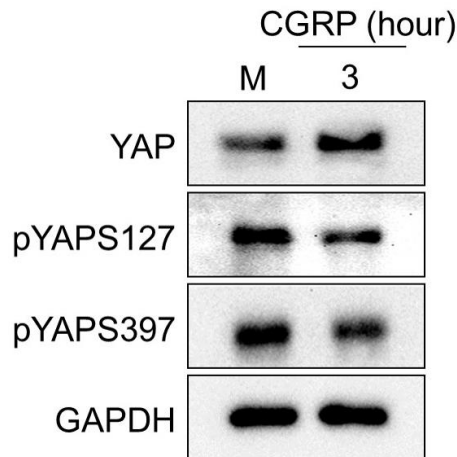
Figure 26. Increased activity of Smad2 in LX-2 cell line stimulated with CGRP. A. mRNA expression of TGFβ1 in LX-2 cells stimulated with CGRP. B. Representative western blot analysis and quantification (C) of p-Smad2 expression in LX-2 cells stimulated with CGRP (n = 4). Results are represented as mean ± SEM. *P < 0.05, **P < 0.01 (two-tailed unpaired Student's t-test or Mann-Whitney U test).

4.13 CGRP/RAMP1 signalling enhances YAP activity in the human primary hepatic stellate cells

We have demonstrated that CGRP signalling promotes YAP activation both in fibrotic mice livers and in the hepatic stellate cell line. To better mimic the *in vivo* situation, we tested the YAP activity in human primary hepatic stellate cells stimulated with CGRP (100nM). Upon 3 hours' stimulation of CGRP, the total YAP expression increased significantly (Figure 27A, B). Furthermore, the stimulation of CGRP decreased the phosphorylation of YAP on both Ser127 and Ser397, indicating that the CGRP treatment attenuated the cytoplasmic retention as well as the degradation of YAP in human primary hepatic stellate

cells. Taken together, the results suggest that CGRP/RAMP1 signalling promotes YAP activation in the human primary hepatic stellate cells.

A



B

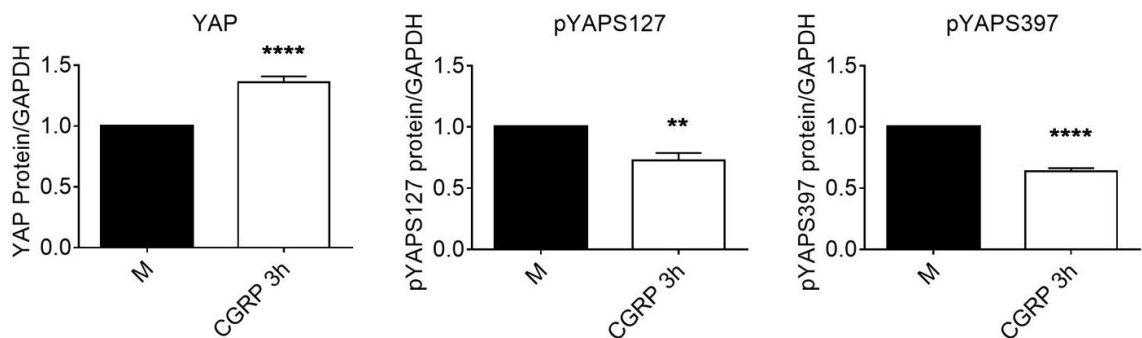


Figure 27. Increased YAP activity in human primary hepatic stellate cells stimulated with CGRP for 3 hours. A. Representative western blot analysis of total and phosphorylated YAP expression in the human primary HSCs stimulated with CGRP. B. Quantification of total and phosphorylated YAP expression in the human primary HSCs (n=4). Results are represented as mean \pm SEM. **P < 0.01, ****P < 0.0001 (two-tailed unpaired Student's t-test or Mann-Whitney U test).

5. Discussion

In human livers, the neuropeptide calcitonin gene-related peptide (CGRP) is mainly found in the autonomic sensory nerves (Franco-Cereceda et al., 1987). The autonomic sensory nerves are known to regulate the function of adrenoreceptors in HSCs, which relates to HSC activation (Oben et al., 2004). Interestingly, in clinic CGRP levels in plasma were significantly increased in cirrhotic patients compared to patients with mild or moderate hepatic steatosis, and increased CGRP levels positively correlated with the severity of cirrhosis (Bendtsen et al., 1991). In both groups of patients, no difference in CGRP level was observed in blood taken from veins that drain the liver, kidney, lung and limb.

The previous results showed that, compared to normal liver tissues, the expression of CGRP and co-receptor activity modifying protein (RAMP1) was highly elevated in cirrhotic liver tissues from mice treated with CCl₄ (Hwang et al., 2006). For the mouse model of bile duct ligation (BDL), which induces acute obstructive jaundice, the increased expression of CGRP was also observed in the liver (Glaser et al., 2007). Moreover, the knockout of α -CGRP reduced cholangiocyte proliferation upon BDL in mice. Furthermore, studies demonstrated that depletion of the neuropeptide CGRP attenuated liver fibrosis, hepatocyte necrosis and inflammation in the bile duct epithelium in the bile duct ligated mice (Wan et al., 2019). In contrast to ligation of the bile duct, CCl₄ mainly exerts its toxic effect in the liver, damaging the endoplasmic reticulum, the mitochondria, and the Golgi apparatus of hepatocytes (Weber et al., 2003). CCl₄ administration better imitates the clinical situation including alcoholic damage or hepatitis virus infection. To induce fibrosis within the murine liver, CCl₄ was injected biweekly for 4 weeks. In our results, we demonstrate that the fibrotic livers from the CCl₄-injected wild type mice express more α CGRP (*Calca*) as well as the CGRP receptor component RAMP1 (*Ramp1*) compared to the untreated wild type mice livers at the RNA level (Figure 6). Another CGRP receptor component, the calcitonin receptor-like receptor (CRLR) (*Crlr*) was not found to be induced upon CCl₄ treatment in wild type mice livers. Notably, CRLR not only acts as a CGRP receptor component, but also heterodimerizes with RAMP2 or RAMP3, forming receptors for adrenomedullin (Chang et al., 2019). Since the HSCs are the main cell type responsible for liver fibrosis, we hypothesised that CGRP/RAMP1 signalling could modulate the activation of HSC during liver fibrosis.

According to our previous study, the absence of the CGRP co-receptor RAMP1 delayed the recovery of liver mass upon partial hepatectomy, and inhibited hepatocyte proliferation (Laschinger et al., 2020). Here, we used the CCl₄ model to induce liver fibrosis in mice. The injection of CCl₄ causes hepatocyte damage, necrosis, inflammation and fibrosis, which better mimic the inflammatory and fibrotic reactions occurring during regeneration in clinic (Dong et al., 2016). Our study demonstrates that CGRP/RAMP1 signalling promotes hepatocyte proliferation upon chronic liver injury induced by CCl₄. The deficiency of CGRP co-receptor RAMP1 reduced the increase of liver-to-body weight ratio after CCl₄ administration (Figure 7A). In the absence of RAMP1, the liver function was ameliorated since alanine aminotransferase (ALT) activity in the serum of CCl₄ injected RAMP1^{-/-} mice was significantly lower upon chronic injury (Figure 7C). ALT is a specific indicator of liver injury because it has a much higher concentration in the liver compared to other tissues (Toita et al., 2018). Thus, we demonstrate that the CGRP/RAMP1 signalling impairs liver function during the chronic liver injury. The analysis of proliferating hepatocytes by Ki67 immunohistochemistry and the cell cycle components revealed that the deficiency of CGRP co-receptor RAMP1 severely diminished the number of proliferating hepatocytes and cell cycle progression in fibrotic livers (Figure 8, 9). Hence, the reduced increase in the liver-to-body weight ratio might be due to the decreased hepatocyte proliferation. Notably, the increase in liver-to-body weight ratio not only relies on hepatocyte proliferation, but also depends on collagen production, the recruitment of inflammatory cells, and the differentiation and proliferation of HSCs. Therefore, the amount of proliferating hepatocytes could not fully reflect the impaired increase of liver mass in RAMP1-deficient mice upon chronic injury. Importantly, the difference between the fibrotic livers of wild type and RAMP1-deficient mice in cell cycle progression was found in the expression of CyclinA2, CyclinB1 and CDK1 on protein level, which regulate the S and G₂/M phases of cell division (Lim et al., 2013). This indicates that the chronic liver injury induced by CCl₄ mainly affects the later period of the cell cycle during hepatocyte proliferation.

Compared to the BDL model which induces an acute obstructive jaundice, the administration of CCl₄ causes cell necrosis, inflammation, fatty infiltration and fibrosis (Alatsakis et al., 2009). It enhances the production of free radicals, the activation of Kupffer cells and the recruitment of neutrophils to the parenchyma, contributing to the damage of healthy cells (Marques et al., 2012). The collagen in fibrotic livers is mainly

Collagen Type I, which accounts for the increasing stiffness of the stroma and the distortion of the liver architecture (Baiocchi et al., 2016). In our study, we found that after a 4-week CCl₄ injection, the fibrous collagen septa formed around the liver lobules, which was detected by Sirius Red staining. The collagen fibres formed different septa lengths between the liver lobes (Figure 10). Upon CCl₄ treatment, the wild-type tissues showed a significantly stronger collagen expression compared to the RAMP1^{-/-} tissues, even with hepatocyte necrosis around the septa. Wild-type tissue showed a fibrous extension of most portal areas with a clear bridging between the liver lobules, and can therefore be classified as grade 4 for liver fibrosis according to Ishak staging (Ishak et al., 1995), while RAMP1^{-/-} tissues only had fibrous expansion of some portal areas with occasional bridging, which can be rated as grade 3. This finding is supported by previous studies demonstrating that α CGRP deficiency led to reduced collagen deposition detected by Sirius Red staining during chronic liver injury induced by BDL (Wan et al., 2019). Although Sirius Red staining has been used to detect the deposition of all collagens, Collagen Type I seems to be the major type of collagens involved in the process of liver fibrosis. Thus, we specifically detected Collagen Type I using the technique of immunohistochemistry in wild type and RAMP1^{-/-} livers. The distribution of Collagen Type I was found to be in similar areas as Sirius Red staining (Figure 12). Western blot analysis of the two chains of Collagen Type I, alpha 1 and alpha 2, also revealed the difference between wild type and RAMP1^{-/-} fibrotic livers. Here, for the first time, we demonstrate that CGRP/RAMP1 signalling promotes collagen deposition, especially Collagen Type I, upon chronic liver injury.

The urokinase plasminogen activator (uPA) was found to be a negative regulator of the extracellular matrix degradation, by promoting the conversion of plasminogen to plasmin and regulating the activity of specific matrix metalloproteinases (MMPs) (Salas et al., 2008). The synthesis and release of uPA in hepatic stellate cells can be induced by the transforming growth factor- β 1 (TGF β 1) signalling, which plays a major role in liver fibrosis (Pérez-Liz et al., 2005). Previous research showed that CCl₄ treatment induces the expression of uPA and uPA receptor (uPAR), which activate MMP13 (Li et al., 2020). MMP13 facilitates the remission of liver fibrosis by promoting the degradation of newly formed matrix. In our study, we found that the mRNA level of uPA (*Plau*) in wild type livers was significantly higher than the RAMP1^{-/-} livers after CCl₄ administration, indicating less fibrogenesis and matrix proteolysis in absence of RAMP1 (Figure 13A). Protein

expression of uPA did not show a significant difference between wild type and RAMP1^{-/-} livers upon chronic injury. However, whether the detected uPA protein was active needs to be further evaluated, e.g. by analysing downstream effector components.

Various inflammatory cytokines are secreted during the process of liver fibrogenesis, including transforming growth factor- β (TGF β), tumour necrosis factor alpha (TNF α) and interleukins (IL). TGF β has been considered a key initiator of liver fibrosis, inducing the activation of HSC (Tu et al., 2014). TNF α and IL-33 are both pleiotropic cytokines produced by immune cells, and have been reported to be highly expressed during CCl₄-induced liver fibrosis (Weiskirchen et al., 2017; Yang et al., 2015). However, the role of TNF α and IL-33 in HSC activation is not fully understood. In our study, we did not observe a difference in the RNA expression of these cytokines between wild type and RAMP1^{-/-} livers upon CCl₄ treatment (Figure 14). Notably, TGF β , TNF α and IL-33 can be expressed in hepatocytes, which account for most of the liver volume (Jing et al., 2019; Meyer et al., 2013; Sakai et al., 2012). Moreover, the expression of these cytokines in hepatocytes has been reported to increase upon liver injury, mediating hepatocyte apoptosis. Therefore, expression analysis of these cytokines in the whole liver might not reflect the impact of CGRP/RAMP1 signalling on the immune response and HSC activation during chronic liver injury.

CCl₄ administration in mice is known to promote the conversion of quiescent HSCs to activated myofibroblasts, consequently producing different types of collagen (Pritchard et al., 2010). The pivotal role of hepatic stellate cells in the progression of liver fibrosis has been unequivocally identified. HSCs express two collagen receptors, integrins and discoidin domain-containing receptors (DDRs) to interact with collagen (Tsuchida et al., 2017). Specific knockout of the collagen receptor subunit α v integrin in HSCs attenuates the liver fibrosis in mice treated with CCl₄ (Henderson et al., 2013). The present study shows that HSCs were activated in fibrotic livers, detected by the immunohistochemistry of alpha smooth muscle actin (α -SMA) (Figure 16). The areas where HSCs were activated coincided well with those areas in which collagens were highly expressed. The activated HSCs were located in close proximity to vascular walls of the hepatic artery and the portal vein, indicating the impact of contracting HSCs on liver microcirculation and portal hypertension. Interestingly, by quantifying the α -SMA protein, our data implicate significantly more activated HSCs in the wild type tissues compared to the RAMP1^{-/-}

tissues upon chronic injury (Figure 15B), which corroborated the results of collagen expression. Thereby, we demonstrate that *in vivo* CGRP/RAMP1 signalling is able to promote HSC activation as well as collagen production upon chronic liver injury.

To explore whether CGRP signalling could directly activate HSCs *in vitro*, we applied the *in vitro* model of the LX-2 cell line. The LX-2 cell line is a widely used immortal source of human HSC, which retains key features of HSCs such as the retinoid phenotype and induced α -SMA expression (Xu et al., 2005). It has been reported that LX-2 cells were activated upon treatment with the pro-fibrotic factor TGF β 1 for 48 hours, up-regulating α -SMA expression and production of Collagen Type I proteins compared to the medium control. However, there has been no study to date demonstrating a potential impact of neuropeptide stimulation on the activation of HSCs. To the best of our knowledge, we are the first to find that LX-2 cells showed a significantly up-regulated expression of α -SMA at later time-points (2, 3 and 6 hours) upon stimulation of the neuropeptide CGRP (Figure 17A, B). By immunofluorescence, we verified that LX-2 cells were α -SMA positive after 6 hours' stimulation of CGRP (Figure 18). Here, we demonstrate that *in vitro* CGRP/RAMP1 signalling directly activates hepatic stellate cells.

During liver fibrosis, HSCs are the main cell type responsible for collagen production (Liang et al., 2013). Collagen Type I is the predominant type of protein implicated in the fibrogenic process, accounting for 30% of all proteins in the fibrotic liver (Spira et al., 2002). In our study, by stimulating LX-2 cells with CGRP, we observed a significantly elevated level of Collagen Type I Alpha 1 chain (Col1a1) expression at all time-points, especially at 6 hours (Figure 19A). Additionally, we detected an increase in Collagen Type I Alpha 2 (Col1a2) at the 1 hour time-point (Figure 19B). Previous studies have pointed out that the Alpha 1 chain is the main component of Collagen Type I, much more abundant than the Alpha 2 chain (Retief et al., 1985). Hence, it is likely that we observed a clearer induction of Col1a1 expression rather than Col1a2 expression in LX-2 cells stimulated with CGRP. Remarkably, the expression of Col1a1 was induced from 1 the hour time-point and was still increasing at the 6 hour time-point, indicating the long duration of its production.

Previous studies have shown that the migration of HSCs toward the injured areas contributes to wound healing and fibrosis processes (Carloni et al., 1997; Guimarães et al., 2015). The neuropeptide CGRP has been reported to promote the spontaneous

migration of human T lymphocytes isolated from healthy blood donors (Talme et al., 2008). Therefore, we examined whether CGRP could enhance the migration of hepatic stellate cells, thereby accelerating the development of liver fibrosis. In the present study, no significant difference in the migratory capacity of CGRP stimulated LX-2 cells compared to controls was detected at all time-points (14h, 18h, 22h) (Figure 25). The migration of LX-2 cells did not seem to be positively affected by the neuropeptide CGRP. Whether CGRP could affect the migration of the primary HSCs still remains to be determined.

Although the treatment of neuropeptide CGRP was found to increase the expression of TGF β 1 in the kidney proximal tubular cell line as well as in cardiac fibroblasts, the effect of CGRP on TGF β 1 expression in liver cells has not been demonstrated (Li et al., 2016; Yoon et al., 2018). Here, our study revealed that the expression of TGF β 1 in LX-2 cells tend to increase upon CGRP stimulation, while the difference was not significant (Figure 26A). Interestingly, the central component of TGF β 1 signalling, the phosphorylation of Smad2 on Ser465/467, was significantly elevated upon CGRP stimulation at all time-points (Figure 26B, C). It is worth noting that some growth factors in the culture serum could affect the expression of TGF- β 1 on the surface of HSCs, including the hepatocyte growth factor (HGF) (Narmada et al., 2013). Hence the intracellular expression of phospho-Smad2 might better reveal the activation of the TGF- β 1 signalling. Thus, these results suggest that CGRP/RAMP1 may promote TGF β 1 signalling by activating Smad2 in LX-2 cells. Interestingly, the elevation of phospho-Smad2 appeared to peak at the 1 hour time-point, indicating that TGF- β 1 signalling responded very fast upon CGRP stimulus. Further, TGF β 1 has been reported to interact with the yes-associated protein (YAP) signalling in the liver. An *in vitro* study found that YAP expression was increased in the rat hepatic stellate cell line HSC-T6 stimulated with TGF- β 1 (Yu et al., 2019). Moreover, the activation of YAP by knockout of the tumour suppressor kinases 1 and 2 (LATS1/2) up-regulated the expression of TGF β 1 in biliary epithelial cells (Lee et al., 2016). These previous data are in line with our results and suggest that CGRP/RAMP1 signalling might positively regulate both YAP activity and TGF β 1 signalling in hepatic stellate cells.

YAP is a key regulator of HSC activation in response to the extracellular matrix stiffness upon liver injury (Maller et al., 2013). YAP was found to be activated and translocate into the nucleus of HSCs in an early phase during CCl₄-induced liver fibrosis (Mannaerts et al., 2015). The blockade of YAP by the inhibitor verteporfin induced the apoptosis of HSCs

and led to reversion to quiescent HSCs (Yu et al., 2019). Moreover, YAP activation has been involved in other signalling pathways known to control liver fibrogenesis, like TGF β , Wnt/ β -catenin, and Notch signals (Piersma et al., 2015; Totaro et al., 2017). It has been reported that the *in vitro* treatment of the rat HSC line HSC-T6 by the pro-fibrotic factor TGF β 1 for 12, 24 and 48 hours leads to the induction of α -SMA and YAP activity. However, to the best of our knowledge, this study is the first to demonstrate the effect of neuropeptides on YAP activity in HSCs. In the present study, we hypothesised that CGRP/RAMP1 might be able to control YAP activity during liver fibrosis, and thus analysed the expression of YAP in the co-receptor RAMP1-deficient mouse model treated with CCl₄. Upon chronic injury, in murine RAMP1^{-/-} mice livers, the phosphorylation of YAP on Ser127 was significantly increased compared to that in the wild type mice livers, indicating more cytoplasmic retention of YAP in RAMP1^{-/-} livers (Figure 20A, B). Notably, a deficiency of RAMP1 did not influence the phosphorylation of YAP on Ser397 in fibrotic mice livers, suggesting that the degradation of YAP *in vivo*, known to be controlled by phosphorylation of YAP on Ser397, was not affected by CGRP/RAMP1 signalling.

The Hippo pathway has been described in numerous studies as a crucial regulator of cell proliferation and differentiation (Hergovich, 2017). In the Hippo pathway, the kinases, mammalian Sterile 20-like kinases 1 and 2 (MST1/2) together with the adaptor protein salvador (SAV), are known to activate LATS1/2 and the monopolar spindle-one-binder (MOB) 1, which in turn phosphorylate and negatively regulate YAP activity (Patel et al., 2017). Several studies have shown the decreased expression of LATS1/2 and MOB1 as well as elevated YAP activity in the livers of the CCl₄ administered rat model (Mohseni et al., 2020; Perumal et al., 2017). Still, whether CGRP/RAMP1 signalling has an effect on liver fibrosis through regulating YAP activity has not been previously demonstrated. In the present study, upon chronic injury, we detected more activated LATS1/2 and MOB1 in the RAMP1^{-/-} mice livers compared to wild type mice livers (Figure 20C, D), suggesting that YAP is inactivated in the RAMP1^{-/-} livers.

When YAP is activated, it promotes the transcription of the target genes, including *Ctgf*, *Thbs1*, *Ankrd1*, *Bird5* and *Foxm1* (Haskins et al., 2014). The transcription of these genes may activate hepatic stellate cells and stimulate the deposition and remodelling of the extracellular matrix (Filliol et al., 2020; Lipson et al., 2012; Mannaerts et al., 2015; Wang et al., 2011). Previous studies have shown that *Ctgf* and *Ankrd1* expression was highly

induced in the livers upon CCl₄-induced fibrosis (Mannaerts et al., 2015; Park et al., 2016). In our study, we did not observe a difference in the expression of *Ctgf*, *Thbs1*, *Ankrd1*, *Bird5* and *Foxm1* between wild type and RAMP1^{-/-} livers upon CCl₄ treatment (Figure 21). This might be due to the late time-point of liver harvest after CCl₄ administration. *Ctgf* expression has been reported to be induced in fibrotic livers of CCl₄-treated mice or rats, which were harvested 4 hours or 1 day after the last injection (Chen et al., 2020; Zhou et al., 2015). In the present study, livers were harvested 3 days after the last dose of CCl₄, which might affect the gene expression. Importantly, the cell cycle regulators, Cyclins A and B, and CDK1, are also known to be target genes of YAP (Di Agostino et al., 2016; Loforese et al., 2017; Zanconato et al., 2015). Our previous study has demonstrated that the expression of these YAP target genes is reduced in RAMP1^{-/-} mice livers upon partial hepatectomy-induced acute injury, which is associated with impaired YAP activity (Laschinger et al., 2020). In the present study, the expression level of these genes was reduced in RAMP1-deficient livers upon chronic injury (Figure 9). Together, we suggest that CGRP/RAMP1 signalling promotes YAP activation and the transcription of target genes during liver fibrosis.

As a central pathway that controls cell proliferation and activation, the Hippo pathway is regulated by some extracellular mediators. However, to date there has been no study demonstrating the influence of the neuropeptide CGRP signalling on the Hippo pathway during HSC activation. When binding to its receptor complex on the cell surface, composed of CRLR and RAMP1, CGRP activates intracellular signals via either Gα_s or Gα_{q/11} proteins (Deng et al., 2017; Feng et al., 2014). *In vitro*, signalling via Gα_{q/11} protein was reported to increase YAP activity in the human embryonic kidney cell line HEK293A, whereas signalling via Gα_s protein could negatively regulate YAP activity in primary Schwann cells (Deng et al., 2017; Yu et al., 2012). Interestingly, our study observed a significant induction of the Gα₁₁ expression in the livers from CCl₄-treated wild type mice compared to those from untreated wild type mice (Figure 22). Here, for the first time, we hypothesise that the *in vivo* CGRP/RAMP1 complex controls YAP activity via Gα₁₁ protein in the murine livers during liver fibrosis. Furthermore, it has been reported that the expression of mutant Gα₁₁ *in vitro* resulted in the activation of the c-Jun N-terminal kinase (JNK) through a pathway involving protein kinase C (Thomas et al., 2016). The activity of JNK is related to HSC activation during liver fibrosis (Jiang et al., 2017). Taken together, we suggest that CGRP/RAMP1 signalling might activate YAP via the Gα₁₁ protein, thus

promoting HSC activation upon chronic liver injury.

Our *in vivo* data demonstrate that CGRP/RAMP1 signalling positively regulates YAP activity during liver fibrosis. To test whether CGRP/RAMP1 signalling could increase YAP activity specifically in HSCs, we used the human hepatic stellate cell line LX-2. Several studies have shown that active α -SMA-positive LX-2 cells up-regulate the YAP protein and express target genes of YAP including *Ctgf* and *Ankrd1* (Lee et al., 2019; Perumal et al., 2017; Xiang et al., 2020). By treatment with liquiritigenin, an aglycone of liquiritin and also a hepatic protectant, LATS1/2 was shown to be activated, thus inhibiting YAP activity in LX-2 cells (Lee et al., 2019). In our study, upon neuropeptide CGRP treatment, total YAP expression increased at the 2 hour time-point (Figure 23A, B). Although, CGRP did not affect the phosphorylation of YAP on Ser127, it could significantly decrease YAP phosphorylation on Ser397 at the 2 and 3 hour time-points. The results indicate that CGRP directly increases YAP activity by decreasing its degradation in LX-2 cells. Importantly, our *in vivo* data demonstrate that CGRP/RAMP1 signalling positively regulates YAP activity by decreasing its cytoplasmic retention during liver fibrosis, as indicated by the decreased phosphorylation of YAP on Ser127 (Figure 20). Therefore, the mechanism by which CGRP/RAMP1 signalling promotes the nuclear translocation of YAP in HSCs seems to be different in the mouse model of CCl₄ and in LX-2 cells. Further, the down-regulation of phospho-LATS1/2 appeared at the 3 and 6 hour time-points, and phospho-MOB1 expression was reduced at the 3 hour time-point upon stimulation with CGRP (Figure 23C, D). Notably, the LATS1/2-MOB1 complex has been reported to phosphorylate YAP on Ser127 which sequesters YAP in the cytoplasm (Zhao et al., 2020). But whether LATS1/2-MOB1 complex could directly phosphorylate YAP on Ser397 remains unknown. By using immunofluorescence staining, we detected the translocation of YAP into the nucleus of LX-2 cells upon 6 hours' stimulation of CGRP (Figure 24). Altogether, these results demonstrate that CGRP/RAMP1 signalling triggers the activation of YAP by inducing its nuclear translocation in hepatic stellate cells.

Our previous study demonstrated that the primary hepatocytes isolated from the human liver acquired an increased YAP expression upon CGRP treatment, indicating that CGRP/RAMP1 signalling *in vitro* directly caused the up-regulation of YAP activity in hepatocytes (Laschinger et al., 2020). It has also been reported that primary HSCs isolated from fibrotic livers of CCl₄-treated mice expressed elevated YAP, and that the

knockdown of YAP inhibited the activation of primary HSCs (Mannaerts et al., 2015; Yu et al., 2019). In our study, we demonstrate that primary hepatic stellate cells from patients not only express increased YAP protein upon CGRP stimulation, but also showed the decreased phosphorylation of YAP on both Ser127 and Ser397 upon CGRP. These results indicate that the CGRP treatment attenuates cytoplasmic retention as well as the degradation of YAP in human primary hepatic stellate cells (Figure 27A, B). Thus, we demonstrate that CGRP/RAMP1 signalling promotes YAP activation in human primary hepatic stellate cells.

Taken together, our data suggest that CGRP/RAMP1 signalling promotes hepatocyte proliferation and HSC activation by regulating YAP activity during chronic liver injury (Figure 28).

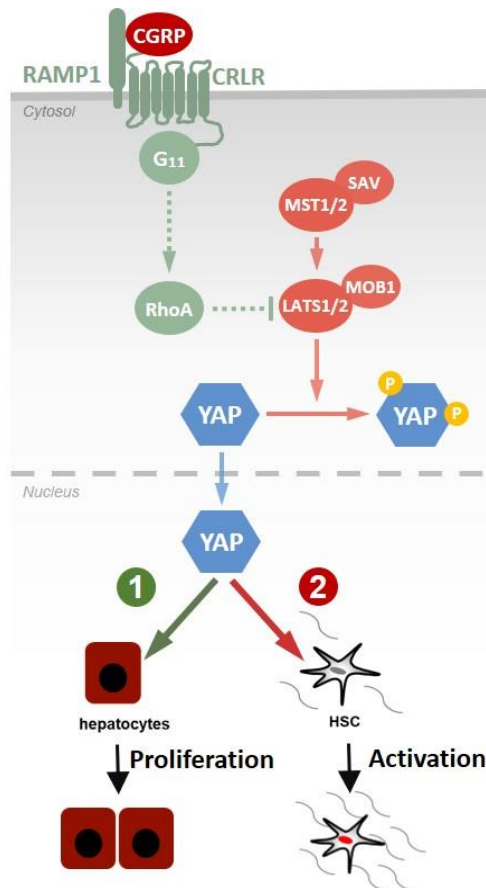


Figure 28. CGRP/RAMP1 signaling promotes hepatocytes proliferation and the activation of hepatic stellate cells (HSCs) through regulating YAP activity during chronic liver injury. CGRP binds to its receptor complex consisting of CRLR and RAMP1. The signal is transmitted into the cell, and inhibits LATS1/2 and MOB1, probably via G_{α11}, thus activating YAP. The activation of YAP consequently promotes hepatocyte proliferation and HSC activation.

Researchers have made great progress in understanding the mechanisms of liver fibrosis and discovered different methods of therapy. The strategies include eliminating the causes of fibrosis (hepatitis viruses, alcohol damage), inhibiting the activation of HSCs and increasing the ECM degradation (Koyama et al., 2015). However, the pivotal player in liver fibrosis, namely HSCs, cannot be reached easily in the liver because of its low proportion in the total cells. Hence, the delivery of targeted medicine to HSCs is critical for the success of treatment, and can avoid extrahepatic complications. Interestingly, our study found that the expression of α CGRP (*Calca*) as well as the CGRP receptor component RAMP1 (*Ramp1*) is highly induced in murine fibrotic livers upon chronic injury. In addition, our preliminary data suggest that livers from cirrhotic patients express more α CGRP (*Calca*), β CGRP (*Calcb*) and RAMP1 (*Ramp1*) compared to normal livers. More importantly, we demonstrate that CGRP/RAMP1 has a role as a pro-fibrotic factor, and specifically promotes HSC activation during liver fibrogenesis. Therefore, therapeutic agents targeted at the CGRP receptor and its downstream signalling pathways might provide a novel strategy for the treatment of liver fibrosis.

6. Summary

In the present study, we explored the role of the CGRP/RAMP1 signalling in the development of liver fibrosis by using the RAMP1 global knockout mouse model. Here, we demonstrate that expression of the CGRP signalling components CRLR and RAMP1 are induced during liver fibrosis in mice upon CCl₄ administration. We found that CGRP/RAMP1 signalling increases the liver-to-body weight ratio and promotes hepatocyte proliferation during chronic liver injury. Importantly, CGRP/RAMP1 signalling promotes collagen deposition in murine livers after CCl₄ administration, accelerating the process of fibrosis. Furthermore, our data suggest that CGRP/RAMP1 signalling positively regulates the activity of the Hippo pathway effector YAP, thus promoting HSC activation during liver fibrosis. *In vitro*, CGRP stimulation directly activates the LX-2 cell line and enhances YAP activity in both LX-2 cells and human primary HSCs. Additionally, CGRP/RAMP1 promotes TGFβ1 signalling by activating Smad2 in LX-2 cells. Therefore, the CGRP/RAMP1 signalling components may act as a potential target of anti-fibrotic therapy for liver disease.

7. Abbreviations

ALT	Alanine aminotransferase
α -SMA	Alpha smooth muscle actin
BDL	Bile duct ligation
cAMP	Cyclic adenosine monophosphate
CGRP	Calcitonin gene-related peptide
CCl ₄	Carbon tetrachloride
CRLR	Calcitonin receptor-like receptor
CTGF	Connective tissue growth factor
Col1a1	Collagen Type I Alpha chain 1
Col1a2	Collagen Type I Alpha chain 2
CREB	cAMP response element-binding protein
DC	Dendritic cell
DDR	Discoid cell domain receptor
ECM	Extracellular matrix
EGF	Epidermal growth factor
EMT	Epithelial-to-mesenchymal transition
FGF	Fibroblast growth factor
GPCR	G protein-coupled receptors
HGF	Hepatocyte growth factor
HSC	Hepatic stellate cell
IL	Interleukin
KC	Kupffer cell
LATS1/2	Tumor suppressor kinases 1 and 2
LBW	Liver-to-body weight
LOX	Lysyl oxidase
LSEC	Liver sinusoidal endothelial cell
MOB	Monopolar spindle-one-binder
MMP	Metalloproteinase
MST	Mammalian Sterile 20-like kinases

NK	Natural killer cell
NPY	Neuropeptide tyrosine
PDGF	Platelet derived growth factor
PKA	Protein kinase A
PKC	Protein kinase C
PLC β	Phospholipase C- β
RAMP1	Receptor activity modifying protein
RCP	Receptor component protein
SAV	Salvador
SNS	Sympathetic nervous system
SPP1	Secreted phosphoprotein 1
TAZ	Transcriptional co-activator with PDZ-binding motif
T β R	T β R
TEAD	TEA domain
TGF β	Transforming growth factor- β
TIMP	Tissue inhibitor of metalloproteinases
TNF α	Tumor necrosis factor alpha
uPA	Urokinase plasminogen activator
VEGF	Vascular endothelial growth factor
VIP	Vasoactive intestinal polypeptide
VP	Verteporfin
YAP	Yes-associated protein

8. List of Figures

Figure 1. The location of liver cells and the dual blood supply	4
Figure 2. Liver injury leads to the conversion of quiescent HSC to activated HSC (myofibroblasts)	7
Figure 3. Regulation of the YAP signaling pathway	12
Figure 4. Anatomy of vagal and spinal afferent innervation of the liver	14
Figure 5. Composition of the CGRP receptor complex	17
Figure 6. Induced expression of CGRP isoforms and receptor subunits during liver fibrosis in mice	42
Figure 7. Liver-to-body weight ratio and serum ALT activity is affected by RAMP1 deficiency	44
Figure 8. Reduced amounts of Ki67-positive proliferating hepatocytes in fibrotic livers of RAMP1 ^{-/-} mice compared to wild type mice	46
Figure 9. Decreased expression of cell cycle regulators in fibrotic livers of RAMP1 ^{-/-} mice compared to wild type mice	47
Figure 10. Reduced collagen fibers in fibrotic livers of RAMP1 ^{-/-} mice compared to wild type mice	48
Figure 11. Reduced expression of collagen in fibrotic livers of RAMP1 ^{-/-} mice compared to wild type mice	49
Figure 12. Less expression of collagen in fibrotic livers of RAMP1 ^{-/-} mice compared to wild type mice	50
Figure 13. Decreased uPA expression on RNA and protein levels in fibrotic livers of RAMP1 ^{-/-} mice compared to wild type mice	51
Figure 14. mRNA expression of modulators in fibrotic livers of wild type and RAMP1 ^{-/-} mice.....	52
Figure 15. Reduced α -SMA expression in fibrotic livers of RAMP1 ^{-/-} mice compared to wild type mice	53
Figure 16. Reduced expression of α -SMA in fibrotic livers of RAMP1 ^{-/-} mice compared to wild type mice	54
Figure 17. Induced expression of α -SMA in LX-2 cells stimulated by CGRP	55
Figure 18. Induced expression of α -SMA in LX-2 cells stimulated with CGRP	56
Figure 19. Induced expression of Collagen Type I in LX-2 cells stimulated with CGRP	57

Figure 20. Increased expression of YAP and decreased expression of the upstream regulators in fibrotic livers of RAMP1 ^{-/-} mice compared to wild type mice	59
Figure 21. mRNA Expression of YAP target genes in fibrotic livers of wild type and RAMP1 ^{-/-} mice	60
Figure 22. Induced mRNA expression of Gα ₁₁ protein in wild type mice livers upon CCl ₄ treatment	61
Figure 23. Increased expression of YAP and decreased expression of the upstream regulators in LX-2 cells stimulated with CGRP	62
Figure 24. YAP translocated from the cytoplasm into the nucleus of LX-2 cells upon 6 hours' stimulation of CGRP	63
Figure 25. Migration of LX-2 cells was not affected by CGRP stimulation	64
Figure 26. Increased activity of Smad2 in LX-2 cell line stimulated with CGRP	66
Figure 27. Increased YAP activity in human primary hepatic stellate cells stimulated with CGRP for 3 hours	67
Figure 28. CGRP/RAMP1 signaling promotes hepatocytes proliferation and the activation of hepatic stellate cells (HSCs) through regulating YAP activity during chronic liver injury	77

9. References

- Akiyoshi, H., Gonda, T., Terada, T. (1998). A comparative histochemical and immunohistochemical study of aminergic, cholinergic and peptidergic innervation in rat, hamster, guinea pig, dog and human livers. *Liver*, 18(5), 352-359.
- Alatsakis, M., Ballas, K. D., Pavlidis, T. E., Psarras, K., Rafailidis, S., Tzioufa-Asimakopoulou, V., Marakis, G. N., Sakantamis, A. K. (2009). Early propranolol administration does not prevent development of esophageal varices in cirrhotic rats. *Eur Surg Res*, 42(1), 11-16.
- Baiocchi, A., Montaldo, C., Conigliaro, A., Grimaldi, A., Correani, V., Mura, F., Ciccocanti, F., Rotiroti, N., Brenna, A., Montalbano, M., D'Offizi, G., Capobianchi, M. R., Alessandro, R., Piacentini, M., Schininà, M. E., Maras, B., Del Nonno, F., Tripodi, M., Mancone, C. (2016). Extracellular Matrix Molecular Remodeling in Human Liver Fibrosis Evolution. *PLoS One*, 11(3), e0151736-e0151749.
- Banales, J. M., Huebert, R. C., Karlsen, T., Strazzabosco, M. (2019). Cholangiocyte pathobiology. *Nat Rev Gastroenterol Hepatol*, 16(5), 269-281.
- Ben-Moshe, S., Itzkovitz, S. (2019). Spatial heterogeneity in the mammalian liver. *Nat Rev Gastroenterol Hepatol*, 16(7), 395-410.
- Bendtsen, F., Schifter, S., Henriksen, J. H. (1991). Increased circulating calcitonin gene-related peptide (CGRP) in cirrhosis. *J Hepatol*, 12(1), 118-123.
- Berthoud, H.-R. (2004). Anatomy and function of sensory hepatic nerves. *Anat Rec A Discov Mol Cell Evol Biol*, 280(1), 827-835.
- Berthoud, H. R., Powley, T. L. (1996). Interaction between parasympathetic and sympathetic nerves in prevertebral ganglia: morphological evidence for vagal efferent innervation of ganglion cells in the rat. *Microsc Res Tech*, 35(1), 80-86.
- Bissell, D. M., Wang, S. S., Jarnagin, W. R., Roll, F. J. (1995). Cell-specific expression of transforming growth factor-beta in rat liver. Evidence for autocrine regulation of hepatocyte proliferation. *J Clin Invest*, 96(1), 447-455.
- Bonnans, C., Chou, J., Werb, Z. (2014). Remodelling the extracellular matrix in development and disease. *Nat Rev Mol Cell Biol*, 15(12), 786-801.
- Boyce, S., Harrison, D. (2008). A detailed methodology of partial hepatectomy in the mouse. *Lab Anim (NY)*, 37(11), 529-532.
- Busnadiego, O., González-Santamaría, J., Lagares, D., Guinea-Viniegra, J., Pichol-Thievend, C., Muller, L., Rodríguez-Pascual, F. (2013). LOXL4 is induced by

- transforming growth factor β 1 through Smad and JunB/Fra2 and contributes to vascular matrix remodeling. *Mol Cell Biol*, 33(12), 2388-2401.
- Carloni, V., Romanelli, R. G., Pinzani, M., Laffi, G., Gentilini, P. (1997). Focal adhesion kinase and phospholipase C gamma involvement in adhesion and migration of human hepatic stellate cells. *Gastroenterology*, 112(2), 522-531.
- Chang, C. L., Hsu, S. Y. T. (2019). Development of chimeric and bifunctional antagonists for CLR/RAMP receptors. *PLoS One*, 14(5), e0216996-e0217015.
- Chen, W., Li, Y., Hsu, C. T., Niu, C. S., Pen, W. H., Cheng, K. C., Niu, H. S. (2020). Connective tissue growth factor in hepatocytes is elevated by carbon tetrachloride via STAT3 activation. *Mol Med Rep*, 21(3), 1390-1398.
- Cheung, P. Y., Zhang, Q., Zhang, Y. O., Bai, G. R., Lin, M. C., Chan, B., Fong, C. C., Shi, L., Shi, Y. F., Chun, J., Kung, H. F., Yang, M. (2006). Effect of WeiJia on carbon tetrachloride induced chronic liver injury. *World J Gastroenterol*, 12(12), 1912-1917.
- Corlu, A., Loyer, P. (2015). Culture Conditions Promoting Hepatocyte Proliferation and Cell Cycle Synchronization. *Methods Mol Biol*, 1250, 27-51.
- Cottrell, G. S. (2019). CGRP Receptor Signalling Pathways. *Handb Exp Pharmacol*, 255, 37-64.
- Curado, S., Stainier, D. Y. (2010). deLiver'in regeneration: injury response and development. *Semin Liver Dis*, 30(3), 288-295.
- Dan, I., Watanabe, N. M., Kusumi, A. (2001). The Ste20 group kinases as regulators of MAP kinase cascades. *Trends Cell Biol*, 11(5), 220-230.
- Das, M., Boerma, M., Goree, J. R., Lavoie, E. G., Fausther, M., Gubrij, I. B., Pangle, A. K., Johnson, L. G., Dranoff, J. A. (2014). Pathological changes in pulmonary circulation in carbon tetrachloride (CCl₄)-induced cirrhotic mice. *PLoS One*, 9(4), e96043-e96050.
- Deng, Y., Wu, L. M. N. (2017). A reciprocal regulatory loop between TAZ/YAP and G-protein G α s regulates Schwann cell proliferation and myelination. *Nat Commun*, 8, 15161-15175.
- Dewidar, B., Meyer, C., Dooley, S., Meindl-Beinker, A. N. (2019). TGF- β in Hepatic Stellate Cell Activation and Liver Fibrogenesis-Updated 2019. *Cells*, 8(11), 1419-1451.
- Di Agostino, S., Sorrentino, G., Ingallina, E., Valenti, F., Ferraiuolo, M., Biccato, S., Piazza, S., Strano, S., Del Sal, G., Blandino, G. (2016). YAP enhances the pro-

- proliferative transcriptional activity of mutant p53 proteins. *EMBO reports*, 17(2), 188-201.
- Dickerson, I. M. (2013). Role of CGRP-receptor component protein (RCP) in CLR/RAMP function. *Curr Protein Pept Sci*, 14(5), 407-415.
- Dixon, L. J., Barnes, M., Tang, H., Pritchard, M. T., Nagy, L. E. (2013). Kupffer cells in the liver. *Compr Physiol*, 3(2), 785-797.
- Dong, S., Chen, Q. L., Song, Y. N., Sun, Y., Wei, B., Li, X. Y., Hu, Y. Y., Liu, P., Su, S. B. (2016). Mechanisms of CCl₄-induced liver fibrosis with combined transcriptomic and proteomic analysis. *J Toxicol Sci*, 41(4), 561-572.
- Dooley, S., Streckert, M., Delvoux, B., Gressner, A. M. (2001). Expression of Smads during in vitro transdifferentiation of hepatic stellate cells to myofibroblasts. *Biochemical and biophysical research communications*, 283(3), 554-562.
- Downes, G. B., Gautam, N. (1999). The G protein subunit gene families. *Genomics*, 62(3), 544-552.
- Drissi, H., Lasmoles, F., Le Mellay, V., Marie, P. J., Lieberherr, M. (1998). Activation of phospholipase C-beta1 via Galphaq/11 during calcium mobilization by calcitonin gene-related peptide. *J Biol Chem*, 273(32), 20168-20174.
- El Taghdouini, A., van Grunsven, L. A. (2016). Epigenetic regulation of hepatic stellate cell activation and liver fibrosis. *Expert Rev Gastroenterol Hepatol*, 10(12), 1397-1408.
- Ellis, E. L., Mann, D. A. (2012). Clinical evidence for the regression of liver fibrosis. *J Hepatol*, 56(5), 1171-1180.
- Elsharkawy, A. M., Oakley, F., Mann, D. A. (2005). The role and regulation of hepatic stellate cell apoptosis in reversal of liver fibrosis. *Apoptosis*, 10(5), 927-939.
- Fasbender, F., Widera, A., Hengstler, J. G., Watzl, C. (2016). Natural Killer Cells and Liver Fibrosis. *Front Immunol*, 7, 19-25.
- Fausto, N. (2004). Liver regeneration and repair: hepatocytes, progenitor cells, and stem cells. *Hepatology*, 39(6), 1477-1487.
- Feng, X., Degese, M. S., Iglesias-Bartolome, R., Vaque, J. P., Molinolo, A. A., Rodrigues, M., Zaidi, M. R., Ksander, B. R., Merlino, G., Sodhi, A., Chen, Q., Gutkind, J. S. (2014). Hippo-independent activation of YAP by the GNAQ uveal melanoma oncogene through a trio-regulated rho GTPase signaling circuitry. *Cancer Cell*, 25(6), 831-845.
- Filliol, A., Schwabe, R. F. (2020). FoxM1 Induces CCl₂ Secretion From Hepatocytes

- Triggering Hepatic Inflammation, Injury, Fibrosis, and Liver Cancer. *Cell Mol Gastroenterol Hepatol*, 9(3), 555-556.
- Fisher, L. A., Kikkawa, D. O., Rivier, J. E., Amara, S. G., Evans, R. M., Rosenfeld, M. G., Vale, W. W., Brown, M. R. (1983). Stimulation of noradrenergic sympathetic outflow by calcitonin gene-related peptide. *Nature*, 305(5934), 534-536.
- Franco-Belussi, L., Santos, L. R., Zieri, R., Vicentini, C. A., Taboga, S. R., de Oliveira, C. (2012). Liver anatomy, histochemistry, and ultrastructure of *Eupemphix nattereri* (Anura: Leiuperidae) during the breeding season. *Zoolog Sci*, 29(12), 844-848.
- Franco-Cereceda, A., Henke, H., Lundberg, J. M., Petermann, J. B., Hökfelt, T., Fischer, J. A. (1987). Calcitonin gene-related peptide (CGRP) in capsaicin-sensitive substance P-immunoreactive sensory neurons in animals and man: distribution and release by capsaicin. *Peptides*, 8(2), 399-410.
- Frevert, U., Engelmann, S., Zougbedé, S., Stange, J., Ng, B., Matuschewski, K., Liebes, L., Yee, H. (2005). Intravital Observation of *Plasmodium berghei* Sporozoite Infection of the Liver. *PLoS Biol*, 3(6), e192-e205.
- Friedman, S. L. (2008). Hepatic stellate cells: protean, multifunctional, and enigmatic cells of the liver. *Physiol Rev*, 88(1), 125-172.
- Frolik, C. A., Dart, L. L., Meyers, C. A., Smith, D. M., Sporn, M. B. (1983). Purification and initial characterization of a type beta transforming growth factor from human placenta. *Proc Natl Acad Sci U S A*, 80(12), 3676-3680.
- Gardemann, A., Püschel, G. P., Jungermann, K. (1992). Nervous control of liver metabolism and hemodynamics. *Eur J Biochem*, 207(2), 399-411.
- Gaul, S., Leszczynska, A., Alegre, F., Kaufmann, B., Johnson, C. D., Adams, L. A., Wree, A., Damm, G., Seehofer, D., Calvente, C. J., Povero, D., Kisseleva, T., Eguchi, A., McGeough, M. D., Hoffman, H. M., Pelegrin, P., Laufs, U., Feldstein, A. E. (2021). Hepatocyte pyroptosis and release of inflammasome particles induce stellate cell activation and liver fibrosis. *J Hepatol*, 74(1), 156-167.
- Glaser, S. S., Ueno, Y., DeMorrow, S., Chiasson, V. L., Katki, K. A., Venter, J., Francis, H. L., Dickerson, I. M., DiPette, D. J., Supowit, S. C., Alpini, G. D. (2007). Knockout of alpha-calcitonin gene-related peptide reduces cholangiocyte proliferation in bile duct ligated mice. *Lab Invest*, 87(9), 914-926.
- Grunebaum, E., Avitzur, Y. (2019). Liver-associated immune abnormalities. *Autoimmun Rev*, 18(1), 15-20.
- Guimarães, E. L., Stradiot, L., Mannaerts, I., Schroyen, B., van Grunsven, L. A. (2015).

- P311 modulates hepatic stellate cells migration. *Liver Int*, 35(4), 1253-1264.
- Haskins, J. W., Nguyen, D. X., Stern, D. F. (2014). Neuregulin 1-activated ERBB4 interacts with YAP to induce Hippo pathway target genes and promote cell migration. *Sci Signal*, 7(355), ra116-ra116.
- Hellerbrand, C., Stefanovic, B., Giordano, F., Burchardt, E. R., Brenner, D. A. (1999). The role of TGFbeta1 in initiating hepatic stellate cell activation in vivo. *J Hepatol*, 30(1), 77-87.
- Henderson, N. C., Arnold, T. D., Katamura, Y., Giacomini, M. M., Rodriguez, J. D., McCarty, J. H., Pellicoro, A., Raschperger, E., Betsholtz, C., Ruminski, P. G., Griggs, D. W., Prinsen, M. J., Maher, J. J., Iredale, J. P., Lacy-Hulbert, A., Adams, R. H., Sheppard, D. (2013). Targeting of αv integrin identifies a core molecular pathway that regulates fibrosis in several organs. *Nat Med*, 19(12), 1617-1624.
- Hergovich, A. (2017). YAP needs Nemo to guide a Hippo. *EMBO reports*, 18(1), 3-4.
- Herrera, J., Henke, C. A., Bitterman, P. B. (2018). Extracellular matrix as a driver of progressive fibrosis. *J Clin Invest*, 128(1), 45-53.
- Higashi, T., Friedman, S. L., Hoshida, Y. (2017). Hepatic stellate cells as key target in liver fibrosis. *Adv Drug Deliv Rev*, 121, 27-42.
- Hinz, B., Phan, S. H., Thannickal, V. J., Galli, A., Bochaton-Piallat, M.-L., Gabbiani, G. (2007). The myofibroblast: one function, multiple origins. *Am J Pathol*, 170(6), 1807-1816.
- Holzmann, B. (2013). Antiinflammatory activities of CGRP modulating innate immune responses in health and disease. *Curr Protein Pept Sci*, 14(4), 268-274.
- Hsu, C. T. (1992). The role of the sympathetic nervous system in promoting liver cirrhosis induced by carbon tetrachloride, using the essential hypertensive animal (SHR). *J Auton Nerv Syst*, 37(3), 163-173.
- Huang, G., Jiang, H., Lin, Y., Xia, W., Luo, Y., Wu, Y., Cai, W., Zhou, X., Jiang, X. (2018). LncGPR107 drives the self-renewal of liver tumor initiating cells and liver tumorigenesis through GPR107-dependent manner. *J Exp Clin Cancer Res*, 37(1), 121-133.
- Huang, Y., de Boer, W. B., Adams, L. A., MacQuillan, G., Rossi, E., Rigby, P., Raftopoulos, S. C., Bulsara, M., Jeffrey, G. P. (2013). Image analysis of liver collagen using sirius red is more accurate and correlates better with serum fibrosis markers than trichrome. *Liver Int*, 33(8), 1249-1256.
- Huang, Y., Deng, X., Liang, J. (2017). Modulation of hepatic stellate cells and

- reversibility of hepatic fibrosis. *Exp Cell Res*, 352(2), 420-426.
- Hwang, I. S., Tang, F., Leung, P. P., Li, Y. Y., Fan, S. T., Luk, J. M. (2006). The gene expression of adrenomedullin, calcitonin-receptor-like receptor and receptor activity modifying proteins (RAMPs) in CCl₄-induced rat liver cirrhosis. *Regul Pept*, 135(1-2), 69-77.
- Iredale, J. P., Thompson, A., Henderson, N. C. (2013). Extracellular matrix degradation in liver fibrosis: Biochemistry and regulation. *Biochim Biophys Acta*, 1832(7), 876-883.
- Ishak, K., Baptista, A., Bianchi, L., Callea, F., De Groote, J., Gudat, F., Denk, H., Desmet, V., Korb, G., MacSween, R. N., et al. (1995). Histological grading and staging of chronic hepatitis. *J Hepatol*, 22(6), 696-699.
- Jiang, M., Wu, Y. L., Li, X., Zhang, Y., Xia, K. L., Cui, B. W., Lian, L. H., Nan, J. X. (2017). Oligomeric proanthocyanidin derived from grape seeds inhibited NF- κ B signaling in activated HSC: Involvement of JNK/ERK MAPK and PI3K/Akt pathways. *Biomed Pharmacother*, 93, 674-680.
- Jing, Z. T., Liu, W., Xue, C. R., Wu, S. X., Chen, W. N., Lin, X. J., Lin, X. (2019). AKT activator SC79 protects hepatocytes from TNF- α -mediated apoptosis and alleviates d-Gal/LPS-induced liver injury. *Am J Physiol Gastrointest Liver Physiol*, 316(3), G387-G396.
- Johnson, R., Halder, G. (2014). The two faces of Hippo: targeting the Hippo pathway for regenerative medicine and cancer treatment. *Nat Rev Drug Discov*, 13(1), 63-79.
- Kandilis, A. N., Papadopoulou, I. P., Koskinas, J., Sotiropoulos, G., Tiniakos, D. G. (2015). Liver innervation and hepatic function: new insights. *J Surg Res*, 194(2), 511-519.
- Kee, Z., Kodji, X., Brain, S. D. (2018). The Role of Calcitonin Gene Related Peptide (CGRP) in Neurogenic Vasodilation and Its Cardioprotective Effects. *Front Physiol*, 9, 1249-1261.
- Kmieć, Z. (2001). Cooperation of liver cells in health and disease. *Adv Anat Embryol Cell Biol*, 161, 1-151.
- Konishi, T., Schuster, R. M., Lentsch, A. B. (2018). Proliferation of hepatic stellate cells, mediated by YAP and TAZ, contributes to liver repair and regeneration after liver ischemia-reperfusion injury. *Am J Physiol Gastrointest Liver Physiol*, 314(4), G471-G482.
- Koyama, Y., Brenner, D. A. (2015). New therapies for hepatic fibrosis. *Clinics and*

- research in hepatology and gastroenterology*, 39 Suppl 1(0 1), S75-S79.
- Koyama, Y., Brenner, D. A. (2017). Liver inflammation and fibrosis. *J Clin Invest*, 127(1), 55-64.
- Kulkarni, T., O'Reilly, P., Antony, V. B., Gaggar, A., Thannickal, V. J. (2016). Matrix Remodeling in Pulmonary Fibrosis and Emphysema. *Am J Respir Cell Mol Biol*, 54(6), 751-760.
- Kuo, T., Ouchi, Y., Kim, S., Toba, K., Orimo, H. (1994). The role of activation of the sympathetic nervous system in the central pressor action of calcitonin gene-related peptide in conscious rats. *Naunyn Schmiedebergs Arch Pharmacol*, 349(4), 394-400.
- Laschinger, M., Wang, Y., Holzmann, G., Wang, B., Stöß, C., Lu, M., Brugger, M., Schneider, A., Knolle, P., Wohlleber, D., Schulze, S., Steiger, K., Tsujikawa, K., Altmayr, F., Friess, H., Hartmann, D., Hüser, N., Holzmann, B. (2020). The CGRP receptor component RAMP1 links sensory innervation with YAP activity in the regenerating liver. *Faseb j*, 34(6), 8125-8138.
- Lee, D. H., Park, J. O., Kim, T. S., Kim, S. K., Kim, T. H., Kim, M. C., Park, G. S., Kim, J. H., Kuninaka, S., Olson, E. N., Saya, H. (2016). LATS-YAP/TAZ controls lineage specification by regulating TGF β signaling and Hnf4 α expression during liver development. *Nat Commun*, 7, 11961-11974.
- Lee, E. H., Park, K. I., Kim, K. Y., Lee, J. H., Jang, E. J., Ku, S. K., Kim, S. C., Suk, H. Y., Park, J. Y., Baek, S. Y., Kim, Y. W. (2019). Liquiritigenin inhibits hepatic fibrogenesis and TGF- β 1/Smad with Hippo/YAP signal. *Phytomedicine*, 62, 152780-152813.
- Lee, S. M., Schiergens, T. S., Demmel, M., Thasler, R. M., Thasler, W. E. (2017). Isolation of Hepatocytes and Stellate Cells from a Single Piece of Human Liver. *Methods Mol Biol*, 1506, 247-258.
- Li, G., Lin, J., Peng, Y., Qin, K., Wen, L., Zhao, T. (2020). Curcumol may reverse early and advanced liver fibrogenesis through downregulating the uPA/uPAR pathway. *Phytother Res*, 34(6), 1421-1435.
- Li, W. Q., Li, X. H., Du, J., Zhang, W., Li, D., Xiong, X. M., Li, Y. J. (2016). Rutaecarpine attenuates hypoxia-induced right ventricular remodeling in rats. *Naunyn Schmiedebergs Arch Pharmacol*, 389(7), 757-767.
- Liang, F.-F., Liu, C.-P., Li, L.-X., Xue, M.-M., Xie, F., Guo, Y., Bai, L. (2013). Activated effects of parathyroid hormone-related protein on human hepatic stellate cells.

- PLoS One*, 8(10), e76517-e76524.
- Lim, S., Kaldis, P. (2013). Cdks, cyclins and CKIs: roles beyond cell cycle regulation. *Development*, 140(15), 3079-3093.
- Lin, J. C., Peng, Y. J., Wang, S. Y., Lai, M. J. (2016). Sympathetic Nervous System Control of Carbon Tetrachloride-Induced Oxidative Stress in Liver through α -Adrenergic Signaling. *Oxid Med Cell Longev*, 2016, 3190617-3190628.
- Lipson, K. E., Wong, C., Teng, Y., Spong, S. (2012). CTGF is a central mediator of tissue remodeling and fibrosis and its inhibition can reverse the process of fibrosis. *Fibrogenesis Tissue Repair*, 5(Suppl 1), 24-31.
- Liu, P., Chen, L., Zhang, H. (2018). Natural Killer Cells in Liver Disease and Hepatocellular Carcinoma and the NK Cell-Based Immunotherapy. *J Immunol Res*, 2018, 1206737-1206745.
- Loforese, G., Malinka, T., Keogh, A., Baier, F., Simillion, C., Montani, M., Halazonetis, T. D. (2017). Impaired liver regeneration in aged mice can be rescued by silencing Hippo core kinases MST1 and MST2. *EMBO Mol Med*, 9(1), 46-60.
- Lu, L., Finegold, M. J., Johnson, R. L. (2018). Hippo pathway coactivators Yap and Taz are required to coordinate mammalian liver regeneration. *Exp Mol Med*, 50(1), e423-e430.
- Lundberg, J. M., Terenius, L., Hökfelt, T., Martling, C. R., Tatemoto, K., Mutt, V., Polak, J., Bloom, S., Goldstein, M. (1982). Neuropeptide Y (NPY)-like immunoreactivity in peripheral noradrenergic neurons and effects of NPY on sympathetic function. *Acta Physiol Scand*, 116(4), 477-480.
- Ma, J., Benz, C., Grimaldi, R., Stockdale, C., Wyatt, P., Frearson, J., Hammarton, T. C. (2010). Nuclear DBF-2-related kinases are essential regulators of cytokinesis in bloodstream stage *Trypanosoma brucei*. *J Biol Chem*, 285(20), 15356-15368.
- Maller, O., DuFort, C. C., Weaver, V. M. (2013). YAP forces fibroblasts to feel the tension. *Nat Cell Biol*, 15(6), 570-572.
- Mannaerts, I., Leite, S. B., Verhulst, S., Claerhout, S., Eysackers, N., Thoen, L. F. R., Hoorens, A., Reynaert, H., Halder, G., van Grunsven, L. A. (2015). The Hippo pathway effector YAP controls mouse hepatic stellate cell activation. *J Hepatol*, 63(3), 679-688.
- Marques, T. G., Chaib, E., da Fonseca, J. H., Lourenço, A. C., Silva, F. D., Ribeiro, M. A., Jr., Galvão, F. H., D'Albuquerque, L. A. (2012). Review of experimental models for inducing hepatic cirrhosis by bile duct ligation and carbon tetrachloride

- injection. *Acta Cir Bras*, 27(8), 589-594.
- Meyer, C., Liu, Y., Kaul, A., Peipe, I., Dooley, S. (2013). Caveolin-1 abrogates TGF- β mediated hepatocyte apoptosis. *Cell Death Dis*, 4(1), e466-e473.
- Mitchell, C., Willenbring, H. (2008). A reproducible and well-tolerated method for 2/3 partial hepatectomy in mice. *Nat Protoc*, 3(7), 1167-1170.
- Mohseni, R., Alavian, S. M., Sadeghabadi, Z. A., Heiat, M. (2020). Therapeutic effects of *Chlorella vulgaris* on carbon tetrachloride induced liver fibrosis by targeting Hippo signaling pathway and AMPK/FOXO1 axis. *Mol Biol Rep*, 48(1), 117-126.
- Moon, M. Y., Kim, H. J., Kim, M. J., Uhm, S., Park, J. W., Suk, K. T., Park, J. B., Kim, D. J., Kim, S. E. (2019). Rap1 regulates hepatic stellate cell migration through the modulation of RhoA activity in response to TGF- β 1. *Int J Mol Med*, 44(2), 491-502.
- Narmada, B. C., Chia, S. M., Tucker-Kellogg, L., Yu, H. (2013). HGF regulates the activation of TGF- β 1 in rat hepatocytes and hepatic stellate cells. *J Cell Physiol*, 228(2), 393-401.
- Natsis, K., Paraskevas, G., Papaziogas, B., Agiabasis, A. (2004). "Pes anserinus" of the right phrenic nerve innervating the serous membrane of the liver: a case report (anatomical study). *Morphologie*, 88(283), 203-205.
- Negro, A., Lionetto, L., Simmaco, M., Martelletti, P. (2012). CGRP receptor antagonists: an expanding drug class for acute migraine? *Expert Opin Investig Drugs*, 21(6), 807-818.
- Oben, J. A., Diehl, A. M. (2004). Sympathetic nervous system regulation of liver repair. *Anat Rec A Discov Mol Cell Evol Biol*, 280(1), 874-883.
- Oben, J. A., Roskams, T., Yang, S., Lin, H., Sinelli, N., Torbenson, M., Smedh, U., Moran, T. H., Li, Z., Huang, J., Thomas, S. A., Diehl, A. M. (2004). Hepatic fibrogenesis requires sympathetic neurotransmitters. *Gut*, 53(3), 438-445.
- Oh, S. H., Swiderska-Syn, M., Jewell, M. L., Premont, R. T., Diehl, A. M. (2018). Liver regeneration requires Yap1-TGF β -dependent epithelial-mesenchymal transition in hepatocytes. *J Hepatol*, 69(2), 359-367.
- Pérez-Liz, G., Flores-Hernández, J., Arias-Montaño, J. A., Reyes-Esparza, J. A., Rodríguez-Fragoso, L. (2005). Modulation of urokinase-type plasminogen activator by transforming growth factor beta1 in acetaldehyde-activated hepatic stellate cells. *Pharmacology*, 73(1), 23-30.
- Park, H. J., Kim, H. G., Wang, J. H., Choi, M. K., Han, J. M., Lee, J. S., Son, C. G.

- (2016). Comparison of TGF- β , PDGF, and CTGF in hepatic fibrosis models using DMN, CCl₄, and TAA. *Drug Chem Toxicol*, 39(1), 111-118.
- Patel, S. H., Camargo, F. D., Yimlamai, D. (2017). Hippo Signaling in the Liver Regulates Organ Size, Cell Fate, and Carcinogenesis. *Gastroenterology*, 152(3), 533-545.
- Peng, X., Wang, B., Wang, T., Zhao, Q. (2005). Expression of basic fibroblast growth factor in rat liver fibrosis and hepatic stellate cells. *J Huazhong Univ Sci Technolog Med Sci*, 25(2), 166-169.
- Perumal, N., Perumal, M., Halagowder, D., Sivasithamparam, N. (2017). Morin attenuates diethylnitrosamine-induced rat liver fibrosis and hepatic stellate cell activation by co-ordinated regulation of Hippo/Yap and TGF- β 1/Smad signaling. *Biochimie*, 140, 10-19.
- Piersma, B., Bank, R. A., Boersema, M. (2015). Signaling in Fibrosis: TGF- β , WNT, and YAP/TAZ Converge. *Front Med (Lausanne)*, 2, 59-72.
- Pritchard, M. T., Nagy, L. E. (2010). Hepatic fibrosis is enhanced and accompanied by robust oval cell activation after chronic carbon tetrachloride administration to Egr-1-deficient mice. *Am J Pathol*, 176(6), 2743-2752.
- Reilly, F. D., McCuskey, P. A., McCuskey, R. S. (1978). Intrahepatic distribution of nerves in the rat. *Anat Rec*, 191(1), 55-67.
- Retief, E., Parker, M. I., Retief, A. E. (1985). Regional chromosome mapping of human collagen genes alpha 2(I) and alpha 1(I) (COLIA2 and COLIA1). *Hum Genet*, 69(4), 304-308.
- Robert, S., Gicquel, T., Bodin, A., Lagente, V., Boichot, E. (2016). Characterization of the MMP/TIMP Imbalance and Collagen Production Induced by IL-1 β or TNF- α Release from Human Hepatic Stellate Cells. *PLoS One*, 11(4), e0153118-e0153131.
- Russell, F. A., King, R., Smillie, S. J., Kodji, X., Brain, S. D. (2014). Calcitonin gene-related peptide: physiology and pathophysiology. *Physiol Rev*, 94(4), 1099-1142.
- Russo, A. F. (2015). Calcitonin gene-related peptide (CGRP): a new target for migraine. *Annu Rev Pharmacol Toxicol*, 55, 533-552.
- Sørensen, K. K., Simon-Santamaria, J., McCuskey, R. S., Smedsrød, B. (2015). Liver Sinusoidal Endothelial Cells. *Compr Physiol*, 5(4), 1751-1774.
- Sakai, N., Van Sweringen, H. L., Quillin, R. C., Schuster, R., Blanchard, J., Burns, J. M., Tevar, A. D., Edwards, M. J., Lentsch, A. B. (2012). Interleukin-33 is

- hepatoprotective during liver ischemia/reperfusion in mice. *Hepatology*, 56(4), 1468-1478.
- Salas, A. L., Montezuma, T. D., Fariña, G. G., Reyes-Esparza, J., Rodríguez-Fragoso, L. (2008). Genistein modifies liver fibrosis and improves liver function by inducing uPA expression and proteolytic activity in CCl₄-treated rats. *Pharmacology*, 81(1), 41-49.
- Schon, H. T., Bartneck, M., Borkham-Kamphorst, E., Nattermann, J., Lammers, T., Tacke, F., Weiskirchen, R. (2016). Pharmacological Intervention in Hepatic Stellate Cell Activation and Hepatic Fibrosis. *Front Pharmacol*, 7, 33-54.
- Shen, K., Chang, W., Gao, X., Wang, H., Niu, W., Song, L., Qin, X. (2011). Depletion of activated hepatic stellate cell correlates with severe liver damage and abnormal liver regeneration in acetaminophen-induced liver injury. *Acta Biochimica et Biophysica Sinica*, 43(4), 307-315.
- Shi, Y., Massagué, J. (2003). Mechanisms of TGF-beta signaling from cell membrane to the nucleus. *Cell*, 113(6), 685-700.
- Shrestha, N., Chand, L., Han, M. K., Lee, S. O., Kim, C. Y., Jeong, Y. J. (2016). Glutamine inhibits CCl₄ induced liver fibrosis in mice and TGF-β1 mediated epithelial-mesenchymal transition in mouse hepatocytes. *Food Chem Toxicol*, 93, 129-137.
- Si-Tayeb, K., Lemaigre, F. P., Duncan, S. A. (2010). Organogenesis and development of the liver. *Developmental cell*, 18(2), 175-189.
- Spira, G., Mawasi, N., Paizi, M., Anbinder, N., Genina, O., Alexiev, R., Pines, M. (2002). Halofuginone, a collagen type I inhibitor improves liver regeneration in cirrhotic rats. *J Hepatol*, 37(3), 331-339.
- Streba, L. A. M., Vere, C. C., Ionescu, A. G., Streba, C. T., Rogoveanu, I. (2014). Role of intrahepatic innervation in regulating the activity of liver cells. *World J Hepatol*, 6(3), 137-143.
- Talme, T., Liu, Z., Sundqvist, K. G. (2008). The neuropeptide calcitonin gene-related peptide (CGRP) stimulates T cell migration into collagen matrices. *J Neuroimmunol*, 196(1-2), 60-66.
- Tan, S., Lu, Y., Xu, M., Huang, X., Liu, H., Jiang, J., Wu, B. (2019). β-Arrestin1 enhances liver fibrosis through autophagy-mediated Snail signaling. *Faseb j*, 33(2), 2000-2016.
- Tanaka, M., Miyajima, A. (2016). Liver regeneration and fibrosis after inflammation.

Inflamm Regen, 36, 19-24.

- Thomas, A. C., Zeng, Z., Rivière, J.-B., O'Shaughnessy, R., Al-Olabi, L., St-Onge, J., Atherton, D. J., Aubert, H., Bagazgoitia, L., Barbarot, S., Bourrat, E., Chiaverini, C., Chong, W. K., Duffourd, Y., Glover, M., Groesser, L., Hadj-Rabia, S., Hamm, H., Happle, R., Mushtaq, I., Lacour, J.-P., Waelchli, R., Wobser, M., Vabres, P., Patton, E. E., Kinsler, V. A. (2016). Mosaic Activating Mutations in GNA11 and GNAQ Are Associated with Phakomatosis Pigmentovascularis and Extensive Dermal Melanocytosis. *J Invest Dermatol*, 136(4), 770-778.
- Toita, R., Kawano, T., Fujita, S., Murata, M., Kang, J.-H. (2018). Increased hepatic inflammation in a normal-weight mouse after long-term high-fat diet feeding. *J Toxicol Pathol*, 31(1), 43-47.
- Totaro, A., Castellan, M., Battilana, G., Zanconato, F., Azzolin, L., Giulitti, S., Cordenonsi, M., Piccolo, S. (2017). YAP/TAZ link cell mechanics to Notch signalling to control epidermal stem cell fate. *Nat Commun*, 8, 15206-15218.
- Tsuchida, T., Friedman, S. L. (2017). Mechanisms of hepatic stellate cell activation. *Nat Rev Gastroenterol Hepatol*, 14(7), 397-411.
- Tsujikawa, K., Yayama, K., Hayashi, T., Matsushita, H., Yamaguchi, T., Shigeno, T., Ogitani, Y., Hirayama, M., Kato, T., Fukada, S., Takatori, S., Kawasaki, H., Okamoto, H., Ikawa, M., Okabe, M., Yamamoto, H. (2007). Hypertension and dysregulated proinflammatory cytokine production in receptor activity-modifying protein 1-deficient mice. *Proc Natl Acad Sci U S A*, 104(42), 16702-16707.
- Tu, T., Calabro, S. R., Lee, A., Maczurek, A. E., Budzinska, M. A., Warner, F. J., McLennan, S. V., Shackel, N. A. (2015). Hepatocytes in liver injury: Victim, bystander, or accomplice in progressive fibrosis? *J Gastroenterol Hepatol*, 30(12), 1696-1704.
- Tu, X., Zhang, H., Zhang, J., Zhao, S., Zheng, X., Zhang, Z., Zhu, J., Chen, J., Dong, L., Zang, Y., Zhang, J. (2014). MicroRNA-101 suppresses liver fibrosis by targeting the TGF β signalling pathway. *J Pathol*, 234(1), 46-59.
- Varelas, X., Samavarchi-Tehrani, P., Narimatsu, M., Weiss, A., Cockburn, K., Larsen, B. G., Rossant, J., Wrana, J. L. (2010). The Crumbs complex couples cell density sensing to Hippo-dependent control of the TGF- β -SMAD pathway. *Developmental cell*, 19(6), 831-844.
- Wan, Y., Ceci, L., Wu, N., Zhou, T., Chen, L., Venter, J., Francis, H., Bernuzzi, F., Invernizzi, P. (2019). Knockout of α -calcitonin gene-related peptide attenuates

- cholestatic liver injury by differentially regulating cellular senescence of hepatic stellate cells and cholangiocytes. *Lab Invest*, 99(6), 764-776.
- Wang, L., Huang, J., Jiang, M., Sun, L. (2011). Survivin (BIRC5) cell cycle computational network in human no-tumor hepatitis/cirrhosis and hepatocellular carcinoma transformation. *J Cell Biochem*, 112(5), 1286-1294.
- Wang, W., Qiao, Y., Li, Z. (2018). New Insights into Modes of GPCR Activation. *Trends Pharmacol Sci*, 39(4), 367-386.
- Weber, L. W., Boll, M., Stampfl, A. (2003). Hepatotoxicity and mechanism of action of haloalkanes: carbon tetrachloride as a toxicological model. *Crit Rev Toxicol*, 33(2), 105-136.
- Weiskirchen, R., Tacke, F. (2017). Interleukin-33 in the pathogenesis of liver fibrosis: alarming ILC2 and hepatic stellate cells. *Cell Mol Immunol*, 14(2), 143-145.
- Xiang, D., Zou, J., Zhu, X., Chen, X., Luo, J., Kong, L., Zhang, H. (2020). Physalin D attenuates hepatic stellate cell activation and liver fibrosis by blocking TGF- β /Smad and YAP signaling. *Phytomedicine*, 78, 153294-153305.
- Xu, L., Hui, A. Y., Albanis, E., Arthur, M. J., O'Byrne, S. M., Blaner, W. S., Mukherjee, P., Friedman, S. L., Eng, F. J. (2005). Human hepatic stellate cell lines, LX-1 and LX-2: new tools for analysis of hepatic fibrosis. *Gut*, 54(1), 142-151.
- Yagi, R., Chen, L. F., Shigesada, K., Murakami, Y., Ito, Y. (1999). A WW domain-containing yes-associated protein (YAP) is a novel transcriptional co-activator. *The EMBO journal*, 18(9), 2551-2562.
- Yamaoka, K., Nouchi, T., Marumo, F., Sato, C. (1993). Alpha-smooth-muscle actin expression in normal and fibrotic human livers. *Dig Dis Sci*, 38(8), 1473-1479.
- Yang, Y. M., Seki, E. (2015). TNF α in liver fibrosis. *Curr Pathobiol Rep*, 3(4), 253-261.
- Yoon, S. P., Kim, J. (2018). Exogenous CGRP upregulates profibrogenic growth factors through PKC/JNK signaling pathway in kidney proximal tubular cells. *Cell Biol Toxicol*, 34(4), 251-262.
- Yu, F. X., Zhao, B., Panupinthu, N., Jewell, J. L., Lian, I., Wang, L. H., Zhao, J., Yuan, H., Tumaneng, K., Li, H., Fu, X. D., Mills, G. B., Guan, K. L. (2012). Regulation of the Hippo-YAP pathway by G-protein-coupled receptor signaling. *Cell*, 150(4), 780-791.
- Yu, H. X., Yao, Y., Bu, F. T., Chen, Y., Wu, Y. T., Yang, Y., Chen, X., Zhu, Y., Wang, Q., Pan, X. Y., Meng, X. M., Huang, C., Li, J. (2019). Blockade of YAP alleviates hepatic fibrosis through accelerating apoptosis and reversion of activated hepatic

- stellate cells. *Mol Immunol*, 107, 29-40.
- Yu, J., Zhang, L., Chen, A., Xiang, G., Wang, Y., Wu, J., Mitchelson, K., Cheng, J., Zhou, Y. (2008). Identification of the gene transcription and apoptosis mediated by TGF-beta-Smad2/3-Smad4 signaling. *J Cell Physiol*, 215(2), 422-433.
- Zanconato, F., Forcato, M., Battilana, G., Azzolin, L., Quaranta, E., Bodega, B., Rosato, A., Bicciato, S., Cordenonsi, M., Piccolo, S. (2015). Genome-wide association between YAP/TAZ/TEAD and AP-1 at enhancers drives oncogenic growth. *Nat Cell Biol*, 17(9), 1218-1227.
- Zhao, C., Zeng, C., Ye, S., Dai, X., He, Q., Yang, B., Zhu, H. (2020). Yes-associated protein (YAP) and transcriptional coactivator with a PDZ-binding motif (TAZ): a nexus between hypoxia and cancer. *Acta Pharm Sin B*, 10(6), 947-960.
- Zhou, J., Liang, Y., Pan, J. X., Wang, F. F., Lin, X. M., Ma, R. J., Qu, F., Fang, J. Q. (2015). Protein extracts of *Crassostrea gigas* alleviate CCl₄-induced hepatic fibrosis in rats by reducing the expression of CTGF, TGF-β1 and NF-κB in liver tissues. *Mol Med Rep*, 11(4), 2913-2920.
- Zhubanchaliyev, A., Temirbekuly, A., Kongrtay, K., Wanshura, L. C., Kunz, J. (2016). Targeting Mechanotransduction at the Transcriptional Level: YAP and BRD4 Are Novel Therapeutic Targets for the Reversal of Liver Fibrosis. *Front Pharmacol*, 7, 462-472.

10. Curriculum Vitae

Name: Yang Wang

Date of birth: 30/12/1991

Place of birth: Jiangsu, China

Nationality: Chinese

Tel: +49 1630420693

Email: wangyangtum@163.com

Educational career:

- 10.2017 until now Doctoral candidate, TUM Medical Graduate Center, Technical University of Munich, Germany
- 09.2015 – 07.2017 Master's degree of medicine, School of Medicine, Southeast University, Nanjing, China
- 09.2010 – 07.2015 Bachelor's degree of medicine, School of Medicine, Southeast University, Nanjing, China

Publications:

Laschinger, M.*, **Wang, Y.***, Holzmann, G., Wang, B., Stöß, C., Lu, M., Brugger, M., Schneider, A., Knolle, P., Wohlleber, D., Schulze, S., Steiger, K., Tsujikawa, K., Altmayr, F., Friess, H., Hartmann, D., Hüser, N., & Holzmann, B. (2020). The CGRP receptor component RAMP1 links sensory innervation with YAP activity in the regenerating liver. *FASEB journal : official publication of the Federation of American Societies for Experimental Biology*, 34(6), 8125–8138. (* Melanie Laschinger and Yang Wang contributed equally to this work.)

Wang, Y., Yu, X., Hartmann, D., & Zhou, J. (2020). Circulating tumor cells in peripheral blood of pancreatic cancer patients and their prognostic role: a systematic review and

meta-analysis. *HPB : the official journal of the International Hepato Pancreato Biliary Association*, 22(5), 660–669.

Lu, M., Hartmann, D., Braren, R., Gupta, A., Wang, B., **Wang, Y.**, Mogler, C., Cheng, Z., Wirth, T., Friess, H., Kleeff, J., Hüser, N., & Sunami, Y. (2019). Oncogenic Akt-FOXO3 loop favors tumor-promoting modes and enhances oxidative damage-associated hepatocellular carcinogenesis. *BMC cancer*, 19(1), 887.

Cheng, Z., Liu, L., Zhang, X. J., Lu, M., **Wang, Y.**, Assfalg, V., Laschinger, M., von Figura, G., Sunami, Y., Michalski, C. W., Kleeff, J., Friess, H., Hartmann, D., & Hüser, N. (2018). Peroxisome Proliferator-Activated Receptor gamma negatively regulates liver regeneration after partial hepatectomy via the HGF/c-Met/ERK1/2 pathways. *Scientific reports*, 8(1), 11894.

Awards:

Top Abstract Prize & National Scholar Award from the United European Gastroenterology (UEG Barcelona 2019).

11. Acknowledgements

Upon the completion of this thesis, I would like to express my gratitude to all the people who have offered me tremendous support and encouragement during my study in Technical University of Munich.

First of all, I would like to deeply thank Prof. Dr. Helmut Friess for accepting me as a medical doctoral student in the lab of Department of Surgery. I feel lucky to have this chance to work in this fantastic place.

Secondly, I want to express my heartfelt gratitude to my supervisor, Dr. Melanie Laschinger, for her devoted guide and support through my whole project. She led me into the field of basic science, and gave me a lot of precious advice every time I ran into problems. She taught me how to communicate with other group members, and work together as a team. I improved my research strategy, my writing and my presentation skills under her guidance. I could not get any of those achievements without her help.

Thirdly, I would like to thank my mentor, Dr. Daniel Hartmann. He provided me with much support for my research, giving me suggestions on the direction of the project.

Moreover, I owe many thanks to Prof. Dr. Norbert Hüser, who offered me kind support, not only in my project but also in terms of my living in Munich. He helped me solve many problems that I ran into as a foreign student.

Furthermore, I would like to thank Prof. Bernhard Holzmann, Christian Stöß, Gabriela Holzmann, Felicitas Altmayr and Carolin Mogler, for their great contribution to my research. They helped me generate some important data during my experiments.

I also want to thank my colleagues in the lab, Baocai Wang, Xuejun Zhang, Yuhan Yin, Jianye Wang and Hao Ling for the great time together. They supported me in my work and gave me a lot of motivations in the lab.

I also would like to thank Florian Reiter, Tobias Schiergens and Ralf Wimmer from the University Hospital of LMU, for providing me with the human primary hepatic stellate cells,

which were highlight parts of my project.

Last but not least, I am grateful to the China Scholarship Council for funding me during my stay in Germany.